A STRUCTURE-REACTIVITY STUDY OF SELECTED PHOSPHATE ESTERS

A thesis submitted to the
UNIVERSITY OF CAPE TOWN
in fulfilment of the requirements for the degree of
DOCTOR OF PHILOSOPHY

by

DIANNE RUTH BOND
B.Sc.(Hons), M.Sc. (Cape Town)

Department of Physical Chemistry
University of Cape Town
Rondebosch
7700
Republic of South Africa

November 1985

to my Parents

ACKNOWLEDGEMENTS

I wish to extend sincere thanks to

Professor L.R. Nassimbeni for his enthusiastic and expert supervision,

Professor T.A. Modro for his invaluable help and guidance,

Dr M.L. Niven for her expertise with the data collections,

all colleagues for their help and interest and especially to Alfie Le Roux and to Madeleine Moore,

my mother, Ruth, for proof-reading,

my husband, William, for his support and encouragement,

the University of Cape Town for the financial assistance.

PUBLICATIONS

Parts of this work have been published.

1. *N*-Phosphorylated Dimethylsulfoximides. I. Crystal and Molecular Structures.
   Bond, D.R., Modro, T.A., Nassimbeni, L.R. and Wieczorkowski, J.,
   Phosphorus and Sulfur, *22*, p59 (1985).

2. Structural Effects in Phosphates. 1. Comparison of 4-Nitrophenyl
   1-Naphthyl and 4-Nitrophenyl Quinolin-8-yl Phosphates.
   Bond, D.R., Modro, T.A. and Nassimbeni, L.R., *J. Org. Chem.*, *50*, p2281 (1985).

3. Structural effects in phosphates. Part 2. Crystal and molecular structures
   of oxonium bis(*p*-nitrophenyl)phosphate and triethylammonium bis(*p*-nitro=
   phenyl)phosphate.
   Bond, D.R., Modro, T.A., Niven, M.L. and Nassimbeni, L.R., *S. Afr. J. Chem.*,
   38, p78 (1985).

ABSTRACT

A comparative X-ray analysis study of bis(4-nitrophenyl)-8-quinolinyl phosphate (4), 1-naphthyl-bis(4-nitrophenyl) phosphate (5) and 4-nitrophenyl -8-quinolinyl phosphate (6) was undertaken. In compound (4) donor-acceptor nitrogen-phosphorus interactions change the geometry of the molecule from tetrahedral to quasi trigonal bipyramidal, thus the structure may be considered as an "early stage" of the intramolecular displacement of the 4-nitrophenoxide group. In the diester (6) this interaction is replaced by intermolecular N^{+}-H...O^{-} hydrogen bonding. In addition the intramolecular non-bonded potential energies of (4) and (5) were calculated and the minimum-energy conformations were compared with those determined by X-ray diffraction. These results confirm the differences observed in the intramolecular interactions operative in (4) and (5). The mass spectra of (4) and (5) are dramatically different with respect to the fragmentation involving expulsion of the 4-nitrophenoxy radical and formation of the corresponding phosphorylium ion by nitrogen participation. Rate measurements for the base-catalysed hydrolysis of the first P-OPNP linkage show that (4) is not significantly more reactive than (5) and provide no evidence for intramolecular nucleophilic catalysis in the hydrolysis of (4).

The crystal and molecular structure of 1-naphthyl acetate (7) was determined. Attempts to grow suitable crystals of 8-quinolinyl acetate (8) failed and therefore its structure could not be elucidated. Possible intramolecular nitrogen - carbonyl carbon interactions operative in (8) could therefore not be established.

Crystal and molecular structures of oxonium bis(4-nitrophenyl) phosphate (10) and triethylammonium bis(4-nitrophenyl) phosphate (11) were determined. In the oxonium salt (10) three strong hydrogen bonds cross-link the phosphoryl

oxygen atoms with the oxonium oxygen atoms in a double-string formation, running close to the two-fold screw axis. In the triethylammonium salt (11), a single hydrogen bond between the protonated nitrogen atom and a phosphoryl oxygen atom groups the ions in pairs. A correlation between the pKa of the cations and the OPO angle of the common phosphate diester is observed.

The crystal and molecular structures of three *N*-phosphoryl dimethylsulfoximides, $(RO)_2P(O)-N=S(O)Me_2$ (I) have been determined by X-ray diffraction. Values obtained for the P-N bond distances and for the PNS bond angles indicate that the P-N bond in (I) has a partial double bond character, similar to that observed in phosphoramidates. The mutual orientation of the P=O and N=S groups in (13) (R = *i*Pr) and (14) (R = Ph) is close to gauche, while for the 2-oxo-5,5-dimethyl-1,3,2-dioxaphosphorinan-2-yl derivative (15) this orientation is close to anti. The orientation between the P-N and S=O groups in all compounds is nearly gauche. In the cyclic derivative (15) the phosphoryl oxygen is axial, contrary to the usual equatorial preference for the P=O group in 1,3,2-dioxaphosphorinane systems.

From a preliminary structural correlation study of organic phosphates, it was concluded that the inherent reactivity of the phosphate monoester monoanions is manifested in the molecular parameters and thereby this correlation provides further evidence for the proposed dissociative "metaphosphate" mechanism for the cleavage reaction of these organic phosphates.

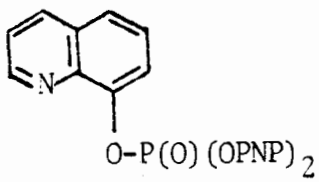

(4)

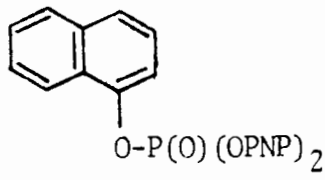

(5)

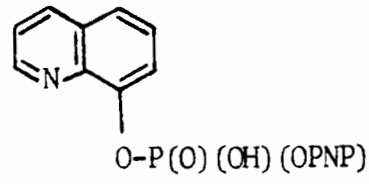

(6)

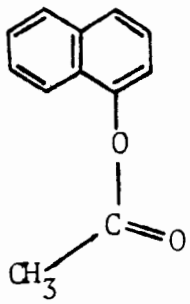

(7)

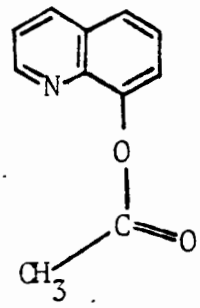

(8)

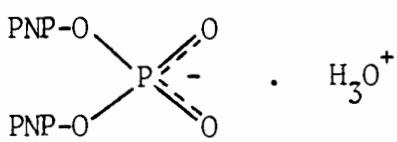

(10)

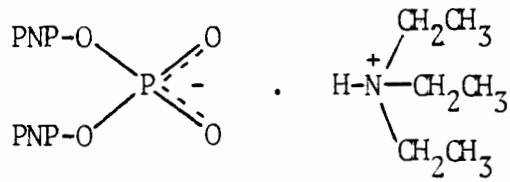

(11)

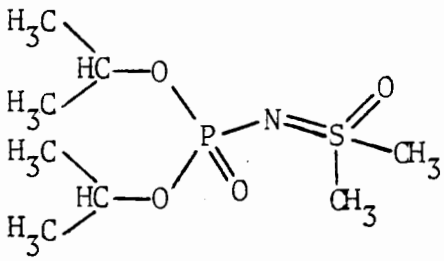

(13)

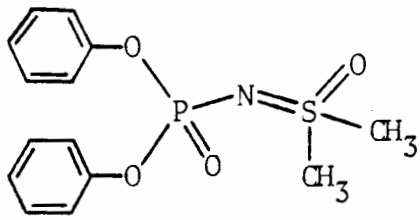

(14)

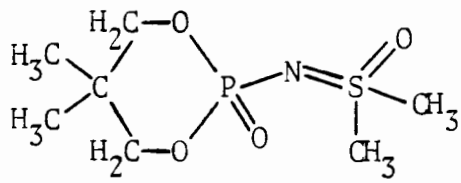

(15)

PNP = O_2N–C$_6$H$_4$–

CONTENTS

CHAPTER 1

CHAPTER 1

GENERAL INTRODUCTION

Phosphorus is present in all living tissue and exists primarily as phosphate esters. These phosphate derivatives are involved in nearly every aspect of cellular function and the focus of this work is on their role in the energy transfer process. The most important carrier of the so-called "high-energy" phosphate group is the adenosine triphosphate (ATP) molecule. The hydrolysis of the ATP molecule occurs by the donation of the "high-energy" phosphate group to an acceptor molecule with simultaneous formation of adenosine diphosphate (ADP) and liberation of energy, as illustrated by the hydrolysis reaction:

$$\text{ATP} + H_2O \rightleftharpoons \text{ADP} + \text{inorganic phosphate}$$

Since 1953 several studies[1] of the hydrolysis of ATP have been undertaken and at best the non-enzymatic behaviour of ATP in solution is reasonably well understood.

An intimate understanding of the phosphoryl transfer reactions in biochemical systems can only be achieved by drawing analogies from model systems. Nucleophilic displacement reactions, at the phosphorus atom, of phosphoric acid esters in both protic and aprotic solvents have therefore been scrutinised. The phosphoryl group transfer occurs by two distinctly different types of mechanisms, namely the formation of a phosphorane or metaphosphate intermediate. These mechanisms are systematically and comprehensively discussed in several review articles[1,2,3].

In addition, various types of catalytic processes must be considered as they may be pertinent to the enzymatic hydrolyses in vivo.

It is generally accepted that divalent metal cations are a prerequisite in the enzymatic reactions involving nucleoside triphosphates. The precise role of these metal ions and the exact nature of their complexation remains unelucidated. To date researchers have considered the metal ion to be co=ordinated to the phosphate thereby increasing its susceptibility to nucleophilic attack. ^{31}P NMR studies[4,5,6] however do not unequivocally specify the site occupied by the metal cation in the polyphosphate chain. It may be concluded that the metal ions interact with the β- and γ-phosphates of ATP. Some researchers[3] have postulated that the metal ion may have a number of possible roles, for example: a) as a template for orientating substrates and enzymatic catalytic groups, b) to promote metaphosphate expulsion by chelation, c) to neutralise charge, d) by complexing with the pentacovalent intermediate in order to control the stereochemical course or enhance the rate of the reaction and finally, e) as a hydroxyl carrier to promote hydrolysis. Their approach was to search for representative model systems which would illustrate the above concepts. A great deal of effort has thus been directed toward the understanding of the metal ion-ATP complexation. In this study metal ion catalysis was not investigated.

Furthermore, enzymatic rate accelerations may be due to a polyfunctional catalytic process whereby several functional groups simultaneously contri=bute to the catalysis. Model systems which demonstrate such cooperative catalytic behaviour have been devised[2].

The possibility of an intramolecular catalytic process operative in enzyme mediated phosphoryl transfer has stimulated much investigation. Carboxyl, carboxylate[7,8,9] and hydroxyl functions[10] have mainly been utilised to displace internally with intermediate ring formation. Relatively few mechanistic investigations have examined the displacement by nitrogen at phosphorus with formation of a cyclic phosphoramidate ester. Several and

sometimes conflicting mechanisms have been proposed for these neighbouring group participation reactions. For example, Chanley and associates[11,12] observe a great rate enhancement in the hydrolysis of the dianion of an *o*-carboxylarylphosphate as compared to the monoanion of phenylphosphate. No such enhanced activities are noticeable for the *m*- and *p*-analogues. They propose that the large rate effect is due to direct interaction between the favourably positioned *o*-carboxyl group and the phosphate rather than to resonance or inductive effects. Bender and Lawlor[13] offer much evidence suggesting that this catalysis is not nucleophilic but instead general acid. Furthermore, three different mechanisms, namely nucleophilic, general base and electrostatic catalysis have been demonstrated[14] in amine-catalysed phosphate triester hydrolyses. In particular, the hydrolysis of nitrophenyl phosphodiesters[15] is catalysed by pyridine type amines via a nucleophilic pathway involving a phosphopyridine intermediate.

The major portion of this work (Chapter 2) was devoted to the understanding of these anchimeric assistance effects.

Finally the most important catalytic process is that mediated by an enzyme. In spite of intensive studies of phosphate ester hydrolysis the details of the processes by which these enzymes function remain unelucidated. There is therefore no satisfactory theory to account for the factors which direct nucleophiles to the P_α, P_β and P_γ centres of ATP in enzymatic displacement reactions.

Medium effects in phosphoryl transfer reactions are also of great importance. Protic solvents participate in the solvation of the ground state of mono- and di-anion arylphosphates to a much greater extent than they do the less polar transition states which result in the formation of a phosphorane or meta-phosphate intermediate[1]. Therefore it is evident that when studying enzymatic

phosphoryl transfer reactions by means of simple model phosphoesters, both the state of ionisation of the molecules and the effect of the medium must be taken into account. In vivo, these reactions occur in aqueous media, hence hydrogen bonding to phosphate groups can be an important factor in the free energy of phosphorylation. A further objective (Chapter 4) was to examine the hydrogen bonding tendencies of two phosphodiesters.

Other "high-energy" reservoirs in vivo include phosphocreatine and phospho= arginine. As in the case of ATP, the reversible phosphoryl transfer reactions involving phosphocreatine and phosphoarginine are catalysed by specific enzymes in the presence of obligatory metal ions. The hydrolytic cleavage however differs from that of ATP in that it occurs at the labile P-N bond. Numerous synthetic phosphoramidic acid derivatives have been prepared and studied in detail in relation to the mode of action of phosphocreatine[16,17].

However this work does not concern itself with the above aspect. Instead three novel *N*-substituted phosphoramidates (the *N*-phosphorylated dimethyl-sulfoximides, $Me_2S(O)N\text{-}P(O)(OR)_2$) have been crystallographically analysed (Chapter 5) in order to examine their structural and bonding characteristics. Comparisons of these compounds with related organo-phosphorus structures may shed light on various aspects including the nature of the P-N bond in the phosphorylation process.

Finally, attempts were made (Part 2) to correlate the structural parameters of a representative number of phosphate esters in some systematic way in order to obtain information which will yield insight into the nature of the bonding in these compounds. In addition a preliminary investigation of selected phosphate monoester monoanions was undertaken in order to establish whether the inherent reactivity of these compounds would be manifested in

their structural parameters, particularly when compared with the much less reactive triester derivatives.

PART 1

CHAPTER 2

CHAPTER 2

INTRAMOLECULAR NUCLEOPHILIC CATALYSIS IN PHOSPHATE ESTERS

2.1 INTRODUCTION

Research has clearly demonstrated intramolecular nucleophilic participation in the displacement at phosphoryl centres[18].

Loran and Williams[15] have observed a ca 350-fold rate increase for the hydrolysis of 4-nitrophenyl-8-quinolinyl phosphate (1) relative to the reactivity of 4-nitrophenyl-phenyl phosphate. They propose that the enhanced expulsion of 4-nitrophenoxide is due to the intramolecular participation of the tertiary nitrogen in (1), to produce a cyclic intermediate (1a) (equation 1).

By comparison, neighbouring carboxy-participation in the hydrolysis of 2-carboxyphenyl-4-nitrophenyl phosphate[19] (2) is, contrary to expectation some 100-fold more efficient (equation 2) than the effect caused by the quinolinyl nitrogen in (1). The large difference in the efficiency of the intramolecular attack is presumably due to the difference in strain in forming the five- and six-membered ring transition states in the quinolinyl and carboxylate participation respectively.

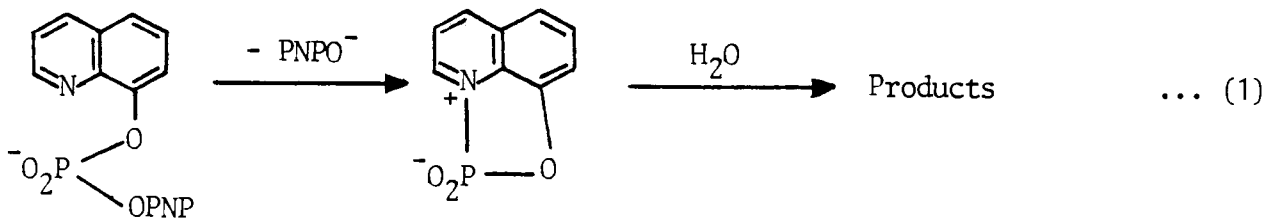

(1) (1a) PNP = $4\text{-}NO_2\text{-}C_6H_4$

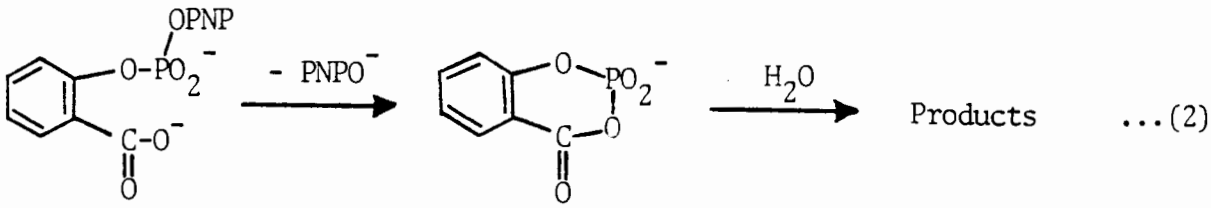

...(2)

(2)

An objective of this study was to determine whether the nitrogen-phosphorus interactions responsible for the intramolecular catalysis in the hydrolysis of phosphates derived from 8-hydroxyquinoline manifest themselves in the molecular parameters of a substrate. Intramolecular displacement of a leaving group (L) by the tertiary nitrogen atom in the quinolinyl phosphate (equation 3) would involve a change in the geometry of the phosphorus from tetrahedral to trigonal bipyramidal, with concomitant modification of bond lengths and angles.

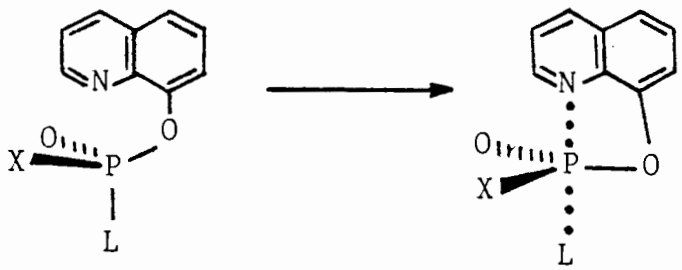

... (3)

If the molecular structure of a suitably selected model compound were to reveal the presence of such interactions, the structure could then be considered as an "early stage"[20] in the intramolecular displacement at the P(IV) centre.

Schmutzler and coworkers[21] have described the structural characterisation of the first intramolecular fluoro-phosphorane complexes (3) containing six-coordinated phosphorus.

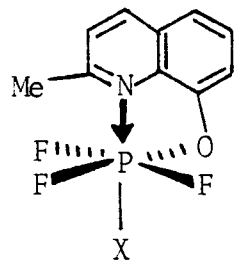

(3) (X = F or Ph)

The N→P co-ordinate bond formation, despite considerable distortion required at the N and O(8) atoms of the quinolinyl moiety, is achieved as a result of the presence of the highly electrophilic fluorine atoms at the P(V) centre. The N→P bond length ranges from 1,9 to 2,0Å and is only slightly longer than a "pure" P-N sigma bond which is reported[22] to be 1,77Å.

Phosphate triesters (4) and (5) were therefore structurally analysed in order to establish, by comparison, whether such specific intramolecular interactions are operative in (4).

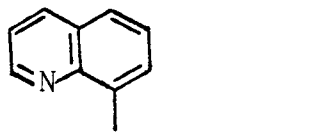

(4)

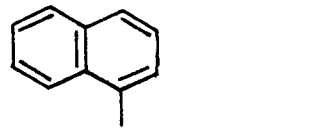

(5)

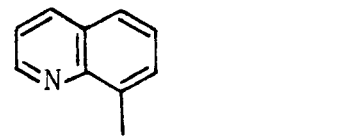

(6)

The structural parameters of compounds (4) and (5) were then correlated with independently obtained sets of reactivity data as follows. The non-bonded potential energies of (4) and (5) were calculated and the conformations corresponding to the minima in total intramolecular energy (T.I.E.) were compared with those determined by X-ray diffraction. The fragmentation patterns of phosphates (4) and (5) resulting from electron impact were obtained and the reactivity of these triesters under conditions of base-

catalysed hydrolysis were investigated.

In this way information pertinent to the neighbouring nitrogen participation effect as well as the dynamics of the phosphate ester groups was accumulated.

Finally the molecular structure of triester (4) was compared to that of its hydrolysis product, 4-nitrophenyl-8-quinolinyl phosphate (6). The hydrolysis of (4) results in the introduction of an acidic hydrogen into the molecule, the nitrogen atom presumably becomes involved in a hydrogen bond formation which prevents its interaction with the phosphoryl centre.

The effect of functional group changes on molecular structure was therefore of further interest.

2.2 CRYSTAL AND MOLECULAR STRUCTURES OF 1-NAPHTHYL-BIS(4-NITROPHENYL) PHOSPHATE (5), BIS(4-NITROPHENYL)-8-QUINOLINYL PHOSPHATE (4) AND 4-NITROPHENYL-8-QUINOLINYL PHOSPHATE (6)

2.2.1 EXPERIMENTAL, SOLUTION AND REFINEMENT OF (5)

Experimental

1-Naphthyl-bis(4-nitrophenyl) phosphate was synthesised according to the following reaction:

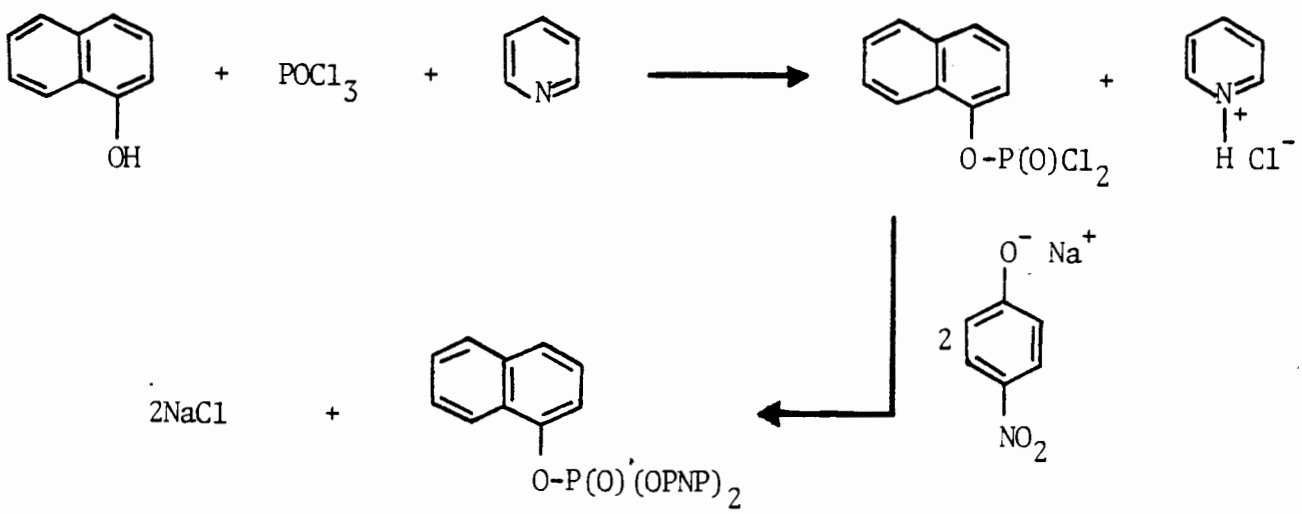

To a stirred solution of 1-naphthyl-phosphorodichloridate (0,02mol) (prepared by refluxing equimolar amounts of 1-naphthol, $POCl_3$ and dry pyridine in benzene; yield 82%; b.p. 150°C/0,7mmHg) in dry ether (25ml), dry sodium 4-nitrophenoxide (0,04mol) was added at room temperature over a period of 30 minutes. The mixture was then refluxed for 2 hours, cooled, the precipitate filtered off and thoroughly washed with water. After drying, the crude product was recrystallised from ethanol-acetone. Yield 60%; m.p. 118-120°C. Anal. Calculated for $C_{22}H_{15}N_2O_8P$: C = 56,66%, H = 3,24%, N = 6,01%. Found: C = 56,50%, H = 3,35%, N = 5,85%. ^1H NMR ($CDCl_3$): δ7,3-7,6 (8H's) hydrogens ortho to the "alcohol" oxygens of the 4-nitrophenyl groups and

four aryl hydrogens of the naphthyl moiety; δ7,94 (3H's) aryl hydrogens of the naphthyl group; δ8,24 (4H's) hydrogens meta to the "alcohol" oxygens of the 4-nitrophenyl groups.

All melting points were taken on a Fisher-Johns apparatus and are uncorrected. All ^1H NMR spectra were recorded in $CDCl_3$ on a 100MHz Varian XL 100 spectrometer with Me_4Si as the internal standard. Microanalyses were performed on a Heraeus Universal combustion analyser. All solvents and substrates used in the syntheses were AnalaR grade reagents and were purified in the usual manner.

Large, rectangular-shaped, transparent, single crystals suitable for X-ray analysis precipitated from an ethanol (96%)-chloroform mixture overnight. The crystal density was determined by flotation in a mixture of saturated potassium iodide and water.

From the preliminary oscillation and Weissenberg photography the conditions for non-extinction of reflections were determined as,

$$hkl \quad : \quad \text{no conditions}$$
$$h0l \quad : \quad h + l = 2n$$
$$0k0 \quad : \quad k = 2n,$$

thus indicating $P2_1/n$, the non-standard setting of the monoclinic space group $P2_1/c$[23]. The relationship between the space groups $P2_1/c$ and $P2_1/n$ is shown in Figure 2.1.

Accurate lattice constants were determined by a least-squares analysis of the χ, ϕ and 2θ angles of 25 reference reflections accurately centred on the Philips PW 1100 four-circle diffractometer, using CuK_α radiation (λ = 1,5418Å). To ensure instrumental stability and to monitor any crystal decomposition, the intensities of three reference reflections were measured at approximately hourly intervals throughout the duration of the data collection. Reflections

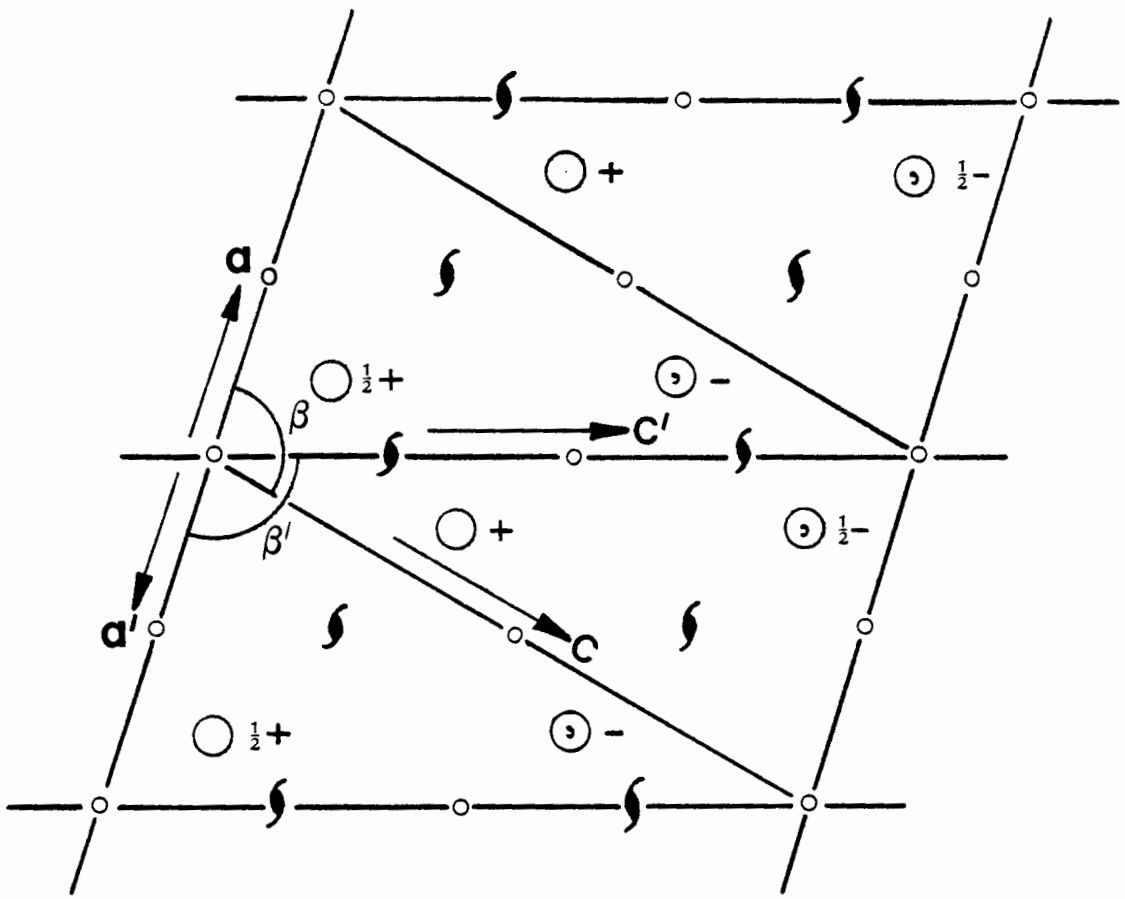

FIGURE 2.1 The relationship between the unit cell (bounded by a, b and c) corresponding to the space group $P2_1/n$ and the unit cell (bounded by a', b' and c') corresponding to the space group $P2_1/c$. The equivalent positions are:

$P2_1/n$: x,y,z; $-x,-y,-z$; $\frac{1}{2}+x,\frac{1}{2}-y,\frac{1}{2}+z$; $\frac{1}{2}-x,\frac{1}{2}+y,\frac{1}{2}-z$

$P2_1/c$: x,y,z; $-x,-y,-z$; $x,\frac{1}{2}-y,\frac{1}{2}+z$; $-x,\frac{1}{2}+y,\frac{1}{2}-z$.

The two cells are projected onto [010].

were considered "present" (observed) if I_{rel} exceeded $2\sigma I_{rel}$. The standard error, σI_{rel}, in the relative standard intensity, I_{rel}, was calculated from the formula:

$$\sigma I_{rel} = [N_{pk} + N_{bg} + N_{instr}]^{\frac{1}{2}}$$

where N_{pk} = gross peak count for a specific reflection

N_{bg} = background count as measured on either side of the peak

$N_{instr} = [0,02(N_{pk} - N_{bg})]^2$

The reflection data were corrected for Lorentz-polarisation but not for absorption as the absorption correction factor, A^{*23} ranged between 2,75 and 2,18 (μR max. = 0,78, μR min. = 0,70) in the entire θ range scanned. This variation was deemed sufficiently small to be neglected.

Solution and Refinement

All relevant crystal data and experimental and refinement parameters for the structure analysis appear in Table 2.1.

The structure was solved in the $P2_1/n$ space group by the automatic centro-symmetric direct methods routine of the SHELX-76[24] program system. An *E*-map yielded the positions of all the non-hydrogen atoms. The positions of several hydrogen atoms were located in a subsequent difference electron-density map calculated after further cycles of least-squares refinement with *R* equal to 0,13. A final refinement was carried out with all the non-hydrogen atoms treated anisotropically and the aromatic hydrogen atoms constrained at 1,00Å from their parent carbon atoms, their positions dictated by the molecular geometry. In the final cycle of least-squares refinement the average shift to error ratio was less than 0,01 indicative of a satisfactory convergence. A final difference electron-density map calculated after the final refinement revealed no peaks of height > 0,2eÅ^{-3}. As a final test of the proposed model

TABLE 2.1 Crystal Data and Experimental and Refinement Parameters for Compound (5)

Crystal Data	
Molecular formula	$C_{22}H_{15}N_2O_8P$
Molecular weight	466,35gmol^{-1}
Space group	$P2_1/n$
a	7,282(4)Å
b	12,683(6)Å
c	22,40(1)Å
β	97,59(2)^{o}
V	2050,86Å^3
Z	4
D_m	1,45gcm^{-3}
D_c	1,51gcm^{-3}
$\mu(CuK_\alpha)$	15,64cm^{-1}
$F(000)$	960
Data Collection	
Crystal dimensions	0,50 x 0,45 x 0,45mm
Scan mode	ω-2θ
Scan width ($\Delta\omega$)	2,0^{o}
Aperture width (Horizontal)	2^{o}
Aperture width (Vertical)	1^{o}
Scan speed	0,067$^{o}\theta$s^{-1}
Range scanned	6$^{o}\leq\theta\leq$60^{o}
Stability of standard reflections	0,05%
Number of reflections collected	3198
Number of "observed" reflections	2743 with $I_{rel} > 2\sigma I_{rel}$
Final Refinement	
Number of variables	301
$R=\Sigma\|\|F_o\|-\|F_c\|\|/\Sigma\|F_o\|$	0,052
$R_w=\Sigma w^{\frac{1}{2}}\|\|F_o\|-\|F_c\|\|/\Sigma w^{\frac{1}{2}}\|F_o\|$	0,054
Weighting scheme w	$(\sigma^2 F)^{-1}$
U_{iso} (aromatic H's)	0,083(4)Å^2

an analysis of variance was calculated and is given in Table 2.2. Final fractional atomic coordinates and their corresponding thermal motion parameters are listed in Tables 2.3 and 2.4 respectively. Observed and calculated structure factors are given on Microfilm in Appendix 2.

TABLE 2.2 Analysis of Variance for Compound (5)

a) By parity groups

Group	*ggg*	*ugg*	*gug*	*uug*	*ggu*	*ugu*	*guu*	*uuu*	All
N	383	310	339	351	308	373	338	341	2743
V	77	79	74	74	65	85	66	76	75

b) As a function of sinθ

sinθ	0,00 - 0,40	0,50 - 0,57	0,63 - 0,68	0,72 - 0,76	0,80 - 0,84	0,87
N	292	276	272	273	293	252	280	292	299	214
V	122	96	76	77	56	60	54	60	57	56

c) As a function of $\sqrt{(F/F_{max})}$

$\sqrt{(F/F_{max})}$	0,00 - 0,12	0,15 - 0,17	0,20 - 0,22	0,25 - 0,28	0,33 - 0,40	1,00
N	291	331	237	334	226	304	226	272	281	241
V	44	57	65	76	86	83	76	78	79	100

d) As a function of |Miller index|

$\|h\|$	0	1	2	3	4	5	6	7	8	9	10	11	12	13	REST
N	253	497	485	438	383	317	229	123	18	0	0	0	0	0	0
V	80	82	74	81	64	72	65	76	52	0	0	0	0	0	0

$\|k\|$	0	1	2	3	4	5	6	7	8	9	10	11	12	13	REST
N	148	289	293	278	261	251	245	214	193	172	144	119	81	46	9
V	119	95	88	65	77	82	64	64	53	52	50	49	69	48	26

$\|l\|$	0	1	2	3	4	5	6	7	8	9	10	11	12	13	REST
N	86	163	173	165	161	162	162	161	147	145	139	134	127	117	701
V	95	83	84	87	96	74	83	78	86	72	59	86	64	78	54

N = Number of reflections in the group; $V = 100[M\Sigma(w|F_o-F_c|^2)/N\Sigma w]^{\frac{1}{2}}$; M = Total number of reflections.

TABLE 2.3 Fractional Atomic Coordinates ($x10^4$) with estimated standard deviations in parentheses for Compound (5)

Atom	*x/a*	*y/b*	*z/c*
P(1)	843(1)	3145(1)	7887(1)
O(1)	690(3)	2524(1)	7281(1)
O(2)	1796(2)	4148(1)	7916(1)
O(3)	1619(3)	2289(2)	8358(1)
O(4)	-1239(3)	3192(2)	7998(1)
C(11)	208(4)	3023(2)	6715(1)
C(12)	1502(4)	3612(2)	6482(1)
C(13)	1041(5)	4046(2)	5904(1)
C(14)	-653(5)	3871(2)	5587(1)
C(15)	-2012(4)	3264(2)	5826(1)
C(16)	-3763(5)	3046(3)	5503(2)
C(17)	-5019(5)	2448(3)	5743(2)
C(18)	-4584(5)	2025(3)	6326(2)
C(19)	-2929(4)	2202(2)	6655(1)
C(20)	-1562(4)	2825(2)	6412(1)
C(31)	3446(4)	1894(2)	8425(1)
C(32)	4014(4)	1262(2)	7984(1)
C(33)	5788(4)	844(2)	8073(1)
C(34)	6898(4)	1054(2)	8601(1)
C(35)	6318(4)	1673(2)	9049(1)
C(36)	4567(5)	2103(2)	8952(1)
N(34)	8775(4)	585(2)	8698(1)
O(341)	9290(3)	91(2)	8287(1)
O(342)	9716(3)	715(2)	9183(1)

TABLE 2.3 Cont/....

TABLE 2.3 Continued

Atom	*x/a*	*y/b*	*z/c*
C(41)	-1947(4)	3871(2)	8406(1)
C(42)	-3615(4)	4328(2)	8202(1)
C(43)	-4435(4)	4966(2)	8591(1)
C(44)	-3555(4)	5123(2)	9154(1)
C(45)	-1909(5)	4644(3)	9362(1)
C(46)	-1078(4)	4000(3)	8979(1)
N(44)	-4372(5)	5837(2)	9566(2)
O(441)	-3499(5)	6014(2)	10057(1)
O(442)	-5883(4)	6209(2)	9391(1)
H(12)	2751(4)	3735(2)	6716(1)
H(13)	1968(5)	4487(2)	5725(1)
H(14)	-945(5)	4178(2)	5174(1)
H(16)	-4085(5)	3339(3)	5088(2)
H(17)	-6257(5)	2308(3)	5506(2)
H(18)	-5524(5)	1584(3)	6499(2)
H(19)	-2653(4)	1899(2)	7069(1)
H(32)	3161(4)	1106(2)	7607(1)
H(33)	6249(4)	399(2)	7756(1)
H(35)	7149(4)	1803(2)	9434(1)
H(36)	4117(5)	2564(2)	9264(1)
H(42)	-4226(4)	4203(2)	7781(1)
H(43)	-5661(4)	5306(2)	8459(1)
H(45)	-1318(5)	4758(3)	9786(1)
H(46)	125(4)	3641(3)	9117(1)

Hydrogen atoms were subjected to constrained refinement.

TABLE 2.4 Anisotropic Thermal Motion Parameters ($Å^2 \times 10^3$) of the Non-Hydrogen Atoms with estimated standard deviations in parentheses for Compound (5)

Atom	U_{11}	U_{22}	U_{33}	U_{12}	U_{13}	U_{23}
P(1)	49(0)	52(0)	59(4)	-1(0)	12(0)	-1(0)
O(1)	66(1)	53(1)	56(1)	5(1)	1(3)	8(2)
O(2)	59(1)	56(1)	75(1)	-11(1)	3(1)	2(1)
O(3)	72(1)	63(1)	62(1)	7(1)	21(1)	10(1)
O(4)	53(1)	76(1)	83(1)	-8(1)	18(1)	-27(1)
C(11)	59(2)	48(2)	53(2)	8(1)	17(1)	-5(1)
C(12)	64(2)	59(2)	69(2)	-2(1)	25(1)	-8(1)
C(13)	87(2)	61(2)	70(2)	-3(2)	35(2)	-2(2)
C(14)	96(2)	63(2)	60(2)	13(2)	26(2)	3(2)
C(15)	68(2)	61(2)	63(2)	14(1)	16(1)	-7(1)
C(16)	82(2)	91(3)	73(2)	21(2)	2(2)	-5(2)
C(17)	59(2)	108(3)	104(3)	10(2)	1(2)	-24(3)
C(18)	60(2)	86(2)	101(3)	-7(2)	27(2)	-19(2)
C(19)	62(2)	62(2)	76(2)	0(1)	22(2)	-10(2)
C(20)	54(2)	49(2)	61(2)	10(1)	19(1)	-8(1)
C(31)	71(2)	46(1)	52(2)	3(1)	15(1)	7(1)
C(32)	72(2)	59(2)	49(2)	2(1)	5(1)	-3(1)
C(33)	71(2)	53(2)	52(2)	1(1)	12(1)	-3(1)
C(34)	66(2)	46(2)	57(2)	-4(1)	8(1)	6(1)
C(35)	83(2)	54(2)	51(2)	-4(2)	2(1)	0(1)
C(36)	93(2)	49(2)	49(2)	3(2)	15(2)	-2(1)
N(34)	70(2)	63(2)	77(2)	8(1)	7(2)	-3(1)
O(341)	85(2)	100(2)	103(2)	15(1)	19(1)	-21(2)
O(342)	83(2)	114(2)	84(2)	6(1)	-15(1)	0(2)

TABLE 2.4 Cont/....

TABLE 2.4 Continued

Atom	U_{11}	U_{22}	U_{33}	U_{12}	U_{13}	U_{23}
C(41)	47(2)	60(2)	61(2)	-5(1)	14(1)	-8(1)
C(42)	51(2)	69(2)	61(2)	-5(1)	4(1)	4(2)
C(43)	49(2)	58(2)	82(2)	3(1)	17(2)	10(2)
C(44)	59(2)	54(2)	69(2)	-1(1)	27(1)	3(1)
C(45)	79(2)	87(2)	59(2)	5(2)	7(2)	-14(2)
C(46)	50(2)	94(2)	70(2)	15(2)	-1(1)	-14(2)
N(44)	107(2)	52(2)	99(2)	0(2)	54(2)	5(2)
O(441)	164(3)	79(2)	93(2)	-1(2)	58(2)	-21(2)
O(442)	116(2)	80(2)	165(3)	31(2)	78(2)	14(2)

All anisotropic thermal motion parameters are of the form:

$$T = \exp[-2\pi^2(U_{11}h^2a^{*2} + U_{22}k^2b^{*2} + U_{33}l^2c^{*2} + 2U_{12}hka^*b^* + 2U_{13}hla^*c^* + 2U_{23}klb^*c^*)]$$

2.2.2 EXPERIMENTAL, SOLUTION AND REFINEMENT OF (4)

Experimental

The preparation of bis(4-nitrophenyl)-8-quinolinyl phosphate proceeded via the following reaction:

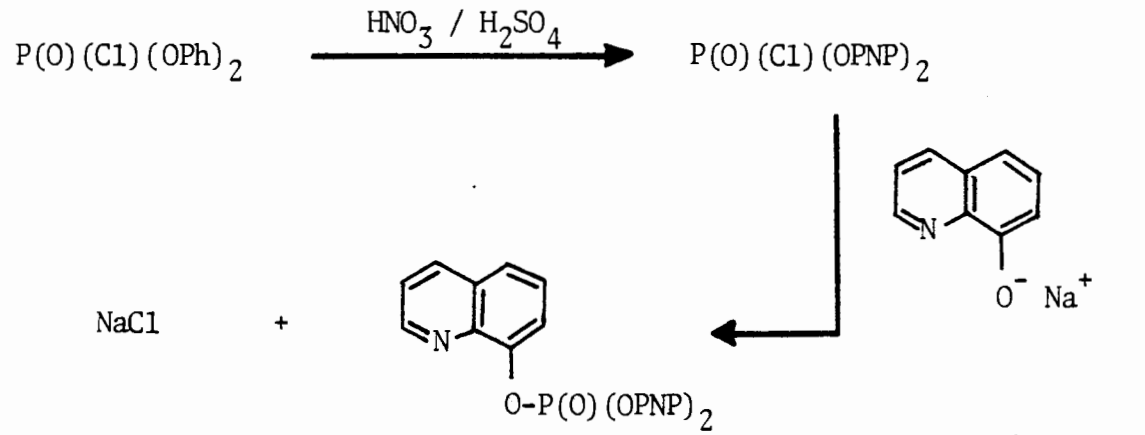

To a stirred solution of bis(4-nitrophenyl)phosphorochloridate (0,005mol) (prepared by nitration of diphenylphosphorochloridate[25]; yield 72%; m.p. 93-95°C) in dry ether (10ml), the dry sodium salt of 8-hydroxyquinoline (0,005mol) was slowly added. The mixture was then refluxed for 2 hours, cooled, the precipitate filtered off and washed with a small volume of water. After drying the crude product was recrystallised from benzene. Yield 64%. m.p. 159-162°C. Anal. Calculated for $C_{21}H_{14}N_3O_8P$: C = 53,97%, H = 3,02%, N = 8,99%. Found: C = 53,90%, H = 3,05%, N = 8,80%. ^1H NMR ($CDCl_3$): δ7,3-7,8 (8H's) hydrogens ortho to the "alcohol" oxygens of the 4-nitrophenyl groups and four aryl hydrogens of the quinolinyl moiety; δ8,2 (1H) aryl hydrogen of the quinolinyl group; δ8,3-8,4 (4H's) hydrogens meta to the "alcohol" oxygens of the 4-nitrophenyl groups; δ8,7 (1H) hydrogen adjacent to the tertiary nitrogen in the quinolinyl group.

Small, white, rectangular single crystals were obtained from a petroleum ether

(80-100°C)-chloroform mixture by slow evaporation. The crystal density was determined by flotation in a mixture of saturated potassium iodide and water.

Preliminary photography revealed the triclinic system [23]. Accurate cell parameters were obtained from a least-squares analysis of the setting angles of 25 reflections in the range $19^{\circ} \leq \theta \leq 23^{\circ}$ automatically located and centred on an Enraf-Nonius CAD4 diffractometer with graphite monochromated MoK_{α} radiation (λ = 0,7107Å). The intensities were collected at room temperature with an ω-2θ scan, $\Delta\omega = (0{,}64 + 0{,}35\tan\theta)^{\circ}$, and aperture of vertical length 4mm and (1,22 + 1,05tanθ)mm wide, to a final acceptance limit of 20σ at $0{,}3^{\circ}s^{-1}$ in ω and a maximum recording time of 40s. The data were corrected for Lorentz-polarisation but not for absorption as the absorption correction factor A* remained equal to 1,0 (μR max. = 0,03, μR min. = 0,01) over the entire range of θ values scanned by the diffractometer.

Solution and Refinement

Crystal data, experimental details of the intensity data collection and refinement parameters are listed in Table 2.5.

The structure was solved by the centrosymmetric direct methods routine of the SHELX-76 [24] program system. An *E*-map yielded the positions of all, except one, (O(442)) non-hydrogen atoms. After further cycles of least-squares refinement the remaining non-hydrogen atom and virtually all the hydrogen atoms were revealed with *R* equal to 0,13. Anisotropic treatment of all the non-hydrogen atoms reduced *R* to 0,07. Further refinement with the aromatic hydrogen atoms constrained 1,00Å from their parent carbon atoms, their positions dictated by the molecular geometry lowered the discrepancy index value, *R*, to 0,05. In the final cycle of refinement, the shift to error ratio of all parameters was always less than 0,03. A final difference electron-density map calculated

TABLE 2.5 Crystal Data and Experimental and Refinement Parameters for Compound (4)

Crystal Data	
Molecular formula	$C_{21}H_{14}N_3O_8P$
Molecular weight	467,34gmol^{-1}
Space group	$P\bar{1}$
a	9,452(3)Å
b	8,751(2)Å
c	13,000(3)Å
α	100,59(2)°
β	107,35(2)°
γ	85,21(2)°
V	1008,43Å^3
Z	2
D_m	1,52gcm^{-3}
D_c	1,54gcm^{-3}
$\mu(MoK_\alpha)$	1,46cm^{-1}
$F(000)$	480
Data Collection	
Crystal dimensions	0,22 x 0,19 x 0,06mm
Scan mode	ω-2θ
Scan width ($\Delta\omega$)	(0,64 + 0,35tanθ)°
Aperture width (Horizontal)	(1,22 + 1,05tanθ)mm
Aperture width (Vertical)	4mm
Range scanned	$1° \leq \theta \leq 25°$
Stability of standard reflections	1,46%
Number of reflections collected	3713
Number of "observed" reflections	1869 with $I_{rel} > 2\sigma I_{rel}$
Final Refinement	
Number of variables	301
$R=\Sigma\|\|F_o\|-\|F_c\|\|/\Sigma\|F_o\|$	0,047
$R_w=\Sigma w^{\frac{1}{2}}\|\|F_o\|-\|F_c\|\|/\Sigma w^{\frac{1}{2}}\|F_o\|$	0,045
Weighting scheme w	$(\sigma^2 F)^{-1}$
U_{iso} (aromatic H's)	0,083(6)Å^2

after the final refinement revealed no peaks of height > 0,3e$\mathring{A}^{-3}$. After the final cycle of refinement an analysis of variance was calculated (Table 2.6) and indicated a satisfactory weighting scheme. Final atomic coordinates and their thermal motion parameters are listed in Tables 2.7 and 2.8 respectively. Observed and calculated structure factors are presented on Microfilm in Appendix 2.

TABLE 2.6 Analysis of Variance for Compound (4)

a) By parity groups

Group	*ggg*	*ugg*	*gug*	*uug*	*ggu*	*ugu*	*guu*	*uuu*	All
N	240	244	239	223	236	243	218	226	1869
V	75	74	71	82	78	81	65	67	75

b) As a function of sinθ

sinθ	0,00 - 0,17	0,21 - 0,25	0,28 - 0,30	0,32 - 0,34	0,36 - 0,39	0,43
N	201	177	238	220	166	168	183	154	208	154
V	128	92	74	54	65	64	56	57	58	57

c) As a function of $\sqrt{(F/F_{max})}$

$\sqrt{(F/F_{max})}$	0,00 - 0,18	0,20 - 0,21	0,23 - 0,25	0,27 - 0,30	0,34 - 0,40	1,00
N	261	214	107	205	188	169	204	170	167	184
V	62	60	65	61	83	73	78	71	76	107

d) As a function of |Miller index|

$\|h\|$	0	1	2	3	4	5	6	7	8	9	10	11	12	13	REST
N	139	282	272	257	242	211	165	133	93	51	22	2	0	0	0
V	76	88	81	81	69	65	68	65	59	48	73	41	0	0	0

$\|k\|$	0	1	2	3	4	5	6	7	8	9	10	11	12	13	REST
N	168	320	306	269	251	191	162	101	69	25	7	0	0	0	0
V	85	84	92	70	68	55	57	63	56	56	53	0	0	0	0

$\|l\|$	0	1	2	3	4	5	6	7	8	9	10	11	12	13	REST
N	108	191	200	198	183	169	153	136	137	131	85	63	60	33	22
V	107	96	84	71	71	74	76	67	58	54	50	53	54	56	70

N = Number of reflections in the group; $V = 100[M\Sigma(w|F_o-F_c|^2)/N\Sigma w]^{\frac{1}{2}}$; M = Total number of reflections.

TABLE 2.7 Fractional Atomic Coordinates ($x10^4$) with estimated standard deviations in parentheses for Compound (4)

Atom	*x/a*	*y/b*	*z/c*
P(1)	2680(1)	-678(1)	7179(1)
O(1)	3181(3)	-1946(3)	7938(2)
O(2)	1119(3)	-613(3)	6588(2)
O(3)	3315(3)	816(3)	8040(2)
O(4)	3834(3)	-726(3)	6528(2)
C(11)	2365(5)	-3269(5)	7854(3)
C(12)	1979(5)	-3498(6)	8729(4)
C(13)	1219(6)	-4824(7)	8667(4)
C(14)	855(5)	-5898(6)	7722(4)
C(15)	1285(5)	-5686(5)	6815(4)
C(16)	981(5)	-6721(5)	5813(4)
C(17)	1437(5)	-6394(5)	4984(4)
C(18)	2185(5)	-5042(5)	5129(3)
N(19)	2512(4)	-4019(4)	6040(3)
C(20)	2057(4)	-4335(5)	6879(3)
C(31)	3006(5)	1301(5)	9030(3)
C(32)	3935(5)	2363(5)	9752(3)
C(33)	3705(5)	2919(5)	10755(3)
C(34)	2551(5)	2364(5)	10996(3)
C(35)	1606(6)	1331(6)	10265(4)
C(36)	1806(5)	801(6)	9253(4)
N(34)	2347(5)	2883(5)	12083(3)
O(341)	3029(4)	3989(5)	12658(3)
O(342)	1494(5)	2193(5)	12349(3)

TABLE 2.7 Cont/....

TABLE 2.7 Continued

Atom	*x/a*	*y/b*	*z/c*
C(41)	3589(5)	-1172(5)	5395(3)
C(42)	2399(5)	-612(5)	4667(4)
C(43)	2242(5)	-1029(5)	3563(4)
C(44)	3317(5)	-1997(5)	3247(3)
C(45)	4504(5)	-2562(6)	3972(4)
C(46)	4655(5)	-2138(5)	5074(3)
N(44)	3156(6)	-2459(5)	2074(3)
O(441)	1991(6)	-2079(6)	1430(3)
O(442)	4128(4)	-3239(5)	1785(3)
H(12)	2241(5)	-2727(6)	9422(4)
H(13)	929(6)	-4990(7)	9317(4)
H(14)	279(5)	-6827(6)	7680(4)
H(16)	432(5)	-7691(5)	5714(4)
H(17)	1238(5)	-7128(5)	4273(4)
H(18)	2502(5)	-4831(5)	4502(3)
H(32)	4778(5)	2737(5)	9557(3)
H(33)	4369(5)	3713(5)	11295(3)
H(35)	765(6)	958(6)	10462(4)
H(36)	1101(5)	63(6)	8693(4)
H(42)	1643(5)	95(5)	4927(4)
H(43)	1373(5)	-643(5)	3006(4)
H(45)	5264(5)	-3261(6)	3712(4)
H(46)	5522(5)	-2526(5)	5630(3)

Hydrogen atoms were subjected to constrained refinement.

TABLE 2.8 Anisotropic Thermal Motion Parameters ($Å^2 \times 10^3$) of the Non-Hydrogen Atoms with estimated standard deviations in parentheses for Compound (4)

Atom	U_{11}	U_{22}	U_{33}	U_{12}	U_{13}	U_{23}
P(1)	56(1)	52(1)	35(1)	-7(1)	16(1)	-3(1)
O(1)	65(2)	62(2)	39(2)	-2(2)	6(2)	3(2)
O(2)	52(2)	57(2)	45(2)	2(1)	16(1)	6(1)
O(3)	82(2)	75(2)	43(2)	-29(2)	33(2)	-16(2)
O(4)	55(2)	84(2)	35(2)	-16(2)	17(1)	-13(2)
C(11)	59(3)	51(3)	45(3)	6(2)	12(2)	7(2)
C(12)	77(4)	74(4)	41(3)	5(3)	13(3)	12(3)
C(13)	93(4)	96(4)	55(3)	18(4)	35(3)	34(3)
C(14)	82(4)	67(4)	75(4)	5(3)	35(3)	25(3)
C(15)	54(3)	50(3)	56(3)	12(2)	19(2)	11(2)
C(16)	65(3)	40(3)	75(3)	3(2)	26(3)	5(3)
C(17)	67(3)	54(3)	61(3)	11(3)	20(3)	-6(3)
C(18)	58(3)	63(3)	47(3)	9(3)	21(2)	4(3)
N(19)	55(2)	55(2)	49(2)	2(2)	19(2)	5(2)
C(20)	50(3)	44(3)	41(3)	13(2)	9(2)	6(2)
C(31)	62(3)	60(3)	35(2)	-9(2)	21(2)	-6(2)
C(32)	54(3)	73(3)	49(3)	-13(3)	18(2)	-13(3)
C(33)	55(3)	72(3)	41(3)	0(3)	11(2)	-8(2)
C(34)	61(3)	64(3)	32(2)	2(3)	15(2)	-2(2)
C(35)	95(4)	80(4)	57(3)	-27(3)	46(3)	-9(3)
C(36)	81(4)	81(4)	49(3)	-33(3)	30(3)	-14(3)
N(34)	87(3)	78(3)	42(3)	5(3)	27(2)	2(2)
O(341)	130(3)	115(3)	54(2)	-32(3)	40(2)	-30(3)
O(342)	153(4)	103(3)	66(3)	-15(3)	67(3)	4(2)

TABLE 2.8 Cont/....

TABLE 2.8 Continued

Atom	U_{11}	U_{22}	U_{33}	U_{12}	U_{13}	U_{23}
C(41)	51(3)	57(3)	38(2)	-10(2)	21(2)	-7(2)
C(42)	64(3)	51(3)	52(3)	10(2)	25(3)	2(2)
C(43)	77(3)	58(3)	45(3)	10(3)	22(3)	10(2)
C(44)	67(3)	60(3)	36(3)	-12(3)	23(2)	-2(2)
C(45)	53(3)	81(4)	51(3)	4(3)	28(3)	-1(3)
C(46)	45(3)	84(4)	46(3)	1(3)	15(2)	-2(3)
N(44)	100(4)	92(3)	41(3)	-7(3)	30(3)	2(3)
O(441)	157(4)	195(5)	39(2)	38(4)	25(3)	12(3)
O(442)	119(3)	115(3)	65(2)	-8(3)	60(2)	-15(2)

The anisotropic thermal parameters of the nitro groups of structure (4) are indeed somewhat higher than those of the other atoms. This may be attributed to enhanced thermal motion of these atoms, which is plausible seeing that they are positioned at the extremities of the molecule. However they could also be a result of relatively poor reflection data. In fact this compound yielded the lowest quality crystal of the series, exhibiting broadened peak profiles. It is well known that in the refinement process the thermal parameters act as a buffer and may yield unrealistic values. Therefore the high U values may also represent partial static disorder of the structure.

2.2.3 EXPERIMENTAL, SOLUTION AND REFINEMENT OF (6)

Experimental

4-Nitrophenyl-8-quinolinyl phosphate was prepared via the method of Loran and Williams[15] as follows:

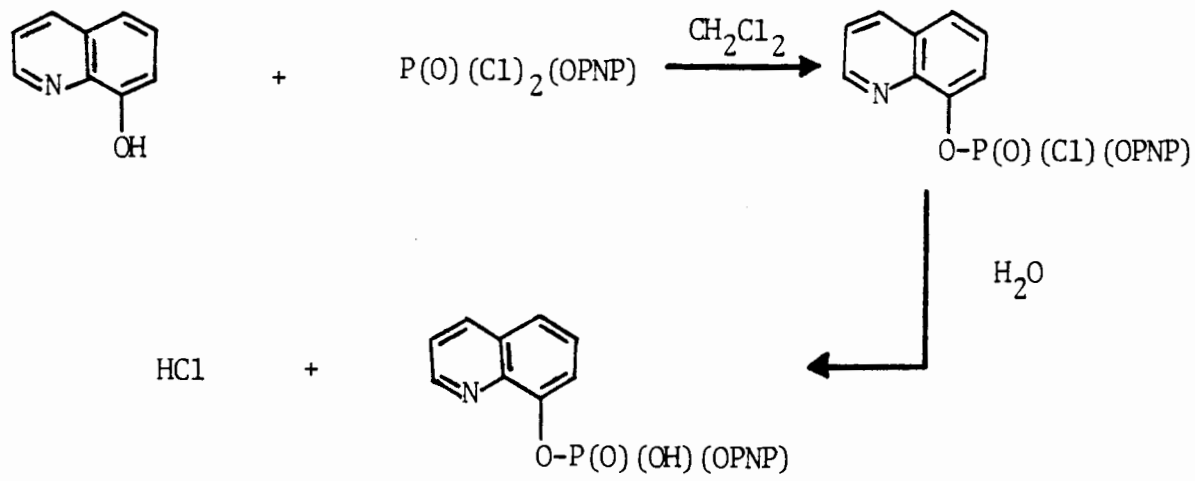

To a solution of 4-nitrophenylphosphorodichloridate (0,02mol) in dry dichloro=methane (12ml), a solution of 8-hydroxyquinoline (0,02mol) in dry dichloro=methane (16ml) was added with stirring. A yellow precipitate slowly appeared and after 1 hour, water (6ml) was slowly added and the stirring continued for 2 hours. The precipitate dissolved and a further precipitate appeared and was filtered off and dried. This highly insoluble product (Yield 79%) was recrystallised from a large volume of n-butanol and isolated as a monohydrate. m.p. 195-200°C. Anal. Calculated for $C_{15}H_{11}N_2O_6P.H_2O$: C = 49,46%, H = 3,60%, N = 7,69%. Found: C = 49,35%, H = 3,60%, N = 7,80%.

Crystals suitable for X-ray analysis were obtained from a petroleum ether (80-100°C)-chloroform mixture in the anhydrous form.

The crystal density was determined by flotation in a saturated ferric sulphate-

water solution.

Accurate cell parameters obtained from a least-squares analysis of 22 stan= dard reflections in the range $16^{o} \leq \theta \leq 17^{o}$ measured on the Enraf-Nonius CAD4 diffractometer indicated a triclinic space group. The intensities were col= lected with the ω-2θ scan mode to a final acceptance limit of 20σ at $0{,}3^{o}s^{-1}$ in ω and a maximum recording time of 40s. A Lorentz-polarisation factor was applied to the data. An absorption correction was not deemed necessary as A^{*} equalled 1,0 (μR max. = 0,05, μR min. = 0,01) over the range of θ scanned.

Solution and Refinement

All details pertaining to experimental and refinement data are listed in Table 2.9.

The structure was solved in the $P\bar{1}^{23}$ space group by a preliminary direct methods routine of the new SHELXS-84[26] program system. All the non-hydrogen atoms appeared in the *E*-map. After a few cycles of least-squares refinement in which eighteen selected non-hydrogen atoms were treated anisotropically, the *R* value was 0,07. Subsequent refinement with the aromatic hydrogen atoms fixed by molecular geometrical requirements reduced *R* to 0,06. Careful analysis of difference electron-density maps showed the quinolinyl nitrogen (N(19)) to be protonated, thus producing a zwitterionic species with electron delocalisation on the two phosphoryl oxygens. In the final refinement H(19) was given a bond length constraint of N(19)-H(19) = 1,063Å. This value was chosen as representing the typical hydrogen bonding geometry as extrapolated from a graph depicting N-H versus N...O distances for a vast number of structures[27]. In the final cycle of refinement, the shift to error ratio of all parameters was always less than 0,02. A final difference electron-density map calculated after the final cycle of least-squares refinement revealed no

TABLE 2.9 Crystal Data and Experimental and Refinement Parameters for Compound (6)

Crystal Data	
Molecular formula	$C_{15}H_{11}N_2O_6P$
Molecular weight	346,24gmol^{-1}
Space group	$P\bar{1}$
a	7,106(7)Å
b	9,559(4)Å
c	10,521(4)Å
α	84,32(3)°
β	82,89(10)°
γ	78,60(7)°
V	693,12Å^3
Z	2
D_m	1,65gcm^{-3}
D_c	1,66gcm^{-3}
$\mu(MoK_\alpha)$	1,84cm^{-1}
$F(000)$	356
Data Collection	
Crystal dimensions	0,28 x 0,12 x 0,06mm
Scan mode	ω-2θ
Scan width ($\Delta\omega$)	(0,75 + 0,35tanθ)°
Aperture width (Horizontal)	(1,29 + 1,05tanθ)mm
Aperture width (Vertical)	4mm
Range scanned	$1° \leq \theta \leq 25°$
Stability of standard reflections	1,55%
Number of reflections collected	2595
Number of "observed" reflections	1212 with $I_{rel} > 2\sigma I_{rel}$
Final Refinement	
Number of variables	192
$R=\Sigma\|\|F_o\|-\|F_c\|\|/\Sigma\|F_o\|$	0,056
$R_w=\Sigma w^{\frac{1}{2}}\|\|F_o\|-\|F_c\|\|/\Sigma w^{\frac{1}{2}}\|F_o\|$	0,051
Weighting scheme w	$(\sigma^2 F)^{-1}$
U_{iso} (aromatic H's)	0,057(6)Å^2
U_{iso} (H(19))	0,081(26)Å^2

peaks of height > $0,4e\text{Å}^{-3}$. An analysis of variance (Table 2.10) computed after the final least-squares cycle showed the weighting scheme to be satis= factory. The refined fractional atomic coordinates and their thermal motion parameters are listed in Tables 2.11 and 2.12. Observed and calculated structure factors are given on Microfilm in Appendix 2.

TABLE 2.10 Analysis of Variance for Compound (6)

a) By parity groups

Group	*ggg*	*ugg*	*gug*	*uug*	*ggu*	*ugu*	*guu*	*uuu*	All
N	146	155	168	157	152	145	151	138	1212
V	119	100	95	92	99	83	96	124	101

b) As a function of sinθ

sinθ	0,00 - 0,17	0,22	0,25	0,28	0,31	0,33	0,35	0,37	0,40	0,43
N	127	149	111	121	144	113	111	115	132	89
V	154	127	100	82	96	96	78	82	75	79

c) As a function of $\sqrt{(F/F_{max})}$

$\sqrt{(F/F_{max})}$	0,00 - 0,21	0,23	0,25	0,27	0,29	0,30	0,33	0,37	0,43	1,00
N	132	124	116	154	135	67	133	122	111	118
V	88	84	68	76	81	98	92	93	110	185

d) As a function of |Miller index|

$\|h\|$	0	1	2	3	4	5	6	7	8	9	10	11	12	13	REST
N	113	240	228	188	169	115	95	52	12	0	0	0	0	0	0
V	80	98	110	108	107	100	102	83	69	0	0	0	0	0	0

$\|k\|$	0	1	2	3	4	5	6	7	8	9	10	11	12	13	REST
N	86	189	173	161	149	132	100	93	67	32	23	7	0	0	0
V	133	123	111	104	93	83	78	81	69	76	102	77	0	0	0

$\|l\|$	0	1	2	3	4	5	6	7	8	9	10	11	12	13	REST
N	99	158	158	151	152	125	114	81	72	52	27	19	4	0	0
V	119	129	123	111	92	78	72	77	91	59	80	65	27	0	0

N = Number of reflections in the group; $V = 100[M\Sigma(w|F_o-F_c|^2)/N\Sigma w]^{\frac{1}{2}}$; M = Total number of reflections.

TABLE 2.11 Fractional Atomic Coordinates ($x10^4$) with estimated standard deviations in parentheses for Compound (6)

Atom	*x/a*	*y/b*	*z/c*
P(1)	2887(2)	5766(2)	1460(2)
O(1)	1796(5)	5859(4)	179(4)
O(2)	3966(5)	4283(4)	1562(4)
O(3)	1058(6)	5961(4)	2566(4)
O(4)	3740(6)	7029(4)	1478(5)
C(11)	544(8)	7106(6)	-211(6)
C(12)	-1362(9)	7288(7)	152(6)
C(13)	-2621(9)	8537(7)	-275(7)
C(14)	-1932(8)	9578(6)	-1074(6)
C(15)	55(8)	9391(6)	-1497(6)
C(16)	879(9)	10408(7)	-2338(6)
C(17)	2819(10)	10156(7)	-2735(6)
C(18)	3954(9)	8880(7)	-2323(6)
N(19)	3218(7)	7922(5)	-1527(5)
C(20)	1294(8)	8122(6)	-1076(6)
C(31)	76(9)	4914(7)	3142(6)
C(32)	1022(10)	3641(7)	3718(7)
C(33)	-22(9)	2664(7)	4370(6)
C(34)	-2027(9)	3009(7)	4440(6)
C(35)	-2963(10)	4274(7)	3862(6)
C(36)	-1925(9)	5232(7)	3228(6)
N(34)	-3146(9)	1991(6)	5138(6)
O(341)	-2308(7)	900(5)	5683(5)
O(342)	-4903(7)	2284(6)	5141(5)

TABLE 2.11 Cont/....

TABLE 2.11 Continued

Atom	*x/a*	*y/b*	*z/c*
H(12)	-1893(9)	6529(7)	727(6)
H(13)	-4034(9)	8659(7)	15(7)
H(14)	-2830(8)	10468(6)	-1355(6)
H(16)	43(9)	11318(7)	-2643(6)
H(17)	3411(10)	10885(7)	-3312(6)
H(18)	5361(9)	8676(7)	-2636(6)
H(19)	4116(82)	6899(34)	-1403(73)
H(32)	2464(10)	3432(7)	3658(7)
H(33)	644(9)	1738(7)	4776(6)
H(35)	-4405(10)	4488(7)	3914(6)
H(36)	-2591(9)	6156(7)	2820(6)

Hydrogen atoms were subjected to constrained refinement.

TABLE 2.12 Anisotropic and Isotropic Thermal Motion Parameters ($Å^2 \times 10^3$) of the Non-Hydrogen Atoms with estimated standard deviations in parentheses for Compound (6)

Atom	U_{11}	U_{22}	U_{33}	U_{12}	U_{13}	U_{23}
P(1)	23(1)	26(1)	38(1)	1(1)	1(1)	4(1)
O(1)	26(2)	25(2)	38(3)	2(2)	-2(2)	2(2)
O(2)	29(2)	29(3)	45(3)	11(2)	5(2)	10(2)
O(3)	34(3)	34(3)	42(3)	-1(2)	14(2)	-1(2)
O(4)	37(3)	32(3)	64(4)	-7(2)	-6(3)	0(3)
C(11)	31(4)	19(3)	33(4)	0(3)	-10(3)	-5(3)
C(12)	29(4)	35(4)	37(4)	-7(3)	-1(3)	2(3)
C(13)	19(3)	39(4)	46(5)	-4(3)	-8(3)	-5(4)
C(14)	22(3)	34(4)	38(4)	4(3)	-9(3)	-1(3)
C(16)	38(4)	31(4)	35(4)	-2(3)	-12(3)	2(3)
C(17)	46(4)	38(4)	29(4)	-6(3)	3(3)	5(3)
C(18)	27(4)	44(4)	32(4)	-5(3)	-1(3)	-6(4)
N(19)	23(3)	25(3)	33(3)	1(2)	-1(3)	-1(3)
C(31)	35(4)	28(3)	24(4)	-2(3)	5(3)	2(3)
C(34)	42(4)	38(4)	27(4)	-11(3)	4(3)	0(3)
N(34)	50(4)	43(4)	37(4)	-8(3)	0(3)	2(3)
O(341)	60(4)	42(3)	62(4)	-13(3)	-4(3)	19(3)
O(342)	34(3)	76(4)	75(4)	-15(3)	0(3)	21(3)

Atom	U_{iso}
C(15)	27(2)
C(20)	26(2)
C(32)	39(2)
C(33)	36(2)
C(35)	38(2)
C(36)	38(2)

2.2.4 DISCUSSION

Perspective views of compounds (4) and (5) with atomic nomenclature are shown in Figures 2.2 and 2.3 respectively. Intramolecular bond lengths and angles are listed in Tables 2.13 and 2.14.

The sp^3 hybridised phosphorus atom, in both substrates (4) and (5) is coordinated to two 4-nitrophenoxy groups, a fused ring moiety (8-hydroxyquinoline and naphthol respectively) and an oxygen atom as the fourth ligand (A).

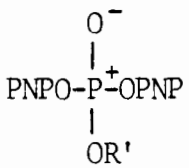

(A)

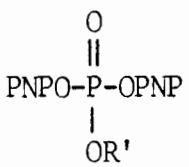

(B)

R' = 8-quinolinyl (4) or naphthyl (5)

The remaining 2p electrons of the oxygen atom interact with the unfilled d_{xy} and d_{yz} orbitals of the phosphorus atom producing the phosphoryl bond, P=O (B)[28].

The phosphorus atom in both triesters has a geometry reasonably close to the regular tetrahedral; the average values of all the O-P-O angles are 108,9° for (4) and 109,1° for (5), but individual angles deviate considerably from the average value (±9,7% for (4) and ±8,2% for (5)). These deviations follow the same pattern observed for other P^{IV} derivatives of the ABCP=Y type, which results in the distortion of the tetrahedral geometry at phosphorus as illustrated in Figure 2.4. The deviations of bond angles from the ideal value of 109,5° result from the greater repulsive effects exerted by the multiple bonding orbitals[29] and can be correlated with the corresponding bond distances

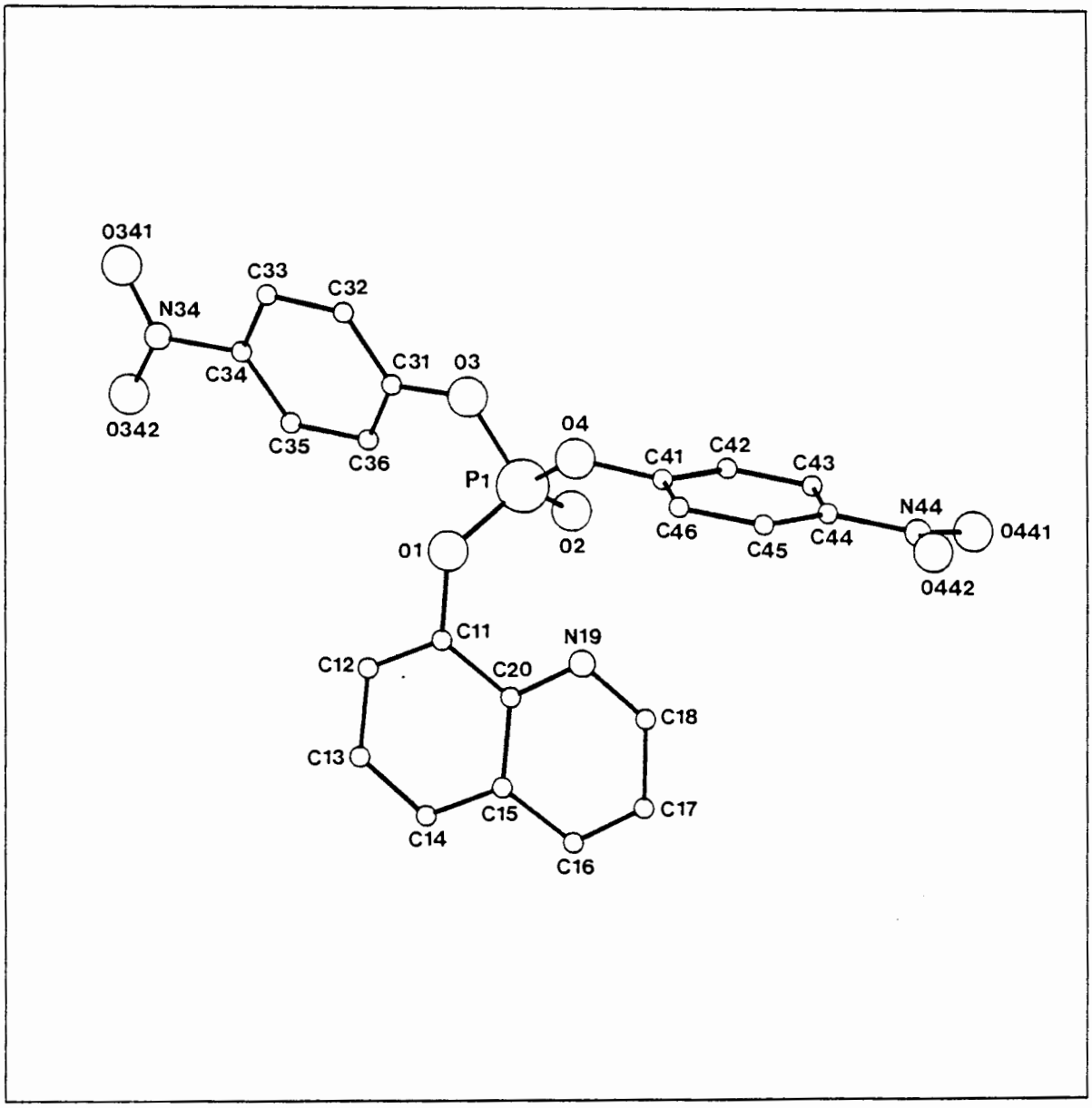

FIGURE 2.2 A perspective view of bis(4-nitrophenyl)-8-quinolinyl phosphate (4).

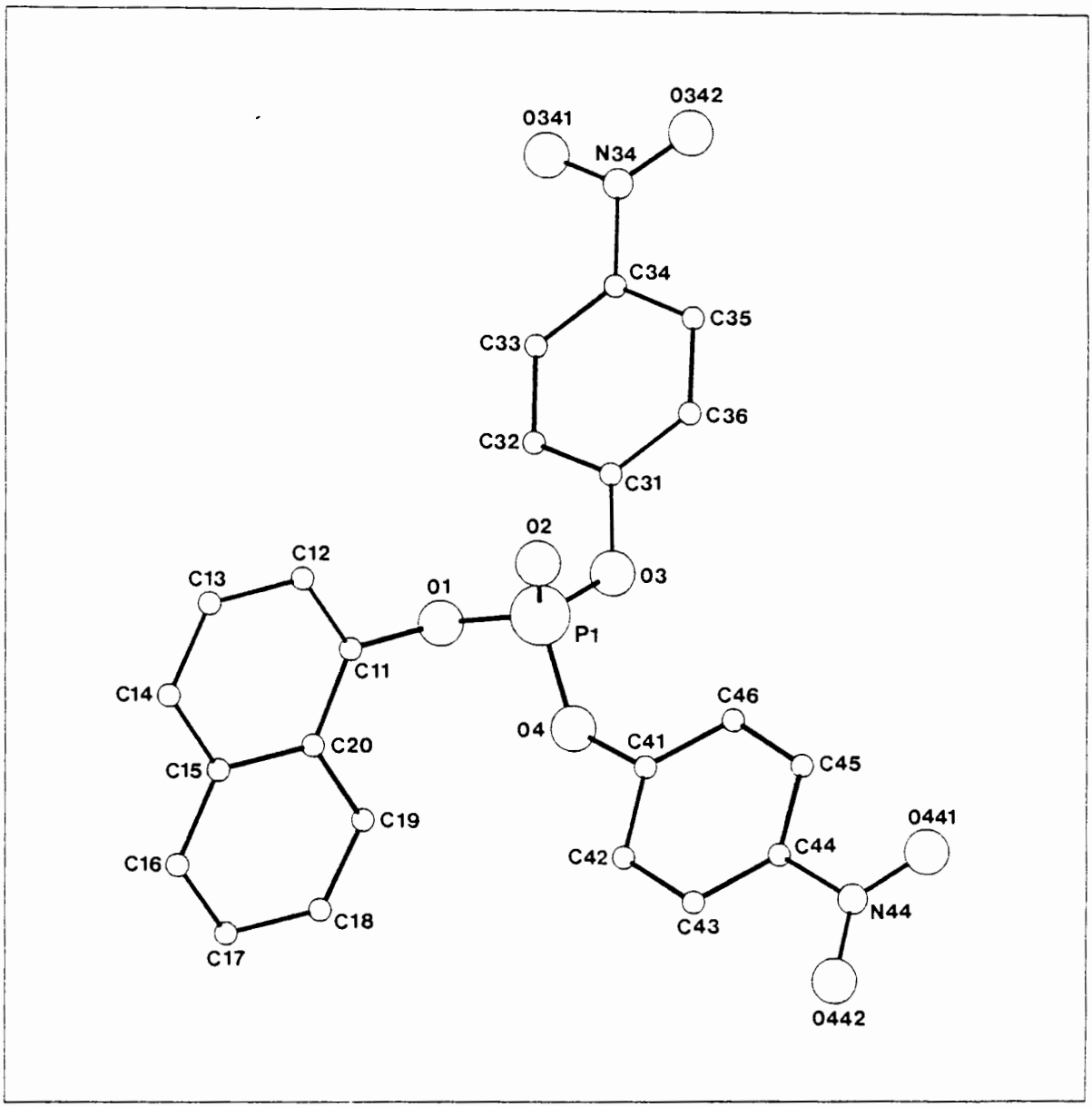

FIGURE 2.3 A perspective view of 1-naphthyl-bis(4-nitrophenyl) phosphate (5).

TABLE 2.13 Bond Lengths (Å) and Angles (°) with estimated standard deviations in parentheses for Compound (4)

Bond Lengths	
P(1) - O(1)	1,571(3)
P(1) - O(2)	1,447(3)
P(1) - O(3)	1,586(3)
P(1) - O(4)	1,560(3)
O(1) - C(11)	1,414(6)
C(11) - C(12)	1,346(7)
C(12) - C(13)	1,392(8)
C(13) - C(14)	1,374(7)
C(14) - C(15)	1,402(8)
C(15) - C(20)	1,418(6)
C(15) - C(16)	1,409(6)
C(16) - C(17)	1,357(8)
C(17) - C(18)	1,383(7)
C(18) - N(19)	1,318(5)
N(19) - C(20)	1,365(6)
C(20) - C(11)	1,397(5)
O(3) - C(31)	1,387(5)
C(31) - C(32)	1,357(5)
C(32) - C(33)	1,379(6)
C(33) - C(34)	1,369(7)
C(34) - C(35)	1,353(6)
C(35) - C(36)	1,375(7)
C(36) - C(31)	1,374(7)
C(34) - N(34)	1,467(6)
N(34) - O(341)	1,209(6)

TABLE 2.13 Cont/....

TABLE 2.13 Continued

N(34) - O(342)	1,209(7)
O(4) - C(41)	1,407(5)
C(41) - C(42)	1,358(6)
C(42) - C(43)	1,381(6)
C(43) - C(44)	1,377(7)
C(44) - C(45)	1,356(6)
C(45) - C(46)	1,379(6)
C(46) - C(41)	1,371(6)
C(44) - N(44)	1,469(6)
N(44) - O(441)	1,208(7)
N(44) - O(442)	1,231(6)

Bond Angles

O(1) - P(1) - O(2)	116,2(2)
O(1) - P(1) - O(3)	99,5(2)
O(1) - P(1) - O(4)	107,6(2)
O(2) - P(1) - O(3)	116,5(2)
O(2) - P(1) - O(4)	118,3(2)
O(3) - P(1) - O(4)	95,3(2)
P(1) - O(1) - C(11)	124,8(2)
O(1) - C(11) - C(12)	119,1(4)
O(1) - C(11) - C(20)	118,4(4)
C(11) - C(12) - C(13)	119,6(4)
C(12) - C(13) - C(14)	120,8(5)
C(13) - C(14) - C(15)	120,0(5)
C(14) - C(15) - C(16)	124,5(4)
C(20) - C(15) - C(16)	116,3(5)
C(15) - C(16) - C(17)	119,6(4)
C(16) - C(17) - C(18)	119,6(4)

TABLE 2.13 Cont/....

TABLE 2.13 Continued

C(17) - C(18) - N(19)	124,4(5)
C(18) - N(19) - C(20)	116,5(4)
N(19) - C(20) - C(15)	123,5(4)
C(15) - C(20) - C(11)	118,1(4)
C(20) - C(11) - C(12)	122,3(4)
P(1) - O(3) - C(31)	125,6(3)
O(3) - C(31) - C(32)	115,3(4)
O(3) - C(31) - C(36)	122,7(3)
C(31) - C(32) - C(33)	119,3(5)
C(32) - C(33) - C(34)	118,7(4)
C(33) - C(34) - C(35)	121,8(4)
C(33) - C(34) - N(34)	119,1(4)
C(34) - C(35) - C(36)	119,8(5)
C(35) - C(36) - C(31)	118,4(4)
C(34) - N(34) - O(341)	118,3(7)
C(34) - N(34) - O(342)	118,2(4)
O(341) - N(34) - O(342)	123,5(4)
P(1) - O(4) - C(41)	127,1(3)
O(4) - C(41) - C(42)	121,4(4)
O(4) - C(41) - C(46)	116,2(3)
C(41) - C(42) - C(43)	119,3(4)
C(42) - C(43) - C(44)	118,0(4)
C(43) - C(44) - C(45)	122,8(4)
C(43) - C(44) - N(44)	118,5(4)
C(44) - C(45) - C(46)	118,8(4)
C(45) - C(46) - C(41)	118,7(4)
C(44) - N(44) - O(441)	117,5(5)
C(44) - N(44) - O(442)	119,3(4)
O(441) - N(44) - O(442)	123,1(4)

TABLE 2.13 Cont/....

TABLE 2.13 Continued

Intramolecular Non-Bonded Distance and Angle

N(19)...P(1)	3,019
N(19)...P(1) - O(3)	158,8

C(14) - C(15) - C(20)	119,2(4)
N(19) - C(20) - C(11)	118,3(4)
C(32) - C(31) - C(36)	121,8(4)
N(34) - C(34) - C(35)	119,1(5)
C(42) - C(41) - C(46)	122,4(4)
N(44) - C(44) - C(45)	118,6(4)

TABLE 2.14 Bond Lengths (Å) and Angles (°) with estimated standard deviations in parentheses for Compound (5)

Bond Lengths	
P(1) - O(1)	1,560(2)
P(1) - O(2)	1,446(2)
P(1) - O(3)	1,568(2)
P(1) - O(4)	1,569(2)
O(1) - C(11)	1,420(3)
C(11) - C(12)	1,360(4)
C(12) - C(13)	1,407(4)
C(13) - C(14)	1,357(5)
C(14) - C(15)	1,414(5)
C(15) - C(20)	1,424(4)
C(15) - C(16)	1,408(4)
C(16) - C(17)	1,354(6)
C(17) - C(18)	1,409(5)
C(18) - C(19)	1,346(4)
C(19) - C(20)	1,433(4)
C(20) - C(11)	1,398(4)
O(3) - C(31)	1,411(3)
C(31) - C(32)	1,377(4)
C(32) - C(33)	1,386(4)
C(33) - C(34)	1,367(4)
C(34) - C(35)	1,384(4)
C(35) - C(36)	1,377(4)
C(36) - C(31)	1,369(4)
C(34) - N(34)	1,480(4)
N(34) - O(341)	1,213(4)

TABLE 2.14 Cont/....

TABLE 2.14 Continued

N(34) - O(342)	1,216(4)
O(4) - C(41)	1,402(4)
C(41) - C(42)	1,369(4)
C(42) - C(43)	1,382(4)
C(43) - C(44)	1,352(4)
C(44) - C(45)	1,370(4)
C(45) - C(46)	1,381(5)
C(46) - C(41)	1,364(4)
C(44) - N(44)	1,474(5)
N(44) - O(441)	1,215(4)
N(44) - O(442)	1,214(5)

Bond Angles

O(1) - P(1) - O(2)	117,5(1)
O(1) - P(1) - O(3)	102,4(1)
O(1) - P(1) - O(4)	101,4(1)
O(2) - P(1) - O(3)	116,8(1)
O(2) - P(1) - O(4)	115,3(1)
O(3) - P(1) - O(4)	100,9(1)
P(1) - O(1) - C(11)	122,2(2)
O(1) - C(11) - C(12)	119,1(2)
O(1) - C(11) - C(20)	117,1(2)
C(11) - C(12) - C(13)	118,4(3)
C(12) - C(13) - C(14)	120,4(3)
C(13) - C(14) - C(15)	121,6(3)
C(14) - C(15) - C(16)	122,9(3)
C(14) - C(15) - C(20)	118,4(3)
C(20) - C(15) - C(16)	118,7(3)
C(15) - C(16) - C(17)	121,3(3)

TABLE 2.14 Cont/....

TABLE 2.14 Continued

C(16) - C(17) - C(18)	120,1(3)
C(17) - C(18) - C(19)	121,3(3)
C(18) - C(19) - C(20)	120,1(3)
C(19) - C(20) - C(15)	118,6(2)
C(15) - C(20) - C(11)	117,5(2)
C(20) - C(11) - C(12)	123,7(2)
P(1) - O(3) - C(31)	124,7(2)
O(3) - C(31) - C(32)	120,0(2)
O(3) - C(31) - C(36)	118,0(2)
C(36) - C(31) - C(32)	121,9(3)
C(31) - C(32) - C(33)	118,9(2)
C(32) - C(33) - C(34)	118,9(3)
C(33) - C(34) - C(35)	122,4(3)
C(33) - C(34) - N(34)	118,6(3)
C(34) - C(35) - C(36)	118,3(2)
C(35) - C(36) - C(31)	119,6(3)
C(34) - N(34) - O(341)	117,9(2)
C(34) - N(34) - O(342)	118,5(3)
O(341) - N(34) - O(342)	123,6(3)
P(1) - O(4) - C(41)	124,9(2)
O(4) - C(41) - C(42)	115,4(2)
O(4) - C(41) - C(46)	121,5(2)
C(42) - C(41) - C(46)	122,9(3)
C(41) - C(42) - C(43)	118,5(3)
C(42) - C(43) - C(44)	118,9(3)
C(43) - C(44) - C(45)	122,5(3)
C(43) - C(44) - N(44)	119,6(3)
C(44) - C(45) - C(46)	119,1(3)
C(45) - C(46) - C(41)	118,0(3)

TABLE 2.14 Cont/....

TABLE 2.14 Continued

C(44) - N(44) - O(441)	118,3(3)
C(44) - N(44) - O(442)	117,4(3)
O(441) - N(44) - O(442)	124,3(4)

Intramolecular Non-Bonded Distance and Angle

C(19)...P(1)	3,790
C(19)...P(1) - O(3)	127,3

C(19) - C(20) - C(11)	123,9(2)
N(34) - C(34) - C(35)	119,0(2)
N(44) - C(44) - C(45)	117,9(3)

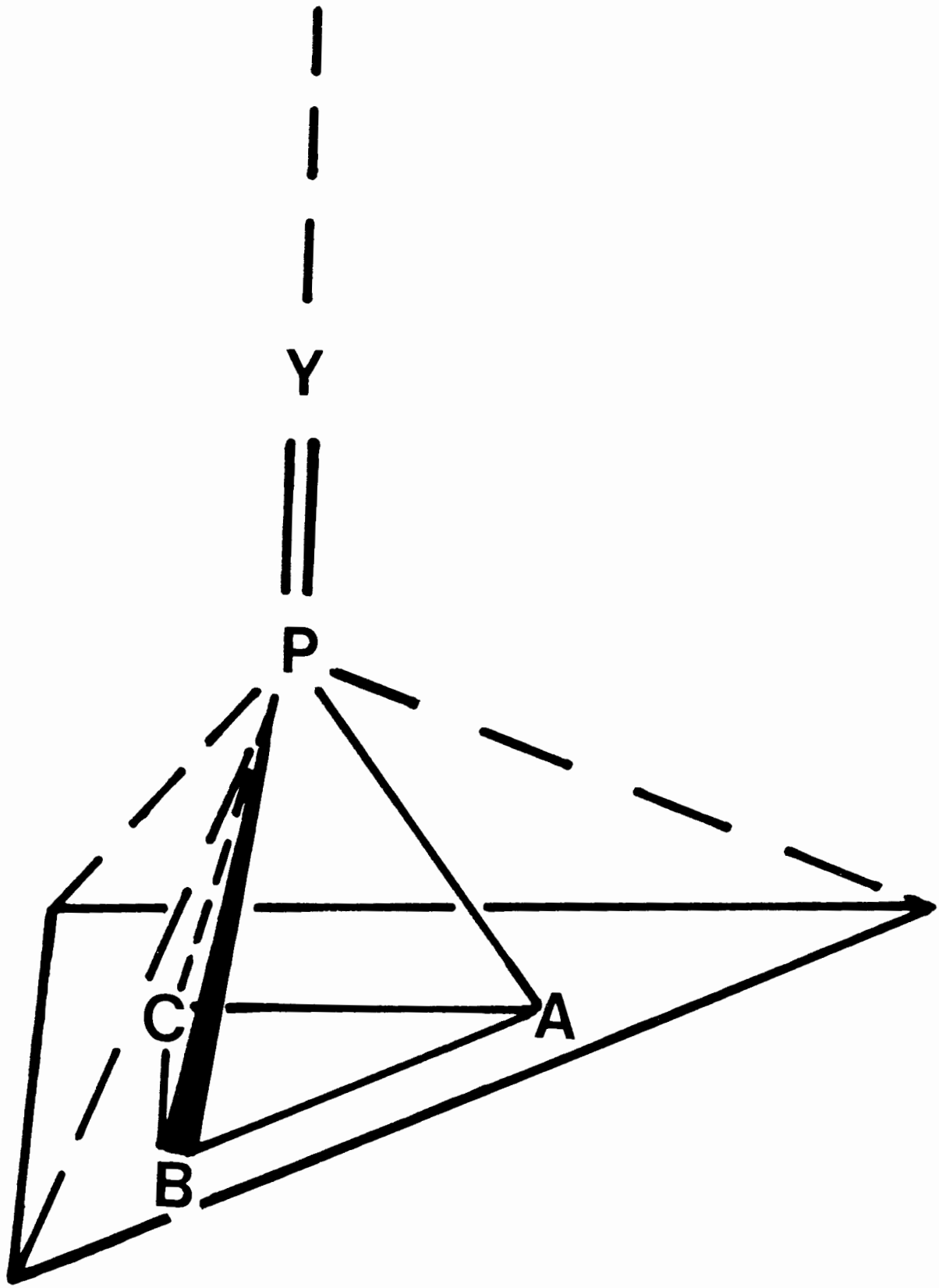

FIGURE 2.4 Distortion of the tetrahedral geometry in an ABCP=Y molecule. Dashed lines represent the ideal tetrahedral geometry.

(see Part 2).

The internal distribution of the individual bond angles at the phosphorus atom is given in Table 2.15.

TABLE 2.15 Average values (with standard deviations) for the O-P-O Bond Angles (^{o}) in compounds (4) and (5)

	(4)	(5)
All six O-P-O angles	108,9 ± 9,7	109,1 ± 8,2
Three O=P-OAr angles	117,0 ± 1,1	116,5 ± 1,1
Three ArO-P-OAr angles	100,8 ± 6,2	101,6 ± 0,8

In this respect, compounds (4) and (5) resemble each other and the "orbitals repulsion" effect appears to be a dominating one in governing the molecular geometry. However in the quinoline derivative (4) additional effects are present, superimposed on the above effect which is common to all tetravalent phosphates. The values of the "narrow" ArO-P-OAr angles in (4) show a scatter of almost an order of magnitude greater than the analogous values for the reference compound (5). This results due to the presence of the nitrogen atom which as expected interacts strongly with the phosphoryl centre. The nitrogen-phosphorus non-bonded distance in (4) is 3,02Å with the corresponding sum of the van der Waals radii equal to 3,44Å[36]. This short contact clearly indicates an intramolecular nucleophilic approach of the nitrogen to the phosphorus and is expected to change the geometry of the molecule toward that of a trigonal bipyramid. Schmutzler et al.[21] observed an even shorter N⟶P close contact of ca 2Å in the fluorophosphorane structures. Structure (4) does indeed show some features of the P^{V} trigonal bipyramidal system. One of

the 4-nitrophenoxy groups tends to apical geometry: the P-O(3) bond (1,586Å) is longer than the P-O(4) bond (1,560Å) and the N...P-O(3) angle of 159° approaches the ideal value of 180°. Furthermore the "quasi apical" O(3)PNP moiety makes angles of 99,5° and 95,3° with the "quasi equatorial" O(1) and O(4) atoms respectively thus tending towards the ideal value of 90°. The phosphoryl group however, deviates strongly from its expected "quasi equatorial" position. As a result of these two overlapping effects, the geometry of (4) can be schematically represented by Figure 2.5.

In contrast, the 4-nitrophenyl moieties in structure (5) have identical P-O bond lengths and lie almost parallel with respect to each other, with a 9,1° discrepancy between the normals to their planes. In addition both these ligands are angled, on average, 71,4° with respect to the naphthyl substituent.

The orientation of the ligands in phosphate (4) is dramatically different from that in (5) further highlighting the remarkable effect produced, by the mere substitution of a carbon with a nitrogen atom, on the geometry of the system. The 4-nitrophenoxy ligands in (4) are orientated at 113° with respect to each other. Their individual orientation with respect to the quinoline moiety is quite different: the O(3)PNP ligand is angled at 25° whereas the O(4)PNP ligand is positioned vertically.

In both triesters (4) and (5) all the aromatic rings are planar to within 0,02Å. The equations of the least-squares mean planes and atomic deviations therefrom are listed in Tables 2.16 and 2.17 respectively.

The difference in the intramolecular interactions operative in the two phos= phates can also be demonstrated by comparing the orientation of the nitrogen atom in (4) with respect to the P^{IV} centre, with the analogous orientation of the C(19) atom in (5). If the quinoline nitrogen atom is considered to be

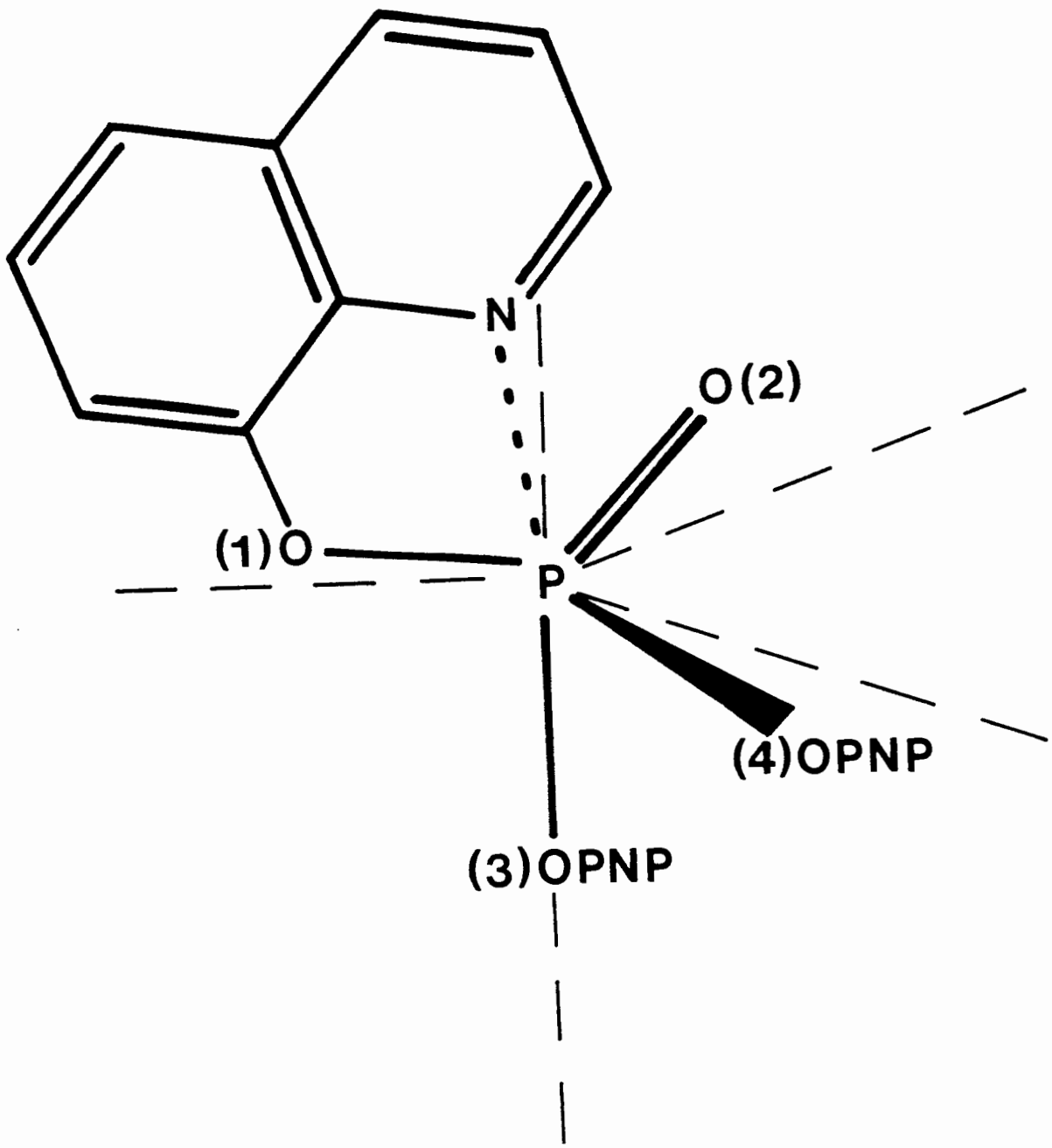

FIGURE 2.5 Distortion of the trigonal bipyramidal geometry in (4). Dashed lines represent ideal trigonal bipyramidal geometry.

TABLE 2.16 Least-Squares Planes for Compound (4)

---

1 (a) Equations of least-squares planes are expressed in orthogonalised space as $pX + qY + rZ = S$.

Plane 1 : The quinolinyl ring atoms (C(11), C(12), C(13), C(14), C(15) C(16), C(17), C(18), N(19), C(20))

$7,2191X - 4,2632Y + 2,2612Z = 4,8884$

Plane 2 : The 4-nitrophenyl ring atoms (C(31), C(32), C(33), C(34), C(35), C(36))

$4,0360X - 6,8699Y + 4,6197Z = 4,4724$

Plane 3 : The 4-nitrophenyl ring atoms (C(41), C(42), C(43), C(44), C(45), C(46))

$5,6644X + 7,4134Y - 3,5836Z = -0,7683$

(b) Deviations from the planes ($\text{Å} \times 10^3$)

Atom	*Plane* 1	*Atom*	*Plane* 2
P(1)	-1042	P(1)	391
O(1)	33	O(1)	1816
O(2)	-2330	O(2)	-556
O(3)	-1025	O(3)	19
O(4)	-335	O(4)	589
C(11)*	-11	C(31)*	19
C(12)*	6	C(32)*	-3
C(13)*	8	C(33)*	-14
C(14)*	-11	C(34)*	13
C(15)*	4	C(35)*	4
C(16)*	0	C(36)*	-19
C(17)*	2	N(34)	76
C(18)*	-2	O(341)	-142
N(19)*	4	O(342)	329
C(20)*	1		

TABLE 2.16 Cont/....

TABLE 2.16 Continued

Atom	*Plane* 3
P(1)	-789
O(1)	-1718
O(2)	-1413
O(3)	370
O(4)	62
C(41)*	-1
C(42)*	1
C(43)*	-2
C(44)*	3
C(45)*	-3
C(46)*	2
N(44)	-10
O(441)	-158
O(442)	66

(c) Angles between normals to planes (^{o})

Plane 1 and Plane 2	25,06
Plane 1 and Plane 3	88,49
Plane 2 and Plane 3	113,00

TABLE 2.17 Least-Squares Planes for Compound (5)

---

1 (a) Equations of least-squares planes are expressed in orthogonalised space as $pX + qY + rZ = S$.

Plane 1 : The naphthyl ring atoms (C(11), C(12), C(13), C(14), C(15), C(16), C(17), C(18), C(19), C(20))

$-2,9910X + 10,4244Y + 9,9790Z = 9,7991$

Plane 2 : The 4-nitrophenyl ring atoms (C(31), C(32), C(33), C(34), C(35), C(36))

$3,0241X + 10,2577Y - 10,4762Z = -5,8462$

Plane 3 : The 4-nitrophenyl ring atoms (C(41), C(42), C(43), C(44), C(45), C(46))

$3,8607X + 10,0139Y - 8,4323Z = -3,9753$

(b) Deviations from the planes ($\text{Å} \times 10^3$)

Atom	*Plane* 1	*Atom*	*Plane* 2
P(1)	1098	P(1)	1065
O(1)	-111	O(1)	1016
O(2)	1886	O(2)	2352
O(3)	443	O(3)	-72
O(4)	1880	O(4)	365
C(11)*	-9	C(31)*	5
C(12)*	-13	C(32)*	-10
C(13)*	-1	C(33)*	7
C(14)*	6	C(34)*	3
C(15)*	19	C(35)*	-9
C(16)*	-7	C(36)*	5
C(17)*	-14	N(34)	-13
C(18)*	-5	O(341)	67
C(19)*	13	O(342)	-100
C(20)*	12		

TABLE 2.17 Cont/....

TABLE 2.17 Continued

Atom	*Plane* 3
P(1)	800
O(1)	629
O(2)	2148
O(3)	-155
O(4)	-53
C(41)*	11
C(42)*	-3
C(43)*	-9
C(44)*	14
C(45)*	-6
C(46)*	-6
N(44)	67
O(441)	165
O(442)	4

(c) Angles between normals to planes (^{o})

Plane 1 and Plane 2	70,74
Plane 1 and Plane 3	71,99
Plane 2 and Plane 3	9,09

an internal nucleophile, it should in agreement with the generally accepted[30] stereochemistry of nucleophilic substitution, approach the phosphoryl centre in a so-called "face" attack. Ideally, nucleophiles (Nu) in "face" approach to a tetrahedral phosphate centre make O-P...Nu angles of 180^{o} (one) and $70,5^{o}$ (three) whereas the alternative "edge" orientation produces two O-P...Nu angles of $54,7^{o}$ and two of $125,3^{o}$ (see Figure 2.6).

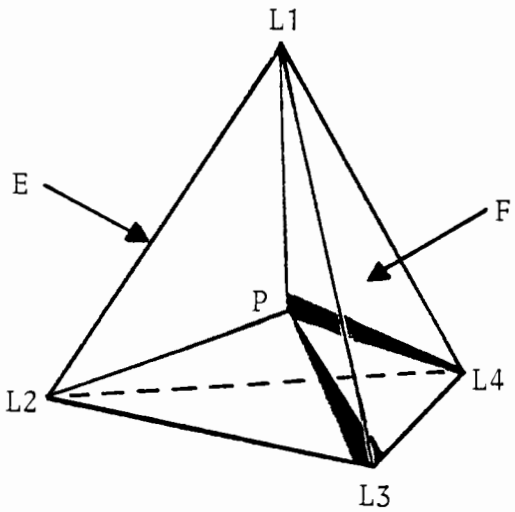

FIGURE 2.6 The Face (F) and Edge (E) directions of nucleophilic attack on a P^{IV} tetrahedral centre.

A plot of the P-N(19) (or P-C(19)) distance versus four O-P...N(19) (or O-P... C(19)) angles for phosphates (4) and (5) is shown in Figure 2.7. The P...X (X = N(19) or C(19)) distance is given relative to the sum of the van der Waals radii, thus $\Delta d = 0$ represents a distance exactly equal to the sum of the van der Waals radii for atom P and X. Figure 2.7 clearly demonstrates the close ($\Delta d < 0$) "face" approach chosen by the nitrogen atom in (4), typically that of an "early stage" nucleophilic substitution. However the α-carbon atom of the naphthalene ring, C(19), in (5) locates itself at a longer range ($\Delta d > 0$) from the phosphoryl centre in an "edge" orientation which is atypical for a nucleophile-tetrahedral electrophile interaction.

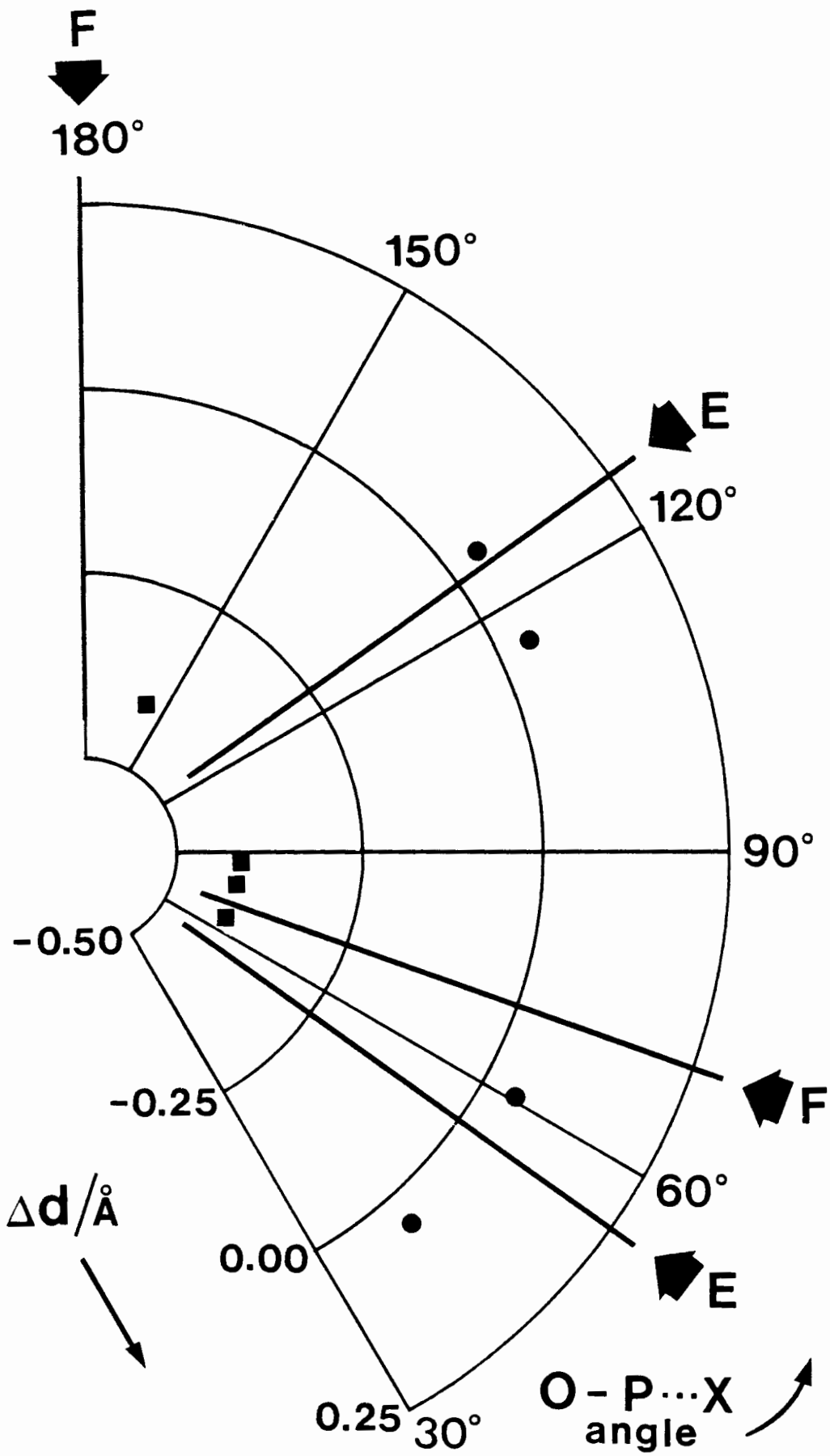

FIGURE 2.7 P...N(19) distance versus O-P...N(19) angles for (4) (squares) and P...C(19) distance versus O-P...C(19) angles for (5) (circles).

Kirby and coworkers are presently investigating the relationship between the length of a bond in the crystal and its reactivity towards heterolytic cleavage in solution. From their study of a series of dialkyl aryl phosphates[88a], aryl tetrahydropyranyl acetals and α-glucoside systems[88b,88c], they observe that the better the leaving group, RO^-, the longer the length of the corresponding P-OR or C-OR bond in the crystal structure.

It appears however that appreciable deviations do arise from this observed linear relationship. For example, in the 1,3,2-dioxaphosphorinane 2-oxide system when good or very good leaving groups ($pK_a \leq 7$) are present, no further bond lengthening is observed.

As phosphate triesters do not react in solution by a dissociative process, implying that the P-OR bond does not break spontaneously and in fact are compounds of relatively low intrinsic reactivity, a good linear correlation between P-O bond length and the nature of the oxyanion leaving group, RO^-, is not expected.

Phosphate triesters (4) and (5) both contain identical good leaving groups, namely the 4-nitrophenoxide moieties. The significant increase in the P-O(3)PNP bond length in (4) as compared to (5) indicates the greater inherent reactivity of triester (4). This can only be attributed to the presence of the tertiary nitrogen atom and provides certain evidence for intramolecular nucleophilic catalysis in (4).

The hydrolysis of one of the PNPO-P functions in (4), producing diester (6), has a profound effect on the molecular structure of the entire system. A perspective view of compound (6) with atomic nomenclature is shown in Figure 2.8 and the bond lengths and angles are listed in Table 2.18. The phosphorus atom in (6) is still tetrahedrally coordinated but now it is the negative

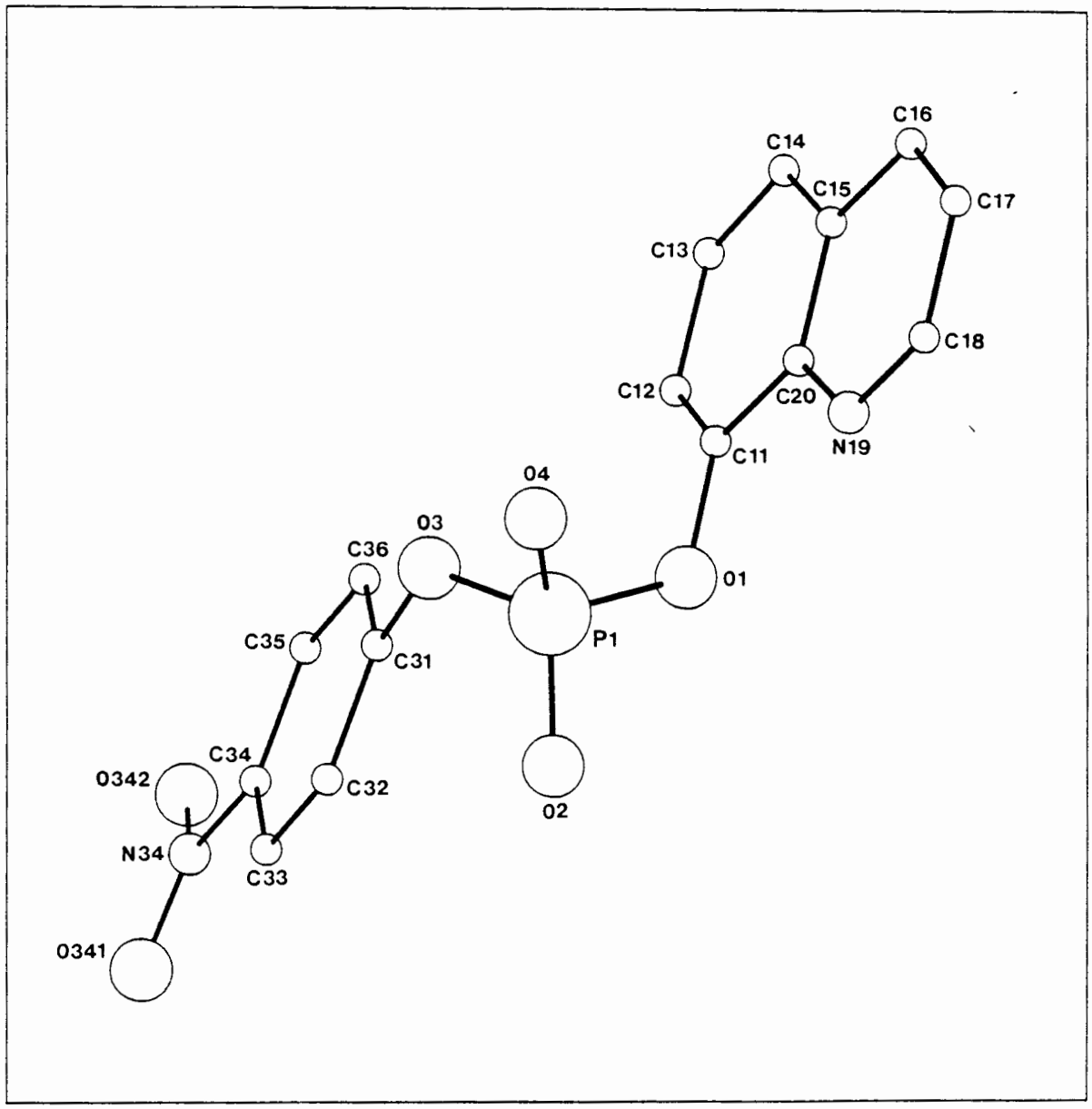

FIGURE 2.8 A perspective view of 4-nitrophenyl-8-quinolinyl phosphate (6).

TABLE 2.18 Bond Lengths (Å) and Angles (°) with estimated standard deviations in parentheses for Compound (6)

Bond Lengths	
P(1) - O(1)	1,622(5)
P(1) - O(2)	1,473(4)
P(1) - O(3)	1,628(4)
P(1) - O(4)	1,457(4)
O(1) - C(11)	1,398(6)
C(11) - C(12)	1,343(8)
C(12) - C(13)	1,414(8)
C(13) - C(14)	1,364(9)
C(14) - C(15)	1,409(8)
C(15) - C(20)	1,418(8)
C(15) - C(16)	1,414(8)
C(16) - C(17)	1,371(8)
C(17) - C(18)	1,386(9)
C(18) - N(19)	1,320(8)
N(19) - C(20)	1,373(7)
C(20) - C(11)	1,402(8)
O(3) - C(31)	1,381(7)
C(31) - C(32)	1,390(8)
C(32) - C(33)	1,383(9)
C(33) - C(34)	1,392(8)
C(34) - C(35)	1,382(9)
C(35) - C(36)	1,361(9)
C(36) - C(31)	1,387(8)
C(34) - N(34)	1,463(8)
N(34) - O(341)	1,221(6)

TABLE 2.18 Cont/....

TABLE 2.18 Continued

N(34) - O(342)	1,224(6)
Bond Angles	
O(1) - P(1) - O(2)	104,1(3)
O(1) - P(1) - O(3)	101,0(2)
O(1) - P(1) - O(4)	110,5(3)
O(2) - P(1) - O(3)	109,8(2)
O(2) - P(1) - O(4)	124,4(3)
O(3) - P(1) - O(4)	104,8(3)
P(1) - O(1) - C(11)	121,2(4)
O(1) - C(11) - C(12)	121,2(6)
O(1) - C(11) - C(20)	118,6(5)
C(11) - C(12) - C(13)	120,7(6)
C(12) - C(13) - C(14)	120,9(6)
C(13) - C(14) - C(15)	119,4(6)
C(14) - C(15) - C(16)	122,9(5)
C(20) - C(15) - C(16)	118,1(6)
C(15) - C(16) - C(17)	120,3(6)
C(16) - C(17) - C(18)	119,2(6)
C(17) - C(18) - N(19)	121,4(6)
C(18) - N(19) - C(20)	122,2(5)
N(19) - C(20) - C(15)	118,7(6)
C(15) - C(20) - C(11)	119,9(5)
C(20) - C(11) - C(12)	120,0(5)
P(1) - O(3) - C(31)	127,1(4)
O(3) - C(31) - C(32)	122,0(6)
O(3) - C(31) - C(36)	117,2(5)
C(32) - C(31) - C(36)	120,6(6)
C(31) - C(32) - C(33)	120,3(6)

TABLE 2.18 Cont/....

TABLE 2.18 Continued

C(32) - C(33) - C(34)	117,9(6)
C(33) - C(34) - C(35)	121,6(6)
C(33) - C(34) - N(34)	118,4(6)
C(34) - C(35) - C(36)	120,1(6)
C(35) - C(36) - C(31)	119,5(6)
C(34) - N(34) - O(341)	119,4(6)
C(34) - N(34) - O(342)	117,4(6)
O(341) - N(34) - O(342)	123,2(6)

Intermolecular Non-Bonded Distance

N(19)...O(2)$^{(i)}$	2,610

Symmetry Code

(i) 1-x, 1-y, -z

C(20) - C(15) - C(14)	119,0(6)
C(11) - C(20) - N(19)	121,4(5)
C(35) - C(34) - N(34)	120,0(6)

charge introduced to the phosphate group which is responsible for the deviation of individual bond angles from the regular tetrahedral value. Electrostatic repulsion between the two negatively charged oxygen atoms increases the O(2)-P-O(4) angle to a value of 124,4° with simultaneous compression of the O(3)-P-O(1) angle to 101°. This counterbalancing effect ensures that on average the O-P-O angles (109,1° ± 8,3°) approximate the ideal 109,5° value.

The most significant difference between compound (6) and its neutral precursor (4) is the nature of the interactions involving the nitrogen atom. Diester (6) crystallises as a zwitterion with the N^+-H function strongly hydrogen bonded to one of the negatively charged oxygen atoms of a neighbouring molecule. As a result the nitrogen atom is removed from the vicinity of the phosphorus atom, thereby eliminating the possibility of any intramolecular interaction. Instead, the nitrogen locates itself close to the $O(2)^{(i)}$ atom producing a $N(19)\ldots O(2)^{(i)}$ intermolecular close contact of 2,61Å (the corresponding sum of the van der Waals radii being 2,94Å). The oxygen atoms, O(2) and O(4), of the PO_2^- group are formally equivalent but the intermolecular hydrogen bonding to the N^+-H group makes the two oxygens clearly non-equivalent. The bond between phosphorus and the hydrogen-bonded O(2) has less multiple character and therefore is longer (1,473Å) than the P-O bond of the "free" negative oxygen atom (1,457Å). This unsymmetrical hydrogen bonding between the PO_2^- acceptor and N^+-H donor group (essentially involving only one oxygen atom) is further evidence (see Chapter 4) for the preferential formation of a "linear" as opposed to a "bifurcated" hydrogen bond. Although recent theoretical calculations[31] predict the "bifurcated" hydrogen bond to be more stable, results of this study are in direct contrast to this proposal.

The geometry of the aromatic rings in the diester (6) is regular: the 4-nitrophenoxy ring is planar to within 0,01Å and the quinoline moiety to within 0,03Å (see Table 2.19). These ligands lie almost coplanar with respect to each other.

TABLE 2.19 Least-Squares Planes for Compound (6)

1 (a) Equations of least-squares planes are expressed in orthogonalised space as $pX + qY + rZ = S$.

Plane 1 : The quinolinyl ring atoms (C(11), C(12), C(13), C(14), C(15), C(16), C(17), C(18), N(19), C(20))

$2{,}5220X + 5{,}4691Y + 9{,}0137Z = 3{,}7889$

Plane 2 : The 4-nitrophenyl ring atoms (C(31), C(32), C(33), C(34), C(35), C(36))

$1{,}1688X + 5{,}0822Y + 9{,}4151Z = 5{,}4680$

(b) Deviations from the planes ($\text{Å} \times 10^3$)

Atom	*Plane* 1	*Atom*	*Plane* 2
P(1)	1408	P(1)	-826
O(1)	30	O(1)	-2112
O(2)	2050	O(2)	101
O(3)	961	O(3)	-1358
O(4)	2331	O(4)	-67
C(11)*	44	C(31)*	-4
C(12)*	-9	C(32)*	2
C(13)*	29	C(33)*	-2
C(14)*	-6	C(34)*	4
C(15)*	11	C(35)*	-6
C(16)*	18	C(36)*	5
C(17)*	11	N(34)	14
C(18)*	-29	O(341)	70
N(19)*	-21	O(342)	-40
C(20)*	9		

(c) Angle between normals to planes ($^\circ$)

Plane 1 and Plane 2	11,51

Molecular Packing

Packing diagrams for compounds (4), (5) and (6) are shown, in projection along the [100] direction, in Figures 2.9, 2.10 and 2.11 respectively.

Compound (4) packs its two molecules in the triclinic unit cell in such a way so as to position all the aromatic rings of one molecule in a parallel formation with respect to the corresponding aromatic ligands of the neighbouring molecules. The shortest intermolecular distances are found between two overlapping 4-nitrophenoxide ligands attached to an O(4). However the interplanar spacing is of the same order of magnitude as the van der Waals separation for aromatic molecules ($\sim$3,6Å), and is therefore unremarkable.

Phosphate (5) crystallises with four molecules in the unit cell. The molecules pack with their phosphoryl oxygen atoms positioned alternatively up and down along the z-axis. No intramolecular interactions are, as is expected, in evidence. The only significantly short intermolecular contacts observed are between C(19) of the naphthyl moiety and C(43) ($C(19)\ldots C(43)^{(i)}$ = 3,40Å) and C(44) ($C(19)\ldots C(44)^{(i)}$ = 3,45Å) of the neighbouring 4-nitrophenoxide ligands.

(i) C(43) and C(44) at $-\frac{1}{2}-x$, $-\frac{1}{2}+y$, $1\frac{1}{2}-z$

In the diester (6) the two molecules in the unit cell are "dimerised" by the formation of two N^{+}-H...O intermolecular hydrogen bonds. These "dimers" stack parallel to the y-axis thereby producing a non-continuous double string hydrogen bonding network. Other intermolecular close contacts are observed and indicate interaction between symmetry related quinolinyl moieties:

$C(16)\ldots C(12)^{(i)}$ = 3,43Å $C(16)\ldots C(13)^{(i)}$ = 3,46Å

$C(15)\ldots C(14)^{(i)}$ = 3,47Å $C(20)\ldots C(14)^{(i)}$ = 3,43Å

(i) $-x$, $2-y$, $-z$

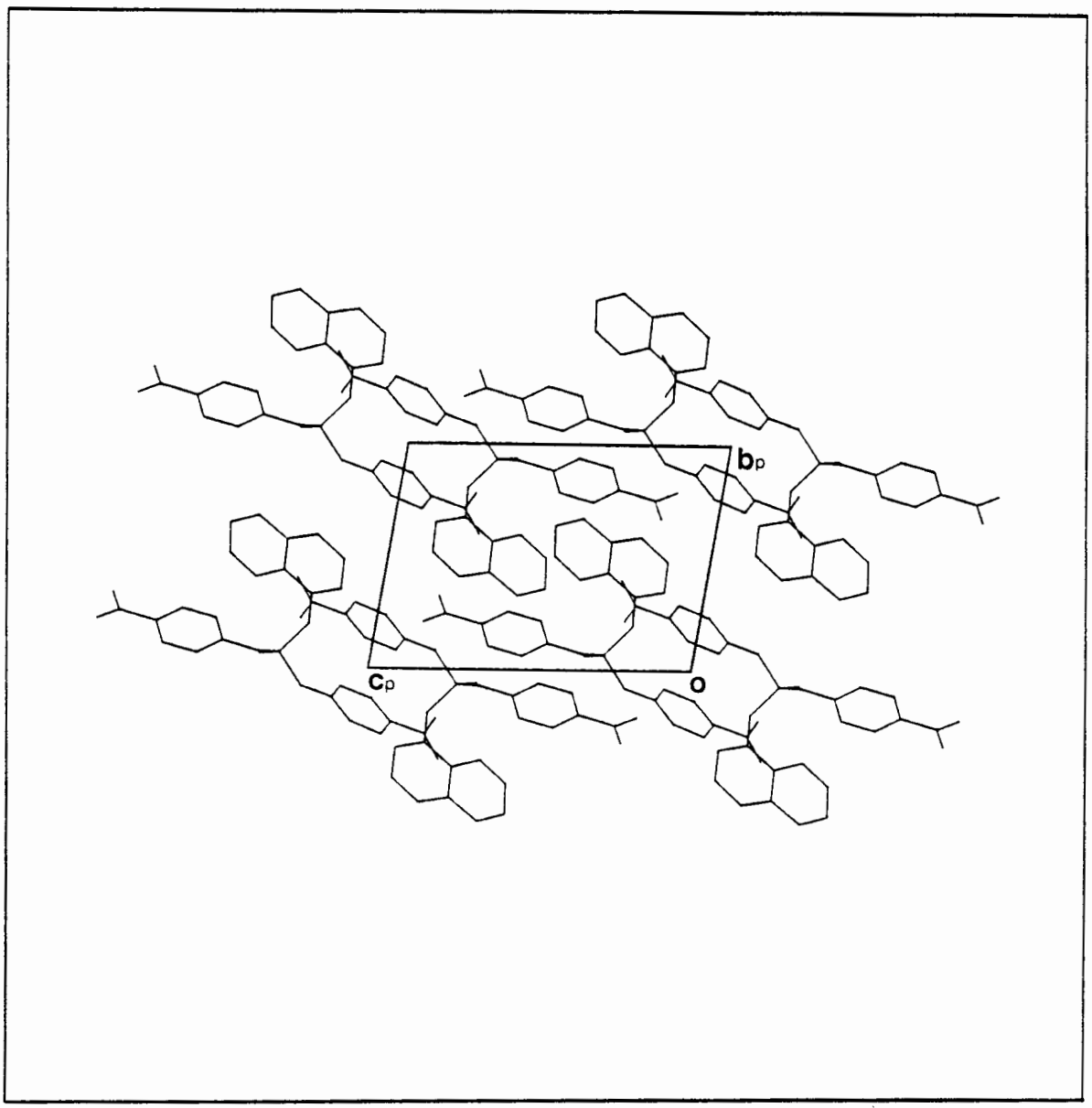

FIGURE 2.9 A packing diagram for compound (4) viewed along [100].

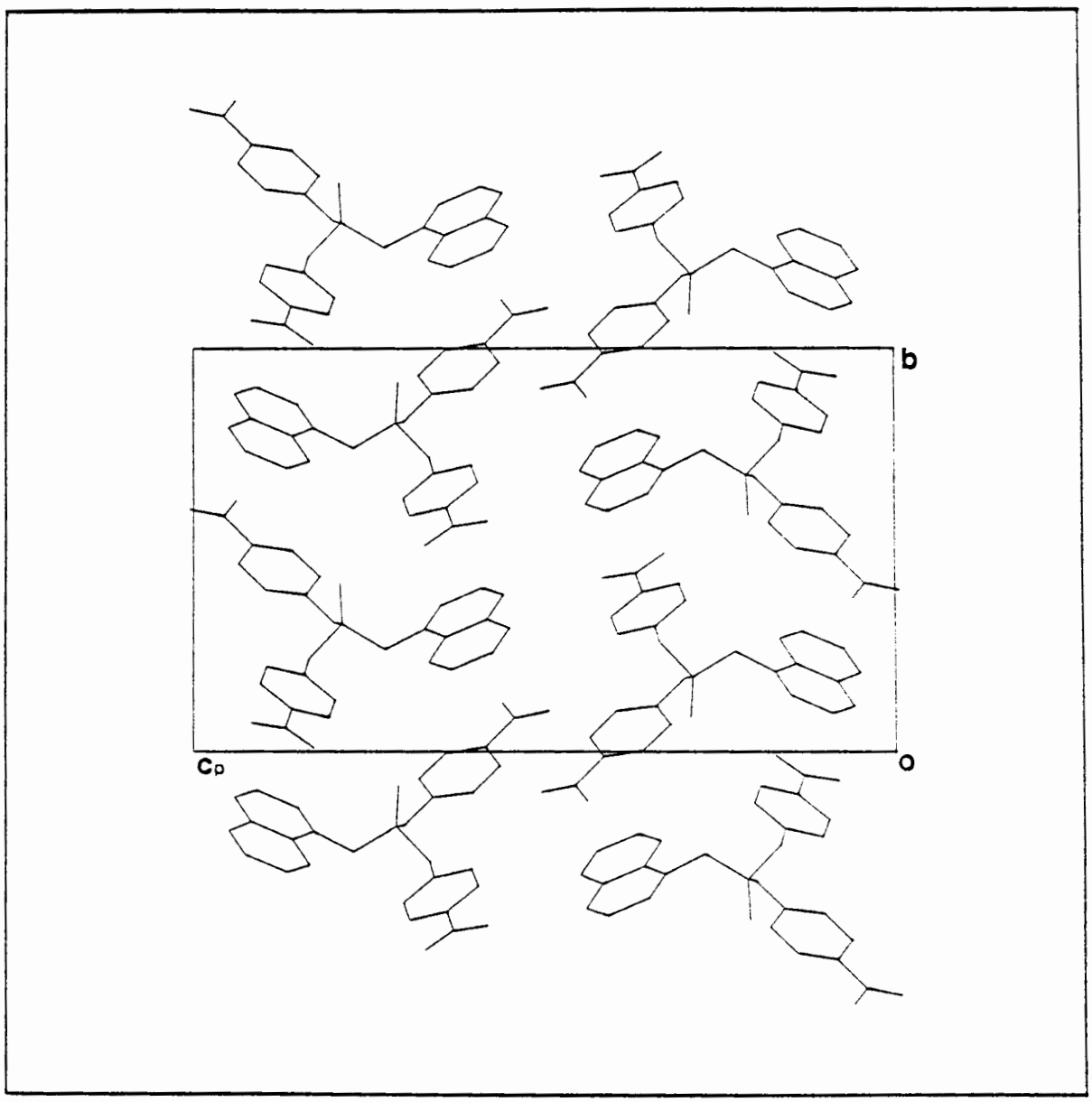

FIGURE 2.10 A projection of the crystal packing for compound (5) viewed along [100].

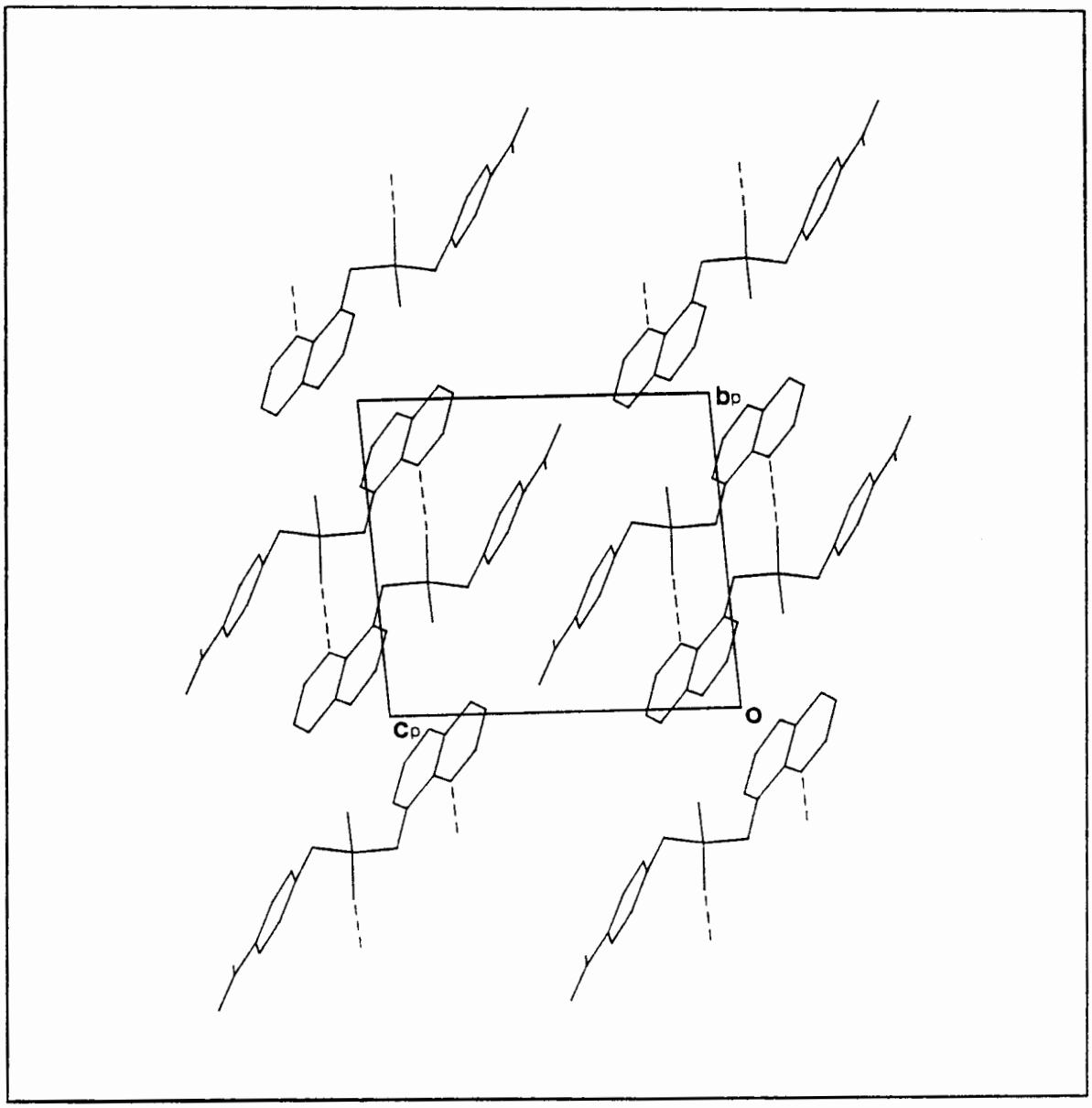

FIGURE 2.11 A packing diagram for compound (6) viewed along [100] showing hydrogen bonds as dashed lines.

2.3 CONFORMATIONAL STUDY

The aim of this study was to determine all other possible low energy conformations for compounds (4) and (5) by calculating the van der Waals energy using empirical atom pair potentials.

If, by comparison, these low energy conformers are similar to their respective crystal structure ones, then it may be established unequivocally that the intramolecular interaction operative in (4) is as a direct result of the presence of the nitrogen atom in the fused ring system and not coincidentally achieved by molecular packing requirements.

This method of evaluating molecular energies is well established and has been reviewed by Kitaigorodsky[32] and Mirsky[33]. The coefficients of the atom-atom potentials are of the form,

$$U(r) = a\exp(-br)/r^d - c/r^6$$

where r is the distance between any pair of atoms and the coefficients a, b, c and d are those given by Giglio[34], such that $U(r)$ is evaluated in kilocalories when r is in Ångströms. These potential energy curves were derived primarily to give good agreement for calculation of molecular position in a crystal structure and the energy values mean little in the absolute sense. No account was taken of possible torsional potentials for sigma bonds, partial atomic charges or dipole interactions. The program EENY[35] calculates molecular coordinates as defined by appropriate torsion angles and sums the energy for all non-bonded pairs of atoms whose separation is dependent upon the torsion angles.

Structures (4) and (5) were analysed by initially dividing the molecules into seven residues linked by six torsion angles as shown in Figure 2.12.

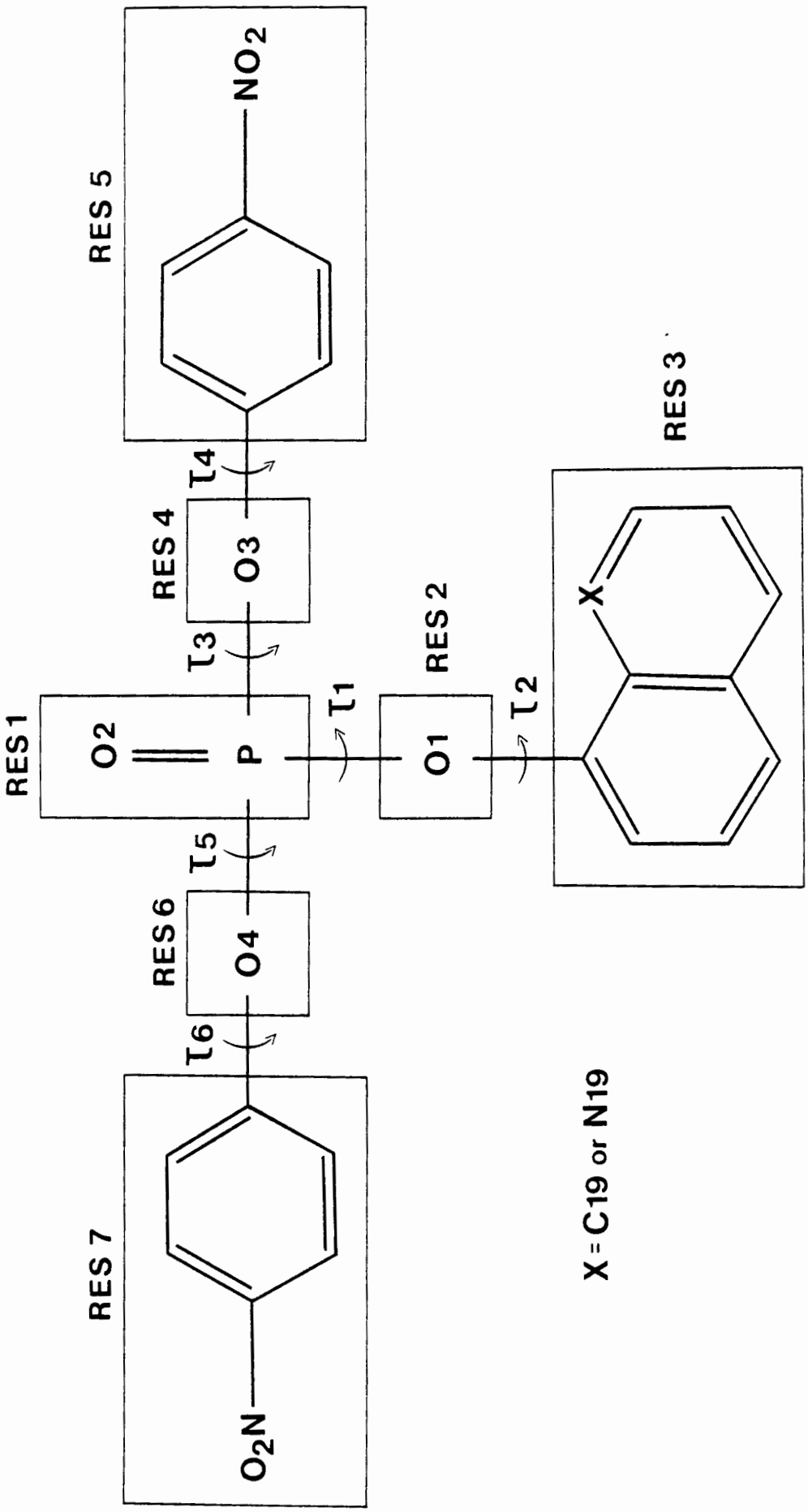

FIGURE 2.12 Structures (4) and (5) divided into seven residues.

A full six-dimensional mapping by varying all six torsion angles simultaneously was not attempted. As an approximation, residues 5 and 7 were initially omitted and an energy map was calculated by varying torsion angles τ_1 and τ_2. Four distinct energy minima were located. With τ_1 and τ_2 fixed at each of these minima, further maps were calculated by varying τ_4 and τ_6. In this way all the important energy valleys could be located and the torsion angles and final energies were refined by a method of steepest descent incorporated in the program. The results of the analysis are summarised in Table 2.20 and Figure 2.13.

Compound (4) yielded six conformations different from that of the crystal structure, all having similar total intramolecular non-bonded energies (T.I.E.). These are shown in Figure 2.14, for the sake of clarity, as Newman projections along the phosphoryl (O=P) bond. If both the 4-nitrophenoxide ($PNPO^-$) "leaving" groups are regarded as being equivalent, then the geometries of the conformations all approximate a "face" approach and are such that the quinolinyl nitrogen, N(19), lies roughly opposite O(3), in conformers (4a) and (4d) and opposite O(4) in conformers (4e) and (4f). The N(19) is located opposite the phosphoryl oxygen atom, O(2), in conformers (4b) and (4c) and as a result these are of less chemical interest. However it is the crystal structure conformation (4) that best models the incipient SN_2 mechanism via a trigonal bipyramidal intermediate. The incoming intramolecular nucleophile, N(19), is positioned opposite ($\sim 160^{\circ}$) to the leaving O(3)PNP group and makes a N(19)...P close contact of 3,02Å (the corresponding sum of the van der Waals radii being 3,44Å).

Four low energy conformations besides the crystal structure were obtained for compound (5), all having similar total intramolecular energies. These are shown in Figure 2.15. The solid state conformer (5) and that closely related to it, (5a), both exhibit an "edge" approach of C(19) to the phos=

TABLE 2.20 Intramolecular Parameters and Calculated Non-Bonded Energies for Compounds (4) and (5) and their Conformers corresponding to the Potential Energy Minima

	(4) (Crystal structure)	(4a)	(4b)	(4c)	(4d)	(4e)	(4f)	(5) (Crystal structure)	(5a)	(5b)	(5c)	(5d)
P(1)...Y (Å) (Y = N(19) or C(19))	3,019	3,486	3,723	3,873	3,197	3,612	3,362	3,790	3,811	3,608	3,629	3,697
Δd (Å) [a]	-0,421	+0,046	+0,283	+0,433	-0,243	+0,172	-0,078	+0,040	+0,061	-0,142	-0,121	-0,053
O(1) - P(1)...Y (°)	63,8	48,7	40,2	34,1	58,2	44,3	52,9	41,2	40,7	48,7	47,6	44,8
O(2) - P(1)...Y (°)	83,7	93,1	152,8	138,5	77,2	88,4	79,3	127,3	112,5	79,5	104,0	92,5
O(3) - P(1)...Y (°)	158,8	145,4	85,8	66,3	157,6	82,7	84,2	115,0	128,7	95,2	138,0	144,8
O(4) - P(1)...Y (°)	78,8	84,7	71,5	101,8	92,6	150,2	159,8	60,0	67,4	148,4	66,5	80,6
T.I.E. (kcal mol^{-1})	15,3	13,1	11,7	12,4	11,5	13,1	13,6	14,4	13,0	12,6	12,8	12,8

[a] Sum of the Van der Waals radii calculated using values (Å):[36] N = 1,54; P = 1,90; C = 1,85

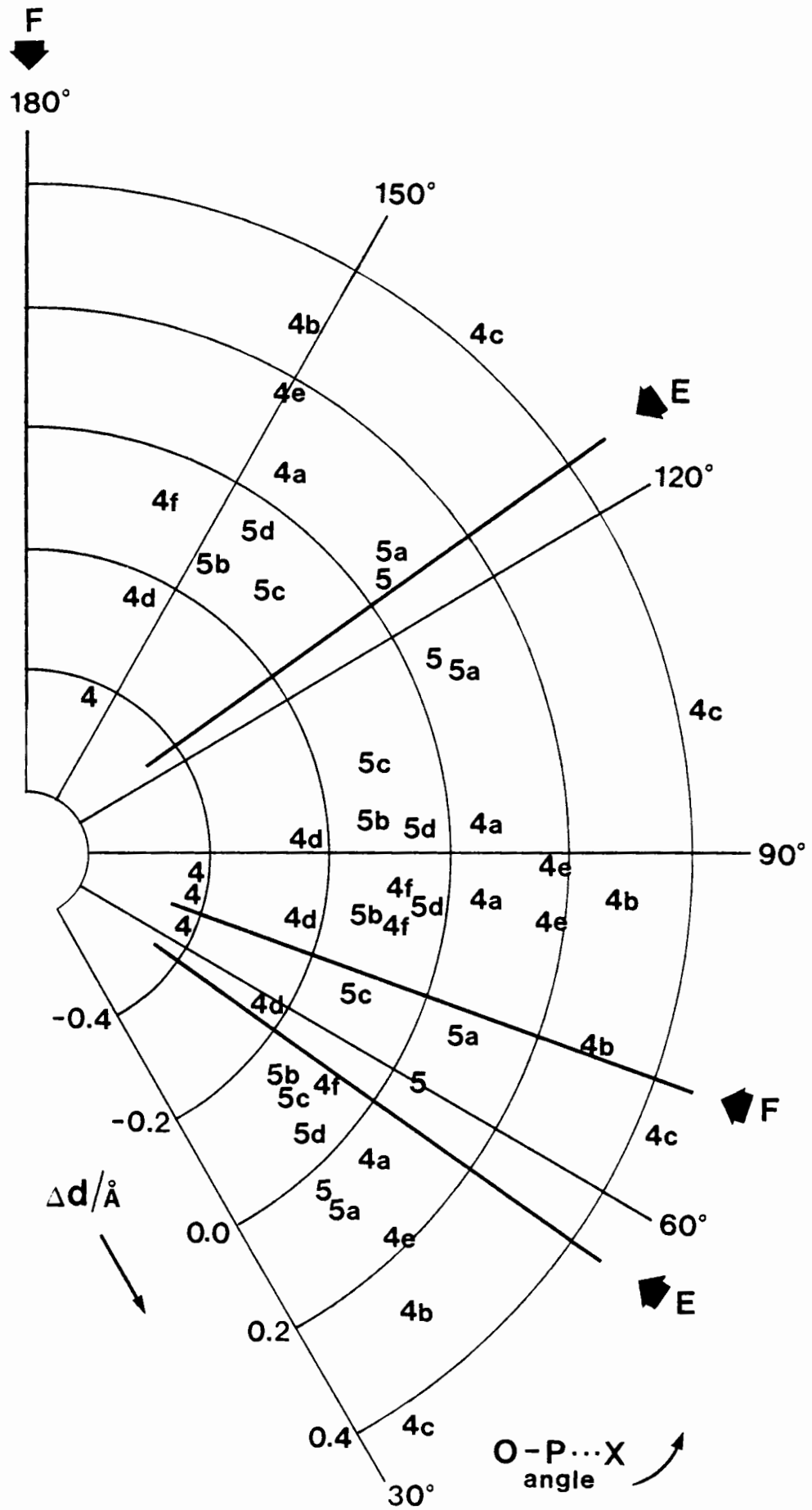

FIGURE 2.13 P...X distance versus O-P...X angles for (4), (4a-f) (X=N) and for (5), (5a-d) (X=CH).

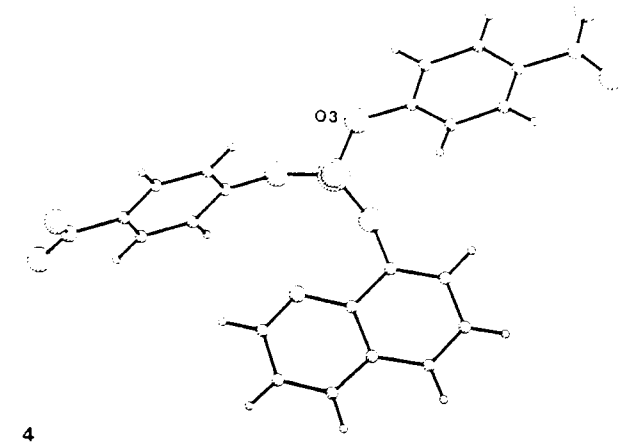

4

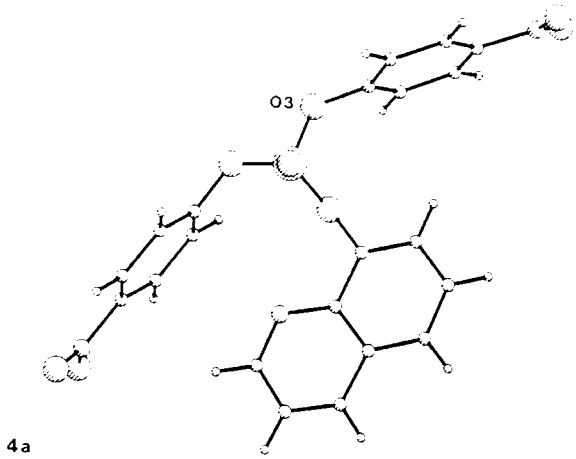

4a

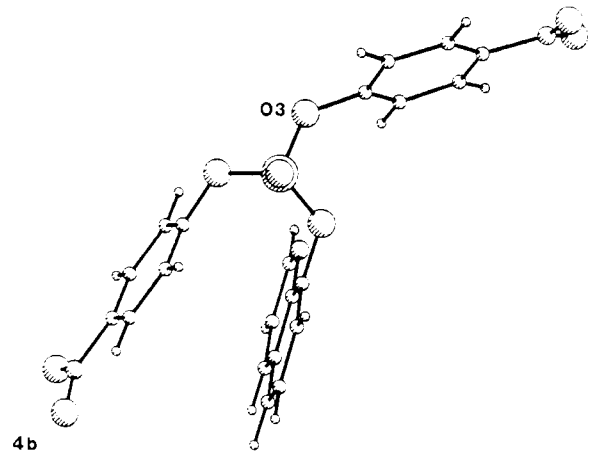

4b

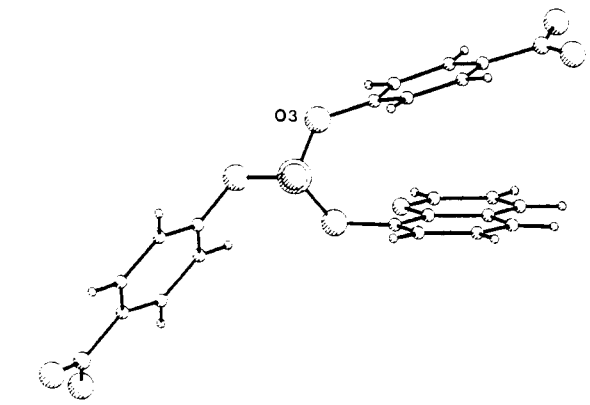

4c

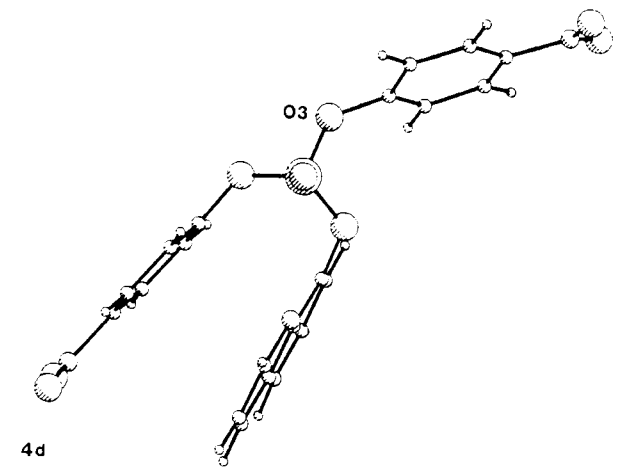

4d

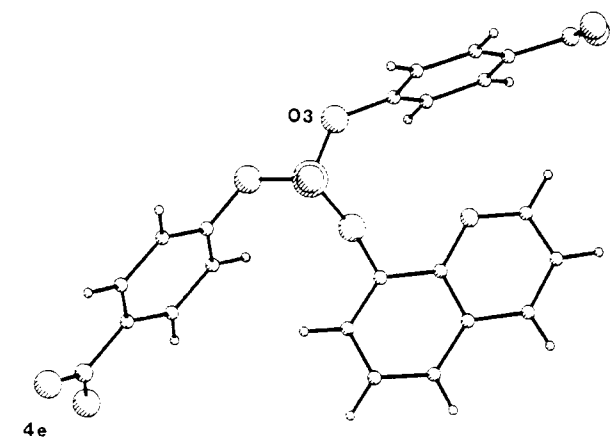

4e

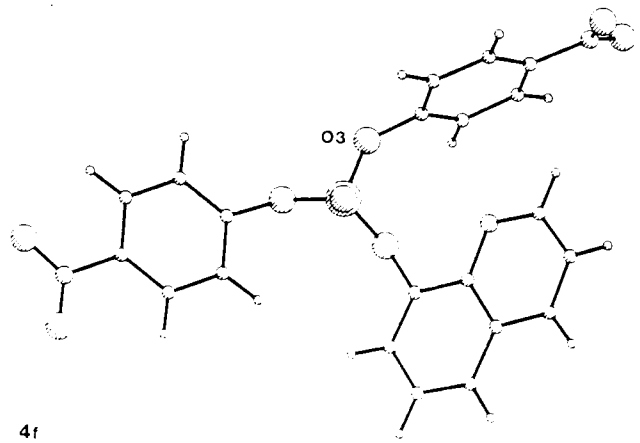

4f

FIGURE 2.14 Perspective views of (4) and (4a-f) projected along the phosphoryl (O=P) bond.

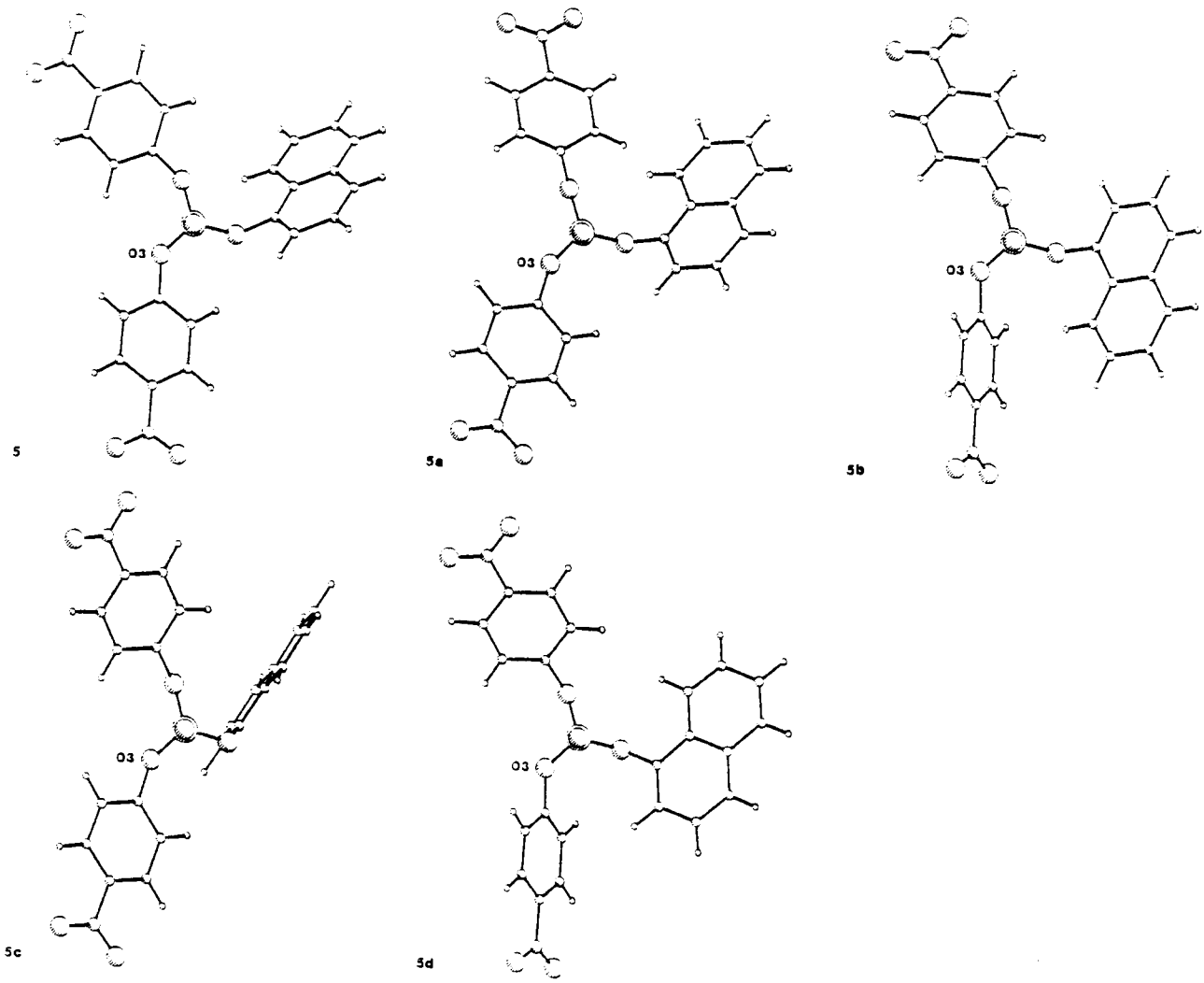

FIGURE 2.15 Perspective views of (5) and (5a-d) projected along the phosphoryl (O=P) bond.

phorus atom, whereas conformers (5b), (5c) and (5d) have geometries which lie somewhere between an "edge" and a "face" approach. Of significance however is that none of the conformers of compound (5) approach the trigonal bipyramidal geometry. No short contacts are observed as the C(19)...P distances are never significantly less than the corresponding sum of the van der Waals radii (with perhaps the exception of conformer (5c)).

In conclusion, it is observed that the geometries of the low energy conformers are not always similar to that of their respective crystal structure ones. The conformers of compound (4) however, do exhibit a preferential "face" approach as opposed to the "edge" approach assumed by compound (5) in accordance with the expected non-participation of the C(19) in intramolecular catalysis.

2.4 MASS SPECTROMETRY STUDY

The mass spectra of triesters (4) and (5) were recorded and interpreted primarily to establish the effect (if any) of the quinolinyl tertiary nitrogen in (4) on the fragmentation patterns obtained upon electron impact induced activation.

Selected ions in the mass spectra, their relative intensities and the proposed assignments are listed in Tables 2.21 and 2.22 for triesters (4) and (5) respectively.

The decomposition modes producing these primary fragments are well documented[37] and typical of the triarylphosphates. Principal modes of fragmentation of aromatic phosphate triesters, $(ArO)_3PO$ result in the formation of the following primary products:

(i) $ArOH^{+\cdot}$ (P-O cleavage with H migration);

(ii) $(ArO)_2PO^+$ (P-O cleavage; loss of $ArO^{\cdot}$);

(iii) Ar^+ (C-O cleavage; loss of $(ArO)_2PO_2^{\cdot}$);

(iv) $(ArO)_2PO_2^+$ (C-O cleavage; loss of $Ar^{\cdot}$).

Thereafter decomposition of these primary products gives rise to subsequent fragments derived from the aromatic ester groups.

Attention is primarily focused on the fragmentation pathway (ii) yielding the phosphorylium ion, $(ArO)_2PO^+$, as a dramatic difference in the behaviour of (4) and (5) is seen with respect to this fragmentation and is clearly illustrated in Figure 2.16.

The base peak in the mass spectrum of phosphate (5) is the very stable molecular ion (m/e 466). Its decomposition (equation 4) via the loss of a 4-nitrophenoxy radical, to produce the 1-naphthyl-4-nitrophenyl phosphorylium

TABLE 2.21 All the Ions observed in the Mass Spectrum[a] of bis(4-nitrophenyl)-8-quinolinyl phosphate (4)

m/e	% Relative Abundance	Assignment
467	7,2	$C_9H_6NOP(O)(OPNP)_2]^{+\cdot}$
329	100,0	$C_9H_6NOP(O)(OPNP)^+$
283	2,9	$C_9H_6NOP(O)(OC_6H_6)^+$
145	16,2	$C_9H_6N(OH)]^{+\cdot}$

[a]The mass spectrum was recorded on a VG Micromass 16F Spectrophotometer operating at an ionising potential of 10eV and an ion source temperature of 200°C. A spectrum at 70eV did not reveal the molecular ion.

TABLE 2.22 Selected Ions in the Mass Spectrum[b] of 1-naphthyl-bis(4-nitrophenyl) phosphate (5)

m/e	% Relative Abundance	Assignment
466	100,0	$C_{10}H_7OP(O)(OPNP)_2]^{+\cdot}$
328	2,8	$C_{10}H_7OP(O)(OPNP)^+$
218	7,2	$C_{10}H_7OP(OH)_2^+$
201	8,6	$(PNPO)P(O)_2]^{+\cdot}$
144	7,4	$C_{10}H_7(OH)]^{+\cdot}$
139	2,7	$PNPOH]^{+\cdot}$

[b]The spectrum was recorded at 70eV and 200°C.

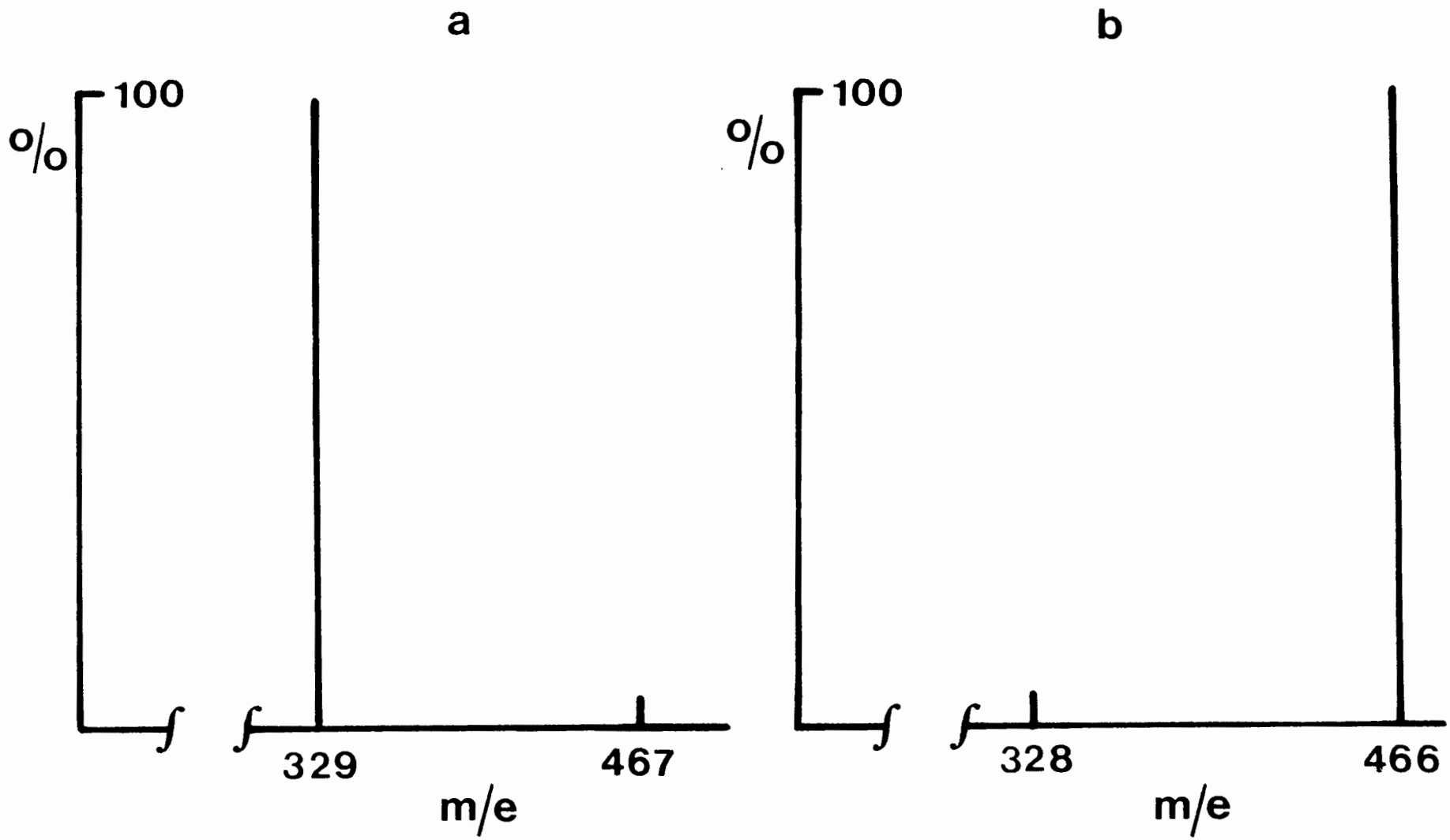

FIGURE 2.16 Sections (m/e > 300) of the mass spectra of (4) (a) and (5) (b).

ion (m/e 328) is clearly not favoured (rel. ab. 2,8%).

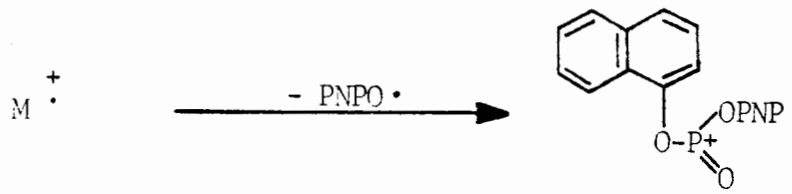

...(4)

(5)

In contrast the molecular ion (m/e 467) of phosphate (4) is very unstable (rel. ab. 7,2%) but the fragmentation producing the corresponding phosphorylium ion (m/e 329), which exists as the base peak, is the most favoured of all the decomposition modes. This is certainly surprising in view of the fact that phosphorylium ions $(RO)_2P(O)^+$ are generally considered to be highly unstable species[38]. This enhanced P-OPNP fragmentation is ascribed to the assistance of the quinolinyl nitrogen. Loss of the PNPO· radical results in the highly abundant resonance-stabilised phosphorylium-ammonium ion (equation 5).

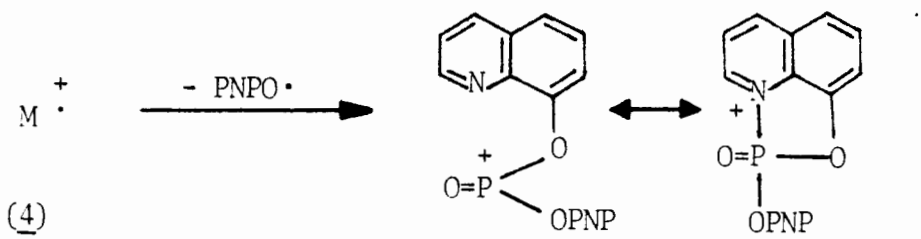

...(5)

(4)

It is concluded that the difference in the fragmentation behaviour of (4) and (5) is simply determined by the relative stability of the phosphorylium ion formation.

In addition the fragmentation of the diester (6) was examined. Without the possibility of a camouflaging hydrogen bond formation (present in the solid state) nucleophilic interaction with the phosphoryl centre (as asserted by Loran and Williams[15]) should be observed.

The major ions in the mass spectrum are given in Table 2.23.

TABLE 2.23 The Major Ions observed in the Mass Spectrum[c] of 4-nitrophenyl-8-quinolinyl phosphate (6)

m/e	% Relative Abundance	Assignment
329	44,3	$C_9H_6NOP(O)(OPNP)^{+\cdot}$
208	3,4	$C_9H_6NOP(O)(OH)^{+}$
145	100,0	$C_9H_6N(OH)^{+\cdot}$
139	69,4	$PNPOH^{+\cdot}$

[c]The spectrum was recorded at 10eV and 200°C.

The molecular ion (m/e 346) is highly unstable and even at operating conditions as low as 10eV could not be detected.

The phosphorylium ion (m/e 208) is present but not as the base peak. It is of low intensity (rel. ab. 3,4%) indicating minimum resonance stabilisation via intramolecular nitrogen participation.

Of further interest is the highly abundant fragments m/e 145 (base peak) and m/e 139 (rel. ab. 69%) observed for (6), whereas in the case of the triester (4), these ions are considerably less abundant. Fragmentation of the molecular ion (m/e 346) occurs with H abstraction to give rise to the two stable molecular ions, 8-hydroxyquinoline (m/e 145) and 4-nitrophenol (m/e 139).

The behaviour of the diester (6) in the gas phase differs markedly from that of its triester precursor (4) and does not parallel that observed in solution[15].

2.5 ALKALINE HYDROLYSIS STUDY

The possible catalytic effect of an intramolecular nitrogen function on the hydrolysis of phosphate triester (4) was explored in view of the previously observed great rate enhancements for the hydrolyses of notoriously stable phosphate diester analogues.

The mechanism (equation 6) could be proposed to involve intramolecular nucleophilic attack on the phosphorus displacing 4-nitrophenoxide via a five-membered cyclic intermediate which is subsequently rapidly hydrolysed to the diester product. Thereafter a second 4-nitrophenoxide may be similarly released to yield the monoester in accordance with the hydrolysis proposal by Loran and Williams[15].

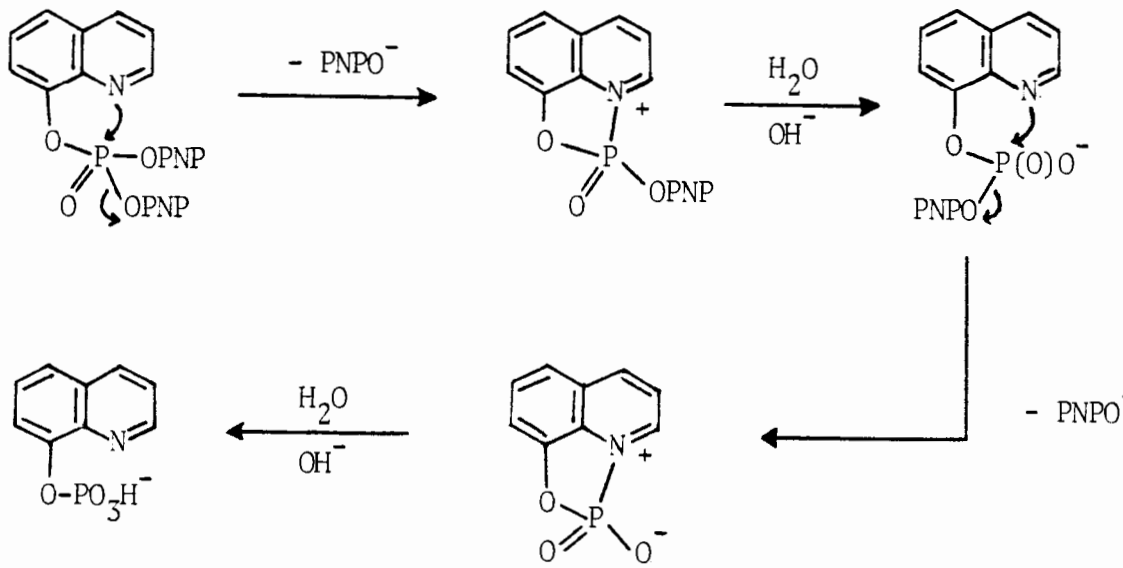

...(6)

Preliminary spectrophotometric scanning experiments indicated that both esters (4) and (5) were hydrolysed in aqueous solutions of NaOH in a 1:2 stoicheiometry, the molar quantity of 4-nitrophenoxide released being double the amount of ester used as substrate. However the step measured in the kinetic experiments was the cleavage of the first 4-nitrophenyl ester linkage, the very slow

release of the second occurring only after completion of the first and the possible cleavage of the P-OAr bond providing if any, a negligible contribu=tion.

$$ArO\text{-}P(O)(OPNP)_2 \xrightarrow{H_2O,\ OH^-} ArO(PNPO)PO_2^- + PNPO^- \quad ...(7)$$

Ar = 8-Quinolinyl in (4) and 1-Naphthyl in (5)

The hydrolysis reactions were carried out in a large excess of NaOH in the absence of buffers* so the rate equation may be represented as

$$Rate = k_{obs}\,[S] \quad ...(8)$$

and the observed, pseudo first-order rate constant as,

$$k_{obs} = k_{spont} + k_{OH^-}\,[OH^-] \quad ...(9)$$

For the simple triester (5), k_{spont} represents the rate constant for the hydrolysis by water alone whereas for substrate (4) it can include any catalytic effect arising due to the presence of the tertiary quinolinyl nitrogen.

The rate constants obtained for the hydrolysis of phosphates (4) and (5) are summarised in Table 2.24.

The k_{obs} versus $[OH^-]$ plots for triesters (4) and (5) are linear (r = 0,994 and 0,997 respectively) with slopes and intercepts yielding the following individual rate constants:

---

*The rate determinations in buffered solutions of constant ionic strength have also been attempted. It was found however that the reaction rate depends on the buffer concentration indicating catalysis by some of the buffer components. Since the objective of the rate study was to find evidence for intramolecular catalysis in (4), the more complex kinetic measurements under buffered condi=tions have been abandoned.

TABLE 2.24 Observed Rate Constants for the hydrolysis of bis(4-nitrophenyl)-8-quinolinyl phosphate (4) and 1-naphthyl-bis(4-nitrophenyl) phosphate (5) in aqueous NaOH; 25,0°C; $[S]_o = 1,5 \times 10^{-5}$M

[NaOH]	$10^3 \times k_{obs}$ (s^{-1}) [a]	
M	(4)	(5)
0,0010	0,91	
0,0016	1,23	
0,0025	1,59	0,19
0,0037	2,38	0,29
0,0050	2,79	0,34
0,0075		0,53
0,0100		0,68

[a] Average of two to three runs; ±3-6%

Triester	$10^2 \times k_{OH^-}$ ($s^{-1}M^{-1}$)	$10^2 \times k_{spont}$ (s^{-1})
(4)	47,8	0,046
(5)	6,5	0,0031

The phosphate triester derived from 8-hydroxyquinoline is more reactive than its 1-naphthyl analogue. However, the increase in reactivity with respect to the "spontaneous" rate constant, k_{spont}, (k_{rel} = 14,8) is only about twice as big as the increase with respect to the "specific" rate constant, k_{OH^-} (k_{rel} = 7,3). Although the intramolecular catalytic effect of the nitrogen is known to be greater in phosphoric diesters than in the triesters[18], reactivity data for substrates (4) and (5) provide little evidence for any significant specific effects of this type in triester (4). Furthermore as in triester (5) a hydroxide concentration term is noticed in the hydrolysis of the quinolinyl triester, indicating the nucleophilic participation of the hydroxide ion. The seven-fold increase in the k_{OH^-} value observed for (4) relative to (5) is as a result of the inductive effect of the quinolinyl nitrogen atom, which by increasing the electron deficiency of the phosphorus atom, lowers the activation energy for the approach of the hydroxide ion. The extrapolated k_{spont} values obtained from the intercepts of the plots are less accurate, so the value of k_{rel} must only be considered as approximate. If the general inductive effect of the quinolinyl nitrogen upon the rate of hydrolysis by neutral water is subtracted from the relative reactivity, then the increase in the reactivity of (4) relative to (5), due to any "specific" catalytic effect of the nitrogen, does not exceed a factor of two. Such a rate enhancement (if any at all) contrasts sharply to the factor of 350 observed by Loran and Williams[15] for the analogous diesters.

The intermolecular approach of the strong charged nucleophile (OH^-) to the phosphoryl centre of triester (4) thus appears to be far more effective as the

intramolecular attack by the tertiary quinolinyl nitrogen involves unfavourable angle strain. In addition, in aqueous media the nucleophilicity of this nitrogen atom is significantly decreased due to its certain involvement in hydrogen bond formation. In the diester case[15] (1) however, the presence of the negative charge on the substrate makes the approach of the OH^- ion more difficult, relative to the intramolecular attack of the electrically neutral nitrogen atom, hence creates better conditions for intramolecular catalysis.

Comparative hydrolysis investigations undertaken in this laboratory, involving active triesters derived from 2-pyridylmethyl- and 2-pyridylethyl-phosphates have yielded almost identical results.

The kinetic studies do not support the proposed intramolecular mechanism (equation 6) even though anchimeric assistance is clearly demonstrated in the solid state and in the gas phase after electron-impact induced activation of the molecule.

Experimental

Rate Measurements

Hydrolyses of the triesters (4) and (5) were carried out at 25±0,5°C in standardised NaOH (0,001 - 0,01M) in a 1cm quartz cell in the thermostatted cell compartment of a Beckman UV-vis 5260 spectrophotometer. Stock solutions of the esters (1,8 x 10^{-3}M) were prepared in dioxane. Reactions were initiated by the addition of stock solution (25µl) by means of a calibrated syringe to the NaOH (3ml) in a cuvette which had been equilibrated for 15 minutes in the cell holder. The hydrolyses of the triesters were monitored for the first 4-nitrophenoxide release at 405nm (ε = 1786m^2mol^{-1}). The extinction coeffi= cient was determined from a linear (r = 0,999) Beer Lambert's plot of Absor= bance versus concentration (1,7 x 10^{-5} - 4,3 x 10^{-5}M NaOH). Reactions were followed for three half-lives and infinity readings taken after ten. Pseudo first-order rate constants (k_{obs}) were calculated from the slopes of linear plots (r = 0,997 - 0,999) of $\ln(A_\infty - A_t)$ versus time; A_t being the absorbance at time t and A_∞ the absorbance at infinite time. Kinetic runs for triesters (4) and (5) were performed in duplicate and triplicate respectively. The calculated rate constants were reproducible to 3-6% of the average value.

Chemicals

The solvent dioxane was of AnalaR grade and was further purified by distil= lation. The standard NaOH solution was obtained from BDH Chemicals Ltd and prepared using glass distilled water. The substrates were recrystallised as mentioned previously.

CHAPTER 3

CHAPTER 3

THE CRYSTAL AND MOLECULAR STRUCTURE OF 1-NAPHTHYL ACETATE (7)

3.1 INTRODUCTION

As a continuation of the investigation of intramolecular catalytic effects attempts were made to establish whether nitrogen-carbonyl carbon interactions were present in analogous carboxylic derivatives.

Compounds (7) and (8) were synthesised in order to compare the structural effects operating in (8) with that of its analogue (7) in which no specific intramolecular interactions can be expected.

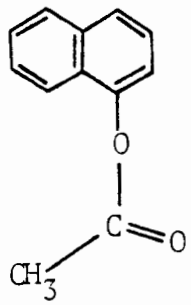

(7)

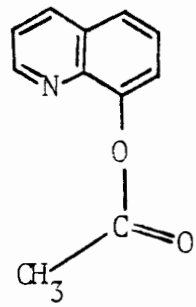

(8)

Nucleophilic displacement at a carbonyl group generally proceeds via tetra= hedral intermediate states to produce a new trigonal centre. Features of the reaction paths for addition/elimination processes involving carbonyl centres have been revealed by structural correlations. The most complete information available concerns molecules containing amino and carbonyl groups. Several examples of unusually short intramolecular N...C distances (ranging from 1,9Å to 2,9Å) have been uncovered by crystal structure analysis. In these molecules, including alkaloids and related structures[39], the carbonyl grouping RR'C=O deviates from the usual coplanar geometry. The carbonyl carbon atom is dis= placed from the plane of the three substituents towards the approaching nitrogen

atom (see Figure 3.1).

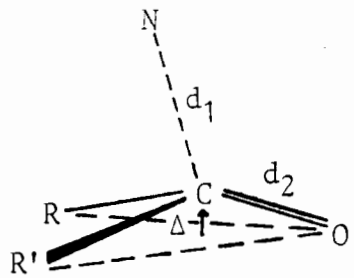

FIGURE 3.1 Interaction of the carbon atom of a carbonyl grouping RR'C=O with a nearby nucleophile (N).

Analytical relationships describe the correlation between the observed out of plane displacement, Δ, and the N...C distances, d_1, and C-O distances, d_2,[40] thereby graphically providing a vivid picture of the geometrical changes that occur during the addition reaction. These results show that as the N...C distance decreases, the carbonyl carbon is increasingly displaced from the plane of its three ligands towards nitrogen and the C-O distance increases. Furthermore, the approach of the nucleophile is along a direction at approximately 109° to the C-O bond and not, as might have been expected, perpendicular to it. There is obviously a preferred orientation for nucleophilic attack of an amine on a carbonyl group, with the lone pair roughly coincident with the N...C direction, i.e. at about 109° to the C-O bond.

An interesting and striking example of crystal distortion from ideal geometry, in order to accommodate intramolecular nucleophilic approach, is seen in the 1,8-disubstituted naphthalene derivatives (9a-c)[41].

The exocyclic C-C bond is splayed outward but the C-N bond is splayed inward; this gives an N...C=O angle of about 100° and tends to orient the lone pair

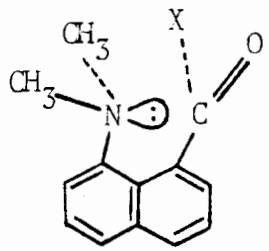

(9) (a) X=OH; (b) X=OMe; (c) X=Me

towards the N...C direction. Thus, the usual pattern of bond angles is distorted to bring the amine nitrogen into a more favourable position for attack than is possible in the undistorted molecule.

3.2 EXPERIMENTAL, SOLUTION AND REFINEMENT AND DESCRIPTION OF (7)

Experimental

1-Naphthyl acetate (7) was synthesised[42] according to the following reaction:

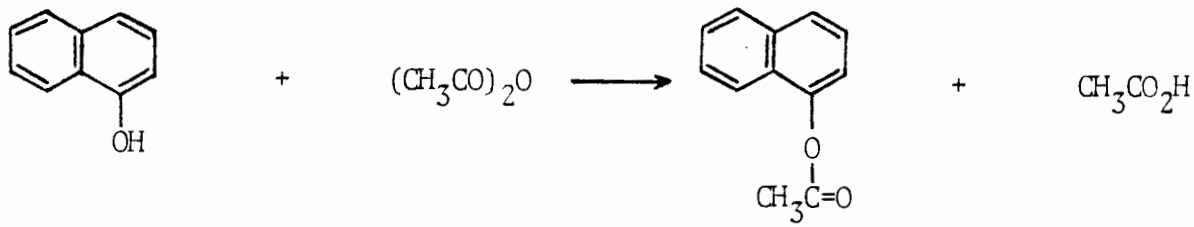

To a solution of 1-naphthol (0,02mol) in 20% aqueous NaOH (12,5ml) crushed ice (30g) and acetic anhydride (2,75ml) was added. The mixture was stirred for a ½ hour, the precipitate filtered off and thoroughly washed with water. After drying the crude product was recrystallised from petroleum ether (30-40°C) to produce transparent, rectangular, single crystals suitable for X-ray diffraction. m.p. 44-46°C. Anal. Calculated for $C_{12}H_{10}O_2$: C = 77,42%, H = 5,38%. Found: C = 77,35%, H = 5,45%.

The crystal density was determined by flotation in a calibrated density column[43] containing a saturated potassium iodide-water mixture.

A suitable crystal was selected under the polarising microscope and accurate unit cell parameters were determined by a least-squares analysis of the setting angles of 24 reflections, ($16^\circ \leq \theta \leq 17^\circ$; graphite monochromated MoK_α radiation), automatically located and centred on the Enraf-Nonius CAD4 diffractometer. The reflection data, collected at room temperature, were corrected by a Lorentz-polarisation factor and an empirical absorption correction[44] was applied.

Solution and Refinement

All relevant crystallographic data are given in Table 3.1.

The structure was solved in the non-centrosymmetric $P2_12_12_1$[23] space group using the SHELXS-84[26] direct methods routine. All the non-hydrogen atoms were revealed in the *E*-map. The positions of all the aromatic hydrogen atoms were located in a difference electron-density map calculated after three cycles of least-squares refinement. In the final refinement the heavy atoms (excluding C(15) and C(20)*) were treated anisotropically, the methyl hydrogen atoms refined as a rigid group and the aromatic hydrogen atoms constrained at 1,00Å from their respective carbon atoms, their positions dictated by the molecular geometry. A final difference electron-density map calculated after the final least-squares refinement revealed no peaks > 0,1eÅ^{-3}. An analysis of variance, listed in Table 3.2, indicates successful convergence and in the final cycle of refinement, the average shift to error ratio was less than 0,03. Upon reversing all the atomic coordinates, the final refinement yielded an identical *R* value. The absolute structure could therefore not be established by a Hamilton's significance test[45] of the *R*-factor ratio. A second more sophisticated procedure (see Appendix 3) was employed to establish the absolute structure, but this also failed.

The final fractional atomic coordinates and thermal motion parameters are given in Tables 3.3 and 3.4 respectively. Lists of observed and calculated structure factors are given on Microfilm in Appendix 2.

*

C(15) and C(20) were left as isotropic in the final refinement because there were insufficient reflection data for the required number of parameters.

TABLE 3.1 Crystal Data and Experimental and Refinement Parameters for Compound (7)

Crystal Data	
Molecular formula	$C_{12}H_{10}O_2$
Molecular weight	$186,21 gmol^{-1}$
Space group	$P2_12_12_1$
a	$5,46(1)\AA$
b	$9,814(3)\AA$
c	$18,090(4)\AA$
$\alpha = \beta = \gamma$	90^o
V	$969,16\AA^3$
Z	4
D_m	$1,26 gcm^{-3}$
D_c	$1,28 gcm^{-3}$
$\mu(MoK_\alpha)$	$0,5 cm^{-1}$
$F(000)$	392
Data Collection	
Crystal dimensions	1,10 x 0,41 x 0,12mm
Scan mode	ω-2θ
Scan width ($\Delta\omega$)	$(0,84 + 0,35\tan\theta)^o$
Aperture width (Horizontal)	$(1,47 + 1,05\tan\theta)$mm
Aperture width (Vertical)	4mm
Range scanned	$1^o \leq \theta \leq 25^o$
Stability of standard reflections	1,23%
Number of reflections collected	1053
Number of "observed" reflections	797
Final Refinement	
Number of variables	123
$R=\Sigma\|\|F_o\|-\|F_c\|\|/\Sigma\|F_o\|$	0,037
$R_w=\Sigma w^{\frac{1}{2}}\|\|F_o\|-\|F_c\|\|/\Sigma w^{\frac{1}{2}}\|F_o\|$	0,035
Weighting scheme w	$(\sigma^2 F)^{-1}$
U_{iso} (aromatic H's)	$0,075(4)\AA^2$
U_{iso} (methyl H's)	$0,114(9)\AA^2$

TABLE 3.2 Analysis of Variance for Compound (7)

a) By parity groups

Group	*ggg*	*ugg*	*gug*	*uug*	*ggu*	*ugu*	*guu*	*uuu*	All
N	119	100	102	90	104	93	101	88	797
V	42	38	33	40	35	34	41	38	38

b) As a function of sinθ

sinθ	0,00 - 0,17	- 0,23	- 0,26	- 0,29	- 0,32	- 0,34	- 0,36	- 0,38	- 0,40	- 0,43
N	80	99	61	86	91	85	79	67	79	70
V	63	46	39	37	33	30	30	25	29	27

c) As a function of $\sqrt{(F/F_{max})}$

$\sqrt{(F/F_{max})}$	0,00 - 0,19	- 0,21	- 0,23	- 0,26	- 0,28	- 0,32	- 0,36	- 0,41	- 0,49	- 1,00
N	93	75	82	95	57	102	72	66	80	75
V	24	26	35	35	33	34	31	37	42	66

d) As a function of |Miller index|

$\|h\|$	0	1	2	3	4	5	6	7	8	9	10	11	12	13	REST
N	137	178	160	133	107	60	22	0	0	0	0	0	0	0	0
V	39	44	39	32	36	26	35	0	0	0	0	0	0	0	0

$\|k\|$	0	1	2	3	4	5	6	7	8	9	10	11	12	13	REST
N	80	96	98	96	87	87	78	59	51	37	22	6	0	0	0
V	46	47	37	41	39	33	39	29	24	28	24	16	0	0	0

$\|l\|$	0	1	2	3	4	5	6	7	8	9	10	11	12	13	REST
N	52	58	58	57	53	52	50	46	50	46	45	43	41	35	111
V	46	46	48	40	40	42	46	31	34	39	30	34	29	25	28

N = Number of reflections in the group; $V = 100[M\Sigma(w|F_o-F_c|^2)/N\Sigma w]^{\frac{1}{2}}$; M = Total number of reflections.

TABLE 3.3 Fractional Atomic Coordinates ($x10^4$) with estimated standard deviations in parentheses for Compound (7)

Atom	*x/a*	*y/b*	*z/c*
C(1)	623(7)	5323(3)	5494(2)
C(2)	-1515(7)	5780(4)	5053(2)
O(11)	202(4)	4054(2)	5766(1)
O(12)	2467(5)	5925(3)	5622(2)
C(11)	2027(6)	3442(3)	6203(2)
C(12)	3831(6)	2711(3)	5882(2)
C(13)	5522(6)	2006(3)	6322(2)
C(14)	5335(6)	2052(3)	7074(2)
C(15)	3464(6)	2806(3)	7423(2)
C(16)	3231(7)	2882(3)	8202(2)
C(17)	1433(7)	3623(3)	8519(2)
C(18)	-257(7)	4349(3)	8085(2)
C(19)	-100(6)	4309(3)	7328(1)
C(20)	1756(6)	3542(3)	6983(1)
H(21)	-1156(7)	6738(4)	4899(2)
H(22)	-3105(7)	5753(4)	5327(2)
H(23)	-1625(7)	5187(4)	4605(2)
H(12)	3962(6)	2673(3)	5331(2)
H(13)	6866(6)	1469(3)	6085(2)
H(14)	6546(6)	1542(3)	7383(2)
H(16)	4418(7)	2378(3)	8522(2)
H(17)	1302(7)	3656(3)	9070(2)
H(18)	-1576(7)	4896(3)	8328(2)
H(19)	-1307(6)	4827(3)	7021(1)

Hydrogen atoms were subjected to constrained refinement.

TABLE 3.4 Anisotropic and Isotropic Thermal Motion Parameters ($Å^2 \times 10^3$) of the Non-Hydrogen Atoms with estimated standard deviations in parentheses for Compound (7)

Atom	U_{11}	U_{22}	U_{33}	U_{12}	U_{13}	U_{23}
C(1)	56(2)	43(2)	46(2)	1(2)	5(2)	2(2)
C(2)	70(3)	60(2)	53(2)	15(2)	-9(2)	4(2)
O(11)	54(1)	50(1)	51(1)	-8(1)	-16(1)	9(1)
O(12)	67(2)	61(2)	122(2)	-14(2)	-16(2)	29(2)
C(11)	48(2)	36(2)	48(2)	-7(2)	-6(2)	3(1)
C(12)	63(2)	49(2)	51(2)	-3(2)	4(2)	-3(2)
C(13)	53(2)	49(2)	74(2)	7(2)	5(2)	-6(2)
C(14)	53(2)	46(2)	68(2)	3(2)	-11(2)	6(2)
C(16)	61(2)	57(2)	52(2)	-3(2)	-12(2)	11(2)
C(17)	73(3)	70(3)	44(2)	-12(2)	3(2)	3(2)
C(18)	64(2)	64(2)	57(2)	-3(2)	9(2)	-8(2)
C(19)	47(2)	45(2)	51(2)	-5(2)	0(2)	2(2)

Atom	U_{iso}
C(15)	45(1)
C(20)	41(1)

Description of the structure

A perspective view of the compound with atomic nomenclature is shown in Figure 3.2. Bond lengths and angles are listed in Table 3.5.

The geometry at the carbonyl centre, C(1), corresponds to the sp^2 bonding arrangement, with the usual deviations expected for a carbon atom forming one double and two single bonds. The O(12)=C(1)-C(2) angle (128,3°) deviates considerably from the ideal 120° and narrowing of the O(11)-C(1)-C(2) angle (109,8°) results due to the greater repulsive effect exerted by the multiple bonding orbitals in the carbonyl bond. The C(1)-O(11), C(1)-C(2) and C(1)=O(12) bond lengths (see Figure 3.3) are slightly shorter than the typical values[46] observed for the corresponding single and double bonds (C-O = 1,41Å, C-C = 1,54Å, C=O = 1,22Å).

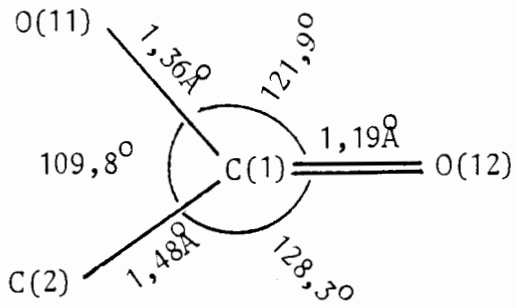

FIGURE 3.3 Bond Lengths and Angles subtended about the sp^2 carbon atom.

In addition the C(1) atom is displaced approximately 0,01Å from the plane of the three substituents, O(11), C(2) and O(12).

The naphthyl moiety has the regular geometry and is planar to within 0,01Å (see Table 3.6).

A packing diagram for compound (7) is shown in projection along the [100]

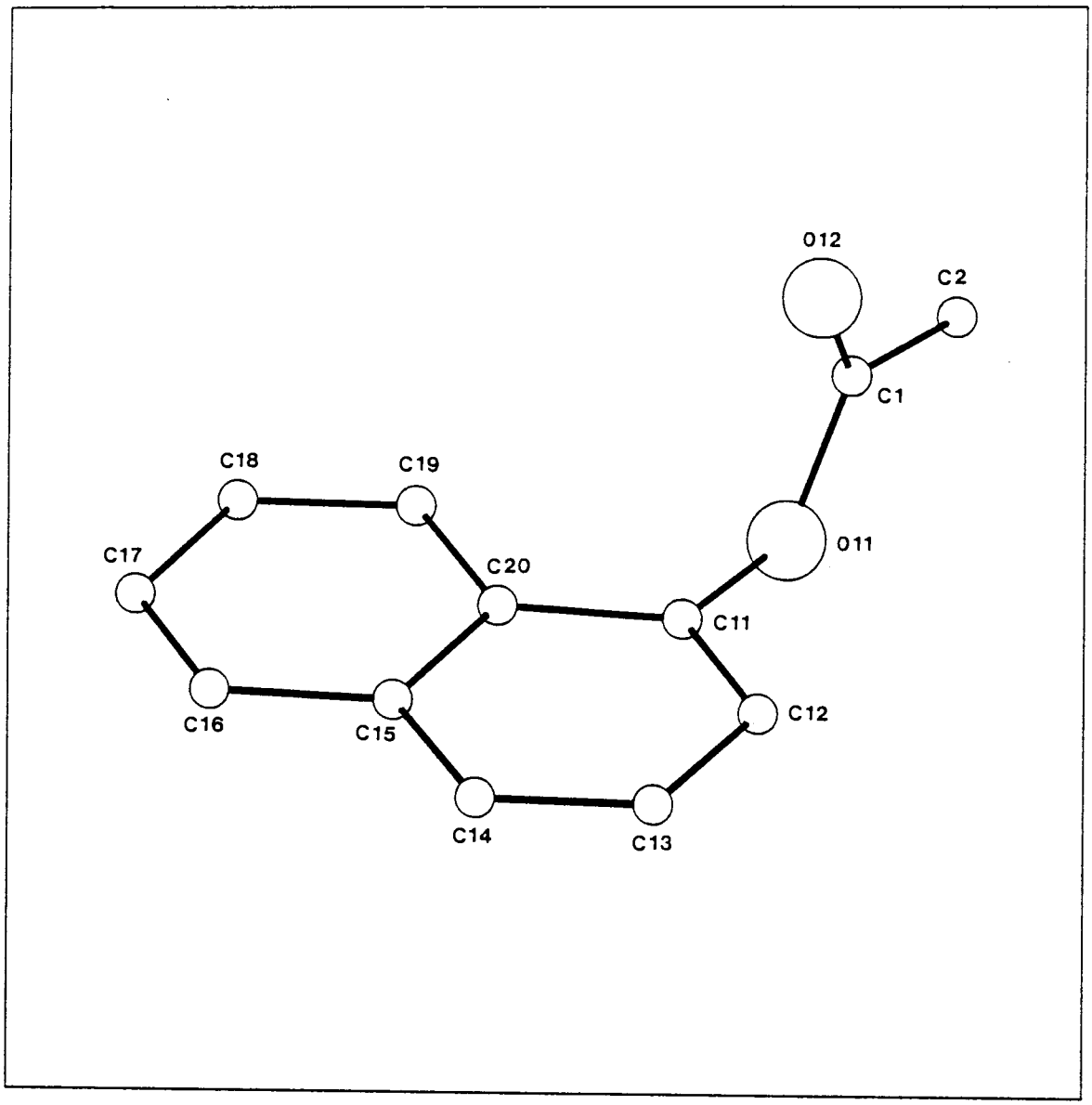

FIGURE 3.2 A perspective view of 1-naphthyl acetate (7)

TABLE 3.5 Bond Lengths (Å) and Angles (°) with estimated standard deviations in parentheses for Compound (7)

Bond Lengths	
C(1) - C(2)	1,483(4)
C(1) - O(11)	1,358(4)
C(1) - O(12)	1,190(4)
O(11) - C(11)	1,407(3)
C(11) - C(12)	1,350(4)
C(12) - C(13)	1,402(4)
C(13) - C(14)	1,365(4)
C(14) - C(15)	1,410(4)
C(15) - C(16)	1,416(4)
C(15) - C(20)	1,424(4)
C(16) - C(17)	1,350(4)
C(17) - C(18)	1,406(4)
C(18) - C(19)	1,372(4)
C(19) - C(20)	1,408(4)
C(20) - C(11)	1,422(3)
Bond Angles	
O(11) - C(1) - C(2)	109,8(3)
O(12) - C(1) - C(2)	128,3(3)
O(12) - C(1) - O(11)	121,9(3)
C(1) - O(11) - C(11)	118,4(3)
O(11) - C(11) - C(12)	120,1(3)
O(11) - C(11) - C(20)	117,0(3)
C(20) - C(11) - C(12)	122,7(3)
C(11) - C(12) - C(13)	119,9(3)
C(12) - C(13) - C(14)	120,1(3)

TABLE 3.5 Cont/....

TABLE 3.5 Continued

C(13) - C(14) - C(15)	121,2(3)
C(14) - C(15) - C(16)	122,5(3)
C(14) - C(15) - C(20)	119,4(3)
C(20) - C(15) - C(16)	118,1(3)
C(15) - C(16) - C(17)	121,1(3)
C(16) - C(17) - C(18)	120,9(3)
C(17) - C(18) - C(19)	120,1(3)
C(18) - C(19) - C(20)	120,2(3)
C(19) - C(20) - C(15)	119,6(2)
C(15) - C(20) - C(11)	116,9(3)
C(19) - C(20) - C(11)	123,5(3)

TABLE 3.6 Least-Squares Plane for Compound (7)

1 (a) Equation of least-squares plane expressed in orthogonalised space as $pX + qY + rZ = S$.

Plane 1 : The naphthyl ring atoms (C(11), C(12), C(13), C(14), C(15), C(16), C(17), C(18), C(19), C(20))

$3{,}2712X + 7{,}8556Y + 0{,}2586Z = 3{,}5366$

(b) Deviations from the plane ($\text{Å} \times 10^3$)

Atom	*Plane* 1
C(1)	991
C(2)	639
O(11)	-137
O(12)	2070
C(11)*	-9
C(12)*	-1
C(13)*	9
C(14)*	3
C(15)*	-8
C(16)*	-4
C(17)*	-2
C(18)*	5
C(19)*	6
C(20)*	1

direction in Figure 3.4.

The compound crystallises so as to pack four molecules in the orthorhombic unit cell in a repetitive alternating head-tail formation. No significant intra- or inter-molecular interactions are in evidence.

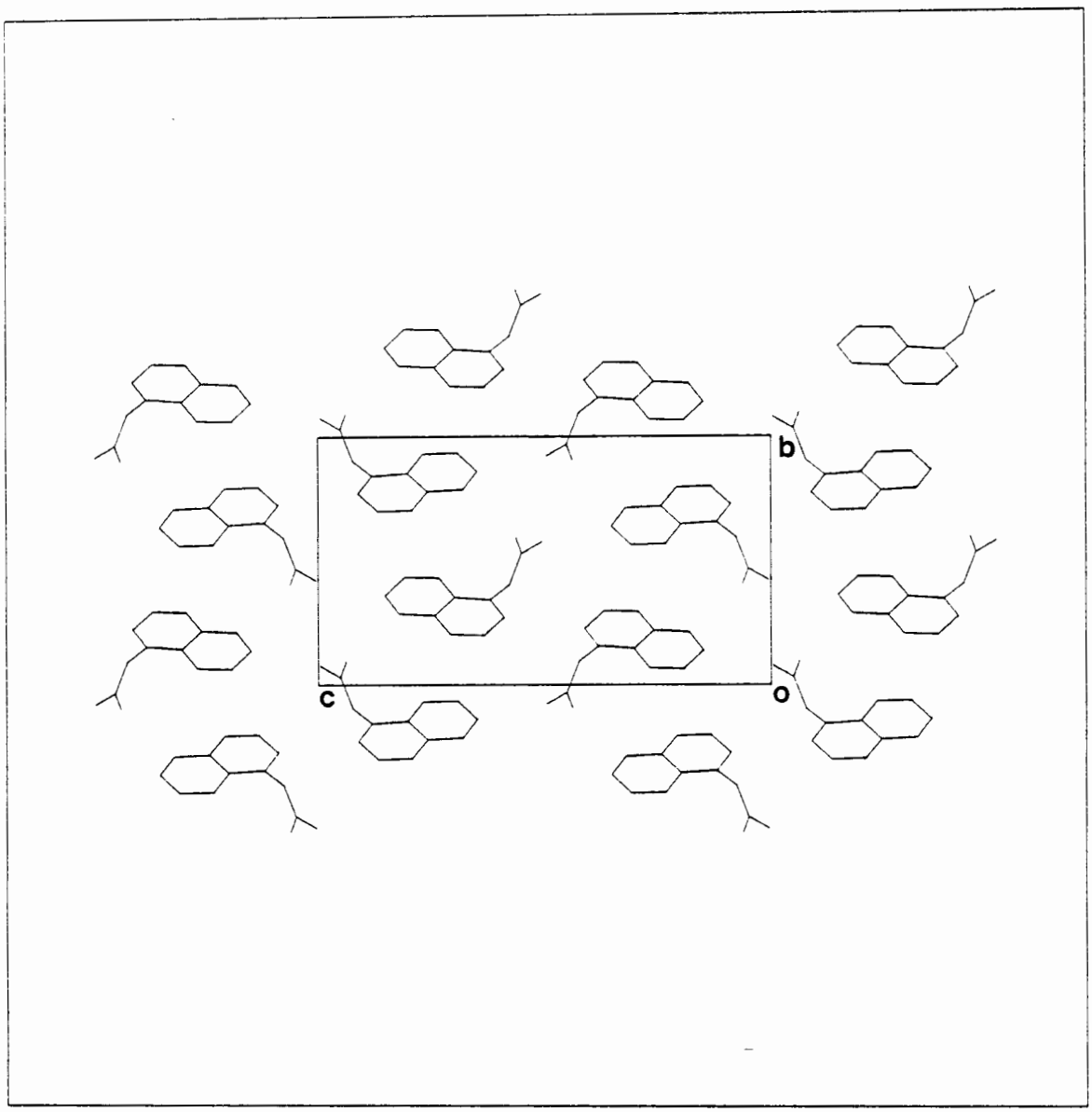

FIGURE 3.4 A packing diagram for compound (7) viewed along [100].

3.3 EXPERIMENTAL PERTAINING TO COMPOUND (8)

8-Quinolinyl acetate (8) was prepared as follows:

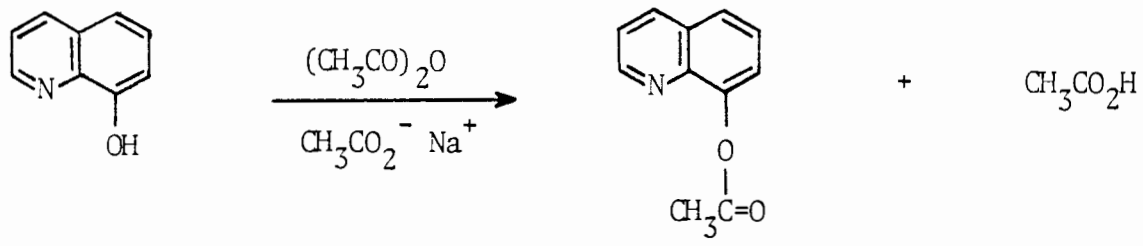

To a ground mixture of anhydrous sodium acetate (0,01mol) and 8-hydroxy= quinoline (0,02mol), acetic anhydride (3,5ml) was added. The solution was refluxed until it became clear and after further mild heating for 2 hours it was poured onto crushed ice (35ml). A white crystalline solid material separated with stirring and was filtered off and washed with cold water. After drying the crude product was recrystallised from a petroleum ether (80-100°C)-chloroform mixture to produce square, colourless single crystals of poor quality. m.p. 55-57°C. Anal. Calculated for $C_{11}H_9NO_2$: C = 70,58%, H = 4,85%, N = 7,48%. Found: C = 70,70%, H = 4,90%, N = 7,50%. ^{1}H NMR ^{1}H NMR ($CDCl_3$): δ2,48 (3H's,s), δ7,37 (3H's,m), δ7,63 (1H,m), δ8,17 (1H, d of d), δ8,88 (1H, d of d).

Oscillation and Weissenberg photography revealed a monoclinic space group with approximate cell parameters as follows: a = 8,48Å, b = 10,82Å, c = 21,70Å and Z = 8.

However, despite repetitive and patient effort crystals of sufficiently good quality for diffractometer data collection could never be grown. All crystal growing attempts, (in various combinations of suitable solvents) yielded poor quality specimens which had very broad peak profiles.

Reluctantly this aspect of the research had to be dropped.

3.4 CONCLUSION

As a result of the incomplete structure analysis, possible intramolecular nitrogen-carbon interactions operative in compound (8) could not be established.

A comparative study of the mass spectra[a] of compounds (7) and (8) was therefore of mechanistic interest in order to determine what effect, if any, the nitrogen heteroatom might have on the electron impact induced fragmentation pattern of compound (8)

In the mass spectrum of compound (7) the molecular ion (m/e 186) is observed and has a relatively low abundance (15%). By comparison the molecular ion (m/e 187) of compound (8) is far more unstable and is not observed. In both compounds the base peak is the stable molecular ion of the corresponding naphthol, i.e. 8-hydroxyquinoline (m/e 145) and 1-naphthol (m/e 144), respec= tively. These ions arise via the C-O bond cleavage with the accompanying hydrogen atom migration and expulsion of a neutral molecule of ketene:

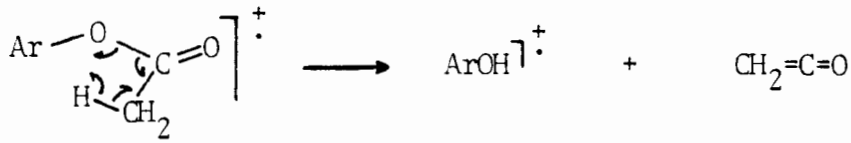

Ar = 8-hydroxyquinolinyl (8) or 1-naphthyl (7)

There is no indication of carboxylium ion formation in (8). This implies that intramolecular nucleophilic attack is viable only if there is a "good" leaving group present at the acyl centre and aligned approximately 180° to the incoming nucleophile as required in the typical SN_2 displacement reaction.

---

[a]The spectra were recorded at 70eV and an ion source temperature of 200°C.

CHAPTER 4

CHAPTER 4

HYDROGEN BONDING IN PHOSPHATE DIESTERS

4.1 INTRODUCTION

In order to improve the understanding of the nature of the "high-energy" phosphate bond and the mechanism of energy release in biological systems, several authors[47,48] have structurally analysed a number of so-called "high-" and "low-energy" phosphates. They attempt to relate precise measurements of selected molecular parameters to kinetic and thermodynamic properties of phosphate esters.

As a further contribution to the study of structure-reactivity relationships of phosphate esters, two different salts of phosphate diesters have been investigated. These compounds are hydrolysis products of bis(4-nitrophenyl) phosphorochloridate - salts of bis(4-nitrophenyl) phosphoric acid, $[X]^+ [(PNPO)_2PO_2]^-$ (PNPO = $4\text{-}NO_2C_6H_4O$; (10), $[X]^+ = [H_3O]^+$; (11), $[X]^+ = [Et_3NH]^+$).

In both cases the cations are O- and N-protonated "onium" species giving rise to interesting hydrogen bonding networks.

These compounds are of biological interest in that phosphate diesters represent substrates (or products) for phosphorylation reactions, often involving the hydrolysis of a phosphate ester with the concomitant cleavage of a so-called "high-energy" P~O bond. As mentioned previously, these processes occur in aqueous media hence hydrogen bonding to phosphate groups is an important factor in the free energy of phosphorylation. In a phosphorylation sequence involving

a series: phosphate triesters - diesters - monoesters - inorganic phosphate, hydrogen bonding ability increases with a decrease in the number of ester groups in a molecule. It has been demonstrated[49] that the affinity of phosphate esters to water increased rapidly in a series: tri-, di- and monoesters. It was also observed in this laboratory[50] that the rates of dealkylation of phosphate triesters to yield phosphate diester anions achieve maximum values in water as a medium, presumably because of the effective hydrogen bonding to the incipient phosphate ion in the transition state.

Many attempts have been made to understand the manner by which smaller molecules such as ATP, bind to macromolecular enzyme molecules and how this binding results in specific activity. The specificity of the interactions between oxygen and/or nitrogen containing molecules suggests that hydrogen bonding is important[51].

Kollman and coworkers[52] have carried out ab initio calculations (using a 4-31G basis set) on the interactions between dimethylphosphate and water and conclude that doubly hydrogen bonded structures (C) are energetically far more stable than linear ones (D).

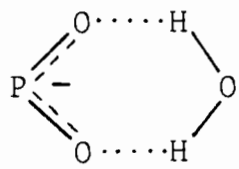

(C)

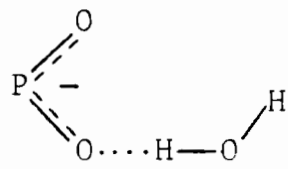

(D)

This is in accordance with Etter[53], who, in his study on carboxylic amides and acids, proposed that the maximum number of proton acceptor sites will participate in hydrogen bond formation.

In contrast, results obtained by Pullman et al.[54,55] from their ab initio

calculations (using a STO-3G basis set) indicate the linear structure (D) to be the more stable.

Of additional interest therefore was to examine the hydrogen bonding geometries of the phosphate salts (10) and (11).

4.2 THE CRYSTAL AND MOLECULAR STRUCTURES OF OXONIUM BIS(4-NITROPHENYL) PHOSPHATE (10) AND TRIETHYLAMMONIUM BIS(4-NITROPHENYL) PHOSPHATE (11)

4.2.1 EXPERIMENTAL, SOLUTION AND REFINEMENT OF (10)

Experimental

The compound was prepared by hydrolysis of bis(4-nitrophenyl)phosphoro= chloridate by water in benzene by gently heating under reflux. The white solid product was recrystallised as the oxonium salt from a petroleum spirit (80-100^{o}C)-chloroform mixture, producing single transparent rectangular crystals suitable for X-ray photography. m.p. 161-163^{o}C. Anal. Calculated for $C_{12}H_{11}N_2O_9P$: C = 40,24%, H = 3,10%, N = 7,82%. Found: C = 40,85%, H = 3,35%, N = 8,25%.

The crystal density was determined by flotation in a saturated ferric sulphate-water mixture.

Accurate cell parameters were determined by a least-squares analysis of the setting angles of 25 high order reflections ($16^{o} \leq \theta \leq 17^{o}$) automatically located and centred on the Enraf-Nonius CAD4 diffractometer. The intensities were collected with a ω-2θ scan to a final acceptance limit of 20σ at $0{,}3^{o}s^{-1}$ in ω and a maximum recording time of 40s. The data were corrected by a Lorentz-polarisation factor, but not for absorption because over the entire range of θ values scanned, the absorption correction factor, A*, remained equal to 1,0 (μR max.= 0,08, μR min.= 0,03).

Solution and Refinement

All relevant crystal data and experimental details are listed in Table 4.1.

The conditions for non-extinction of reflections uniquely determined the space group to be monoclinic $P2_1/c$[23]. The structure was solved using the program MULTAN[56]. The twenty-four non-hydrogen atoms that were revealed were refined by least-squares cycles using the SHELX-76[24] program system. The additional non-hydrogen atom that was revealed in close proximity to the phosphoryl oxygen atoms was intuitively thought to be an oxygen atom of a water molecule. By way of confirmation, this atom along with two other oxygen atoms were purposefully removed in the subsequent least-squares cycles. Scrutiny of the difference electron-density map obtained, revealed three peaks of very similar heights thus establishing the additional atom as an oxygen. Upon anisotropic treatment of all the non-hydrogen atoms R was lowered to 0,06 and all the hydrogen atoms were revealed. Subsequently a structure factor calculation was carried out omitting the oxonium hydrogens, and the difference electron-density map clearly revealed the positions of the three hydrogens of the oxonium ion as shown in Figure 4.1. In the final model the oxonium hydrogens were refined with O-H bond lengths constrained at 1,00±0,01Å, but with individual isotropic temperature factors while the hydrogens belonging to the anion were subjected to constrained refinement with a common isotropic temperature factor. In the final cycle of refinement the shift to error ratio for all parameters was always less than 0,03. A final difference electron-density map calculated after the final refinement revealed no peaks of height > 0,2eÅ^{-3}. An analysis of variance is shown in Table 4.2, indicating a satisfactory weighting scheme. Final fractional atomic coordinates and thermal motion parameters are listed in Tables 4.3 and 4.4. Observed and calculated structure factors are listed on Microfilm in Appendix 2.

TABLE 4.1 Crystal Data and Experimental and Refinement Parameters for Compound (10)

Crystal Data	
Molecular formula	$[H_3O]^+ [C_{12}H_8N_2O_8P]^-$
Molecular weight	358,20gmol^{-1}
Space group	$P2_1/c$
a	9,101(1)Å
b	6,316(1)Å
c	25,450(2)Å
β	96,28(1)°
V	1454,1Å^3
Z	4
D_m	1,62gcm^{-3}
D_c	1,64gcm^{-3}
$\mu(MoK_\alpha)$	1,90cm^{-1}
$F(000)$	736
Data Collection	
Crystal dimensions	0,43 x 0,40 x 0,20mm
Scan mode	ω-2θ
Scan width ($\Delta\omega$)	$(0,65 + 0,35\tan\theta)^\circ$
Aperture width (Horizontal)	$(1,30 + 1,05\tan\theta)$mm
Aperture width (Vertical)	4mm
Range scanned	$1^\circ \leq \theta \leq 20^\circ$
Stability of standard reflections	1,31%
Number of reflections collected	2873
Number of "observed" reflections	1902 with $I_{rel} > 2\sigma I_{rel}$
Final Refinement	
Number of variables	230
$R=\Sigma\|\|F_o\|-\|F_c\|\|/\Sigma\|F_o\|$	0,034
$R_w=\Sigma w^{\frac{1}{2}}\|\|F_o\|-\|F_c\|\|/\Sigma w^{\frac{1}{2}}\|F_o\|$	0,035
Weighting scheme w	$(\sigma^2 F)^{-1}$
U_{iso} (aromatic H's)	0,061(3)Å^2
U_{iso} (H(111))	0,091(11)Å^2
U_{iso} (H(112))	0,114(13)Å^2
U_{iso} (H(113))	0,111(13)Å^2

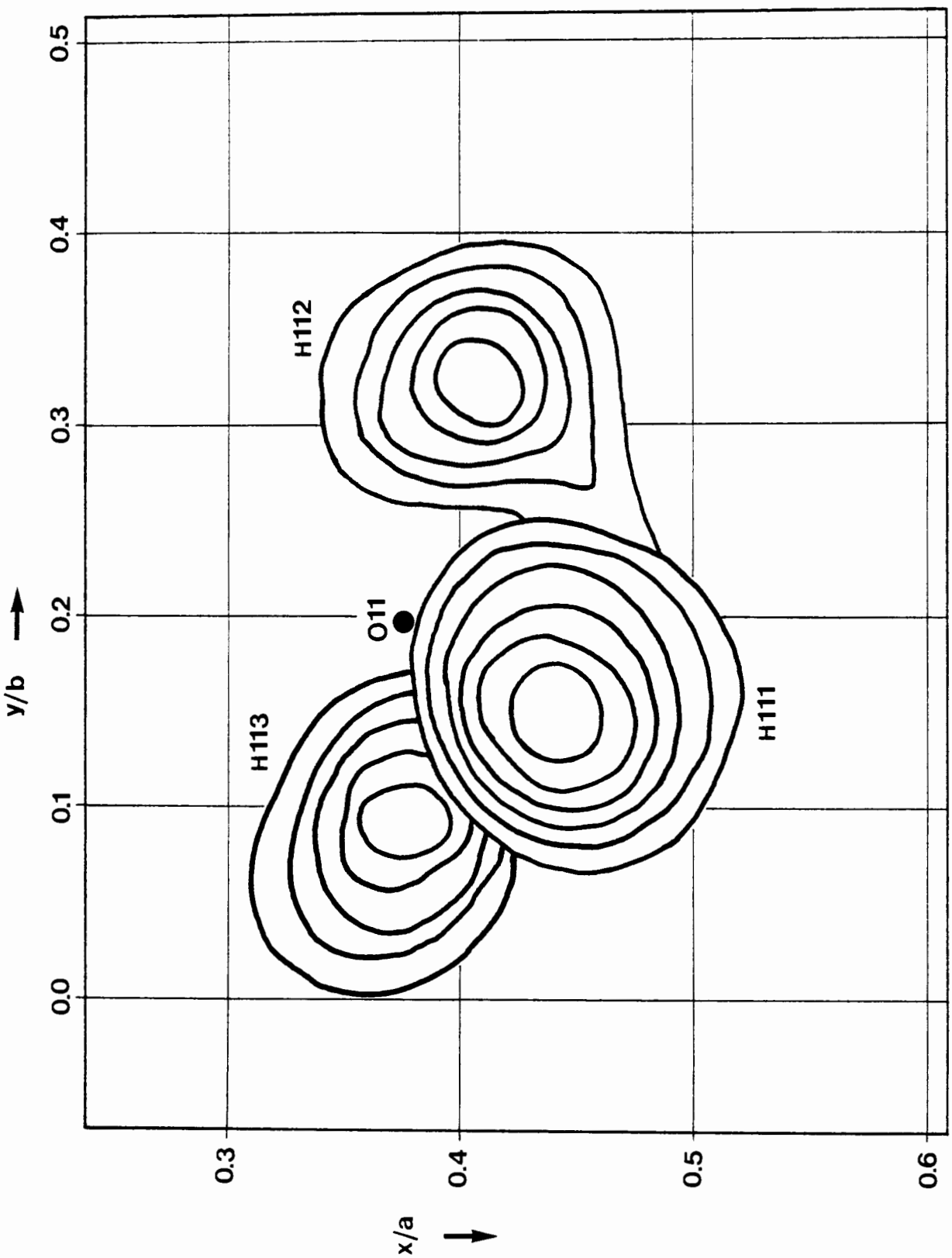

FIGURE 4.1 A difference electron-density map depicting the oxonium hydrogen atoms. Contours are at intervals of 0,05eÅ^{-3} with lowest contour at 0,2eÅ^{-3}.

TABLE 4.2 Analysis of Variance for Compound (10)

a) By parity groups

Group	*ggg*	*ugg*	*gug*	*uug*	*ggu*	*ugu*	*guu*	*uuu*	All
N	297	302	231	231	196	202	214	229	1902
V	68	68	58	64	66	66	62	57	64

b) As a function of sinθ

sinθ	0,00 - 0,19	0,23	0,27	0,30	0,32	0,34	0,36	0,39	0,41 - 0,43
N	214	166	224	209	158	181	179	268	192	111
V	108	79	58	52	55	51	56	49	51	51

c) As a function of $\sqrt{(F/F_{max})}$

$\sqrt{(F/F_{max})}$	0,00 - 0,15	0,18	0,20	0,21	0,24	0,26	0,29	0,33	0,39 - 1,00
N	205	254	216	90	257	163	178	178	182	179
V	53	63	68	66	61	58	65	54	54	93

d) As a function of |Miller index|

$\|h\|$	0	1	2	3	4	5	6	7	8	9	10	11	12	13	REST
N	146	277	278	260	225	217	163	149	103	61	23	0	0	0	0
V	72	77	74	68	59	54	52	47	54	50	36	0	0	0	0

$\|k\|$	0	1	2	3	4	5	6	7	8	9	10	11	12	13	REST
N	214	375	379	314	284	185	120	31	0	0	0	0	0	0	0
V	77	66	73	56	55	55	55	55	0	0	0	0	0	0	0

$\|l\|$	0	1	2	3	4	5	6	7	8	9	10	11	12	13	REST
N	55	87	104	93	106	89	104	88	96	81	97	71	81	70	680
V	76	63	77	68	75	66	63	64	93	74	61	62	54	64	53

N = Number of reflections in the group; $V = 100[M\Sigma(w|F_o-F_c|^2)/N\Sigma w]^{\frac{1}{2}}$; M = Total number of reflections.

TABLE 4.3 Fractional Atomic Coordinates ($x10^4$) with estimated standard deviations in parentheses for Compound (10)

Atom	*x/a*	*y/b*	*z/c*
P(1)	6051(1)	2097(1)	-1473(1)
O(1)	5450(2)	690(3)	-1911(1)
O(2)	6486(2)	4273(3)	-1592(1)
O(3)	4922(2)	2316(3)	-1042(1)
O(4)	7375(2)	920(3)	-1128(1)
C(31)	4171(2)	724(4)	-808(1)
C(32)	2877(3)	1351(4)	-618(1)
C(33)	2135(3)	-31(4)	-326(1)
C(34)	2692(2)	-2029(4)	-236(1)
C(35)	3943(2)	-2709(4)	-444(1)
C(36)	4694(3)	-1316(4)	-735(1)
N(34)	1944(2)	-3488(4)	97(1)
O(341)	738(2)	-2975(3)	228(1)
O(342)	2576(2)	-5137(3)	234(1)
C(41)	8560(2)	-59(4)	-1335(1)
C(42)	8929(3)	-2047(4)	-1145(1)
C(43)	10093(3)	-3106(4)	1328(1)
C(44)	10869(3)	-2114(4)	-1694(1)
C(45)	10520(3)	-105(5)	-1879(1)
C(46)	9338(3)	933(4)	-1699(1)
N(44)	12113(3)	-3238(5)	-1889(1)
O(441)	12823(2)	-2323(4)	-2198(1)
O(442)	12372(3)	-5041(4)	-1734(1)
O(11)	3725(2)	2009(3)	-2726(1)

TABLE 4.3 Cont/....

TABLE 4.3 Continued

Atom	*x/a*	*y/b*	*z/c*
H(32)	2479(3)	2807(4)	-695(1)
H(33)	1203(3)	411(4)	-182(1)
H(35)	4304(2)	-4193(4)	-384(1)
H(36)	5603(3)	-1776(4)	-892(1)
H(42)	8353(3)	-2725(4)	-877(1)
H(43)	10373(3)	-4559(4)	-1198(1)
H(45)	11112(3)	589(5)	-2140(1)
H(46)	9053(3)	933(4)	-1699(1)
H(111)	4433(24)	1642(49)	-2413(8)
H(112)	4059(35)	3353(31)	-2875(13)
H(113)	3644(35)	901(40)	-3007(10)

Hydrogen atoms were subjected to constrained refinement.

TABLE 4.4 Anisotropic Thermal Motion Parameters ($Å^2 \times 10^3$) of the Non-Hydrogen Atoms with estimated standard deviations in parentheses for Compound (10)

Atom	U_{11}	U_{22}	U_{33}	U_{12}	U_{13}	U_{23}
P(1)	44(0)	33(3)	33(3)	-2(0)	3(0)	3(0)
O(1)	53(1)	34(1)	39(1)	1(1)	-1(1)	-1(1)
O(2)	74(1)	38(1)	47(1)	-14(1)	4(1)	6(1)
O(3)	57(1)	34(1)	47(1)	4(1)	17(1)	3(1)
O(4)	45(1)	58(1)	38(1)	5(1)	4(1)	9(1)
C(31)	43(1)	35(1)	32(1)	0(1)	4(1)	-1(1)
C(32)	46(1)	36(1)	53(2)	9(1)	7(1)	-3(1)
C(33)	39(1)	46(2)	52(2)	7(1)	12(1)	-6(1)
C(34)	36(1)	41(1)	34(1)	-3(1)	3(1)	-2(1)
C(35)	41(1)	38(1)	53(2)	7(1)	10(1)	8(1)
C(36)	44(1)	40(1)	56(2)	10(1)	18(1)	5(1)
N(34)	46(1)	49(1)	43(1)	-7(1)	11(1)	-8(1)
O(341)	48(1)	72(1)	73(1)	-8(1)	26(1)	-7(1)
O(342)	71(1)	50(1)	67(1)	4(1)	25(1)	15(1)
C(41)	36(1)	47(2)	37(1)	-3(1)	0(1)	3(1)
C(42)	47(1)	49(2)	46(1)	-7(1)	2(1)	14(1)
C(43)	50(2)	43(2)	54(2)	0(1)	0(1)	6(1)
C(44)	43(1)	53(2)	46(1)	-2(1)	1(1)	-7(1)
C(45)	55(2)	60(2)	52(2)	-6(1)	15(1)	9(1)
C(46)	55(2)	43(2)	54(2)	-2(1)	9(1)	13(1)
N(44)	57(2)	76(2)	62(2)	8(1)	5(1)	-11(2)
O(441)	75(2)	107(2)	96(2)	2(2)	40(1)	-8(2)
O(442)	111(2)	88(2)	121(2)	44(2)	35(2)	12(2)
O(11)	56(1)	35(1)	43(1)	1(1)	-1(1)	0(1)

4.2.2 EXPERIMENTAL, SOLUTION AND REFINEMENT OF (11)

Experimental

Compound (11) was prepared by the hydrolysis of bis(4-nitrophenyl)phosphoro=chloridate in chloroform by water in the presence of triethylamine. The pale orange triethylammonium salt which formed, was recrystallised from a mixture of petroleum spirit (80-100°C) and chloroform producing transparent rectangular single crystals. m.p. 150-154°C. Anal. Calculated for $C_{18}H_{24}N_3O_8P$: C = 48,98%, H = 5,48%, N = 9,52%. Found: C = 49,20%, H = 5,50%, N = 9,50%. A mass spectrum revealed preferential fragmentation of the triethylammonium moiety at lower scan numbers thereafter decomposition of the bis(4-nitrophenyl) phosphate anion at higher scan numbers of the total ion current (see Table 4.5).

The crystal density was determined by flotation in a calibrated density column containing a saturated potassium iodide-water mixture[43].

Accurate cell parameters were obtained from a least-squares analysis of 25 standard reflections in the range $16^\circ \leq \theta \leq 17^\circ$ measured on the Enraf-Nonius CAD4 diffractometer. The intensities were collected with a ω-2θ scan to a final acceptance limit of 20σ at $0{,}3^\circ s^{-1}$ in ω and a maximum recording time of 40s. The reflection data were corrected for Lorentz-polarisation but not for absorption as the absorption correction factor A^*[23] equalled 1,0 (μR max.= 0,04, μR min.= 0,02) over the entire range of θ values scanned.

Solution and Refinement

Crystal data and experimental details of the intensity data collection are listed in Table 4.6.

TABLE 4.5 Selected Ions observed in the Mass Spectrum[a] of compound (11)

m/e	% Relative Abundance	Assignment
1st fragmentation pattern at low scan numbers		
102	4	$(CH_3CH_2)_3NH^+$
86	100	$(CH_3CH_2)_2NCH_2^+$
58	54	$(CH_3CH_2)NCH_3^+$
44	22	$(CH_3)_2N^+$
30	58	CH_3NH^+
2nd fragmentation pattern at higher scan numbers		
340	16	$(PNPO)_2P(O)OH^{]+\cdot}$
323	9	$(PNPO)_2P(O)^{]+\cdot}$
139	100	$PNPOH^{]+\cdot}$
93	24	$C_6H_4OH^{]+\cdot}$

[a]Operating conditions: 70eV and 200°C

TABLE 4.6 Crystal Data and Experimental and Refinement Parameters for Compound (11)

Crystal Data	
Molecular formula	$[C_6H_{16}N]^+ [C_{12}H_8N_2O_8P]^-$
Molecular weight	441,38gmol^{-1}
Space group	*Pc*
a	9,069(2)Å
b	8,616(2)Å
c	13,471(2)Å
β	96,23(1)°
V	1046,4Å^3
Z	2
D_m	1,39gcm^{-3}
D_c	1,40gcm^{-3}
$\mu(MoK_\alpha)$	1,37cm^{-1}
F(000)	464
Data Collection	
Crystal dimensions	0,28 x 0,25 x 0,16mm
Scan mode	ω-2θ
Scan width (Δω)	(0,60 + 0,35tanθ)°
Aperture width (Horizontal)	(1,13 + 1,05tanθ)mm
Aperture width (Vertical)	4mm
Range scanned	$1^\circ \leq \theta \leq 25^\circ$
Stability of standard reflections	1,36%
Number of reflections collected	2058
Number of "observed" reflections	1660 with $I_{rel} > 2\sigma I_{rel}$
Final Refinement	
Number of variables	195
$R=\Sigma\|\|F_o\|-\|F_c\|/\Sigma\|F_o\|$	0,058
$R_w=\Sigma w^{\frac{1}{2}}\|\|F_o\|-\|F_c\|\|/\Sigma w^{\frac{1}{2}}\|F_o\|$	0,061
Weighting scheme w	$(\sigma^2 F)^{-1}$
U_{iso} (aromatic H's)	0,074(8)Å^2
U_{iso} (methylene H's) fixed	0,100(-)Å^2
U_{iso} (methyl H's)	0,103(10)Å^2
U_{iso} (H(10)) fixed	0,100(-)Å^2

The structure was solved in the non-centrosymmetric Pc[23] space group by a direct methods routine of the SHELXS-84[26] program system. Virtually all the non-hydrogen atoms of the bis(4-nitrophenyl) phosphate molecule were located in the *E*-map. After a few cycles of least-squares refinement the remaining non-hydrogen atoms were located as well as a four-atom fragment belonging to a second molecule. Upon subsequent refinement a triethylamine moiety and most of the aromatic hydrogens were revealed where= upon *R* was lowered to 0,09. Refinement of the triethylamine cation gave considerable difficulty in that two of the carbon atoms, C(300) and C(310) yielded unrealistic bond lengths when allowed to refine independently. It was therefore decided to constrain the distances N(10)-C(300) = 1,53Å and C(300)-C(310) = 1,50Å.* Careful analysis of the difference electron-density maps revealed that N(10) was protonated and thus the N(10)-H(10) length was constrained to 1,053Å. This value was chosen as representing the typical hydrogen bonding geometry as extrapolated from a graph depicting N-H versus N...O distances for a large number of crystal structures[57a]. The final refine= ment was carried out with a mixture of anisotropic and isotropic thermal para= meters* assigned to the heavy atoms and common isotropic temperature factors assigned in groups to the aromatic, methylene and methyl hydrogens.
In the final refinement the average shift to error ratio for all parameters was 0,06. This value is higher than that obtained in all the other structural analyses and is attributed to the slight disorder of the triethylammonium cation.

The final refinement was repeated with all the atomic coordinates reversed and yielded an identical *R* value. The absolute structure could therefore not be determined in this way. As mentioned previously, a second, more sophisti= cated procedure (see Appendix 3) was employed to establish the absolute structure, but this also failed.

After the final refinement a difference electron-density map was calculated and no peaks with height > 0,4e$\mathring{A}^{-3}$ were revealed. An analysis of variance computed after the final refinement is given in Table 4.7. The final fractional atomic coordinates and thermal motion parameters are listed in Tables 4.8 and 4.9. Observed and calculated structure factors are listed on Microfilm in Appendix 2.

*

Atoms C(300) and C(310) proved troublesome in the refinement, yielding unreasonable bond lengths. This is probably due to partial disorder and was overcome by applying chemically reasonable bond length constraints.

#

Only the heavy atoms were treated anisotropically. Anisotropic treatment of all non-hydrogen atoms was not possible because there were insufficient reflection data for the required number of parameters.

TABLE 4.7 Analysis of Variance for Compound (11)

a) By parity groups

Group	*ggg*	*ugg*	*gug*	*uug*	*ggu*	*ugu*	*guu*	*uuu*	All
N	252	247	217	228	162	163	196	195	1660
V	81	87	83	74	67	74	61	67	76

b) As a function of sinθ

sinθ	0,00 - 0,19	0,24	0,27	0,30	0,33	0,35	0,37	0,39	0,41 - 0,43
N	189	176	152	174	217	153	158	180	169	92
V	116	85	68	75	76	71	62	63	51	52

c) As a function of $\sqrt{(F/F_{max})}$

$\sqrt{(F/F_{max})}$	0,00 - 0,18	0,20	0,22	0,24	0,26	0,29	0,32	0,36	0,43	1,00
N	209	134	193	161	153	174	162	151	165	158
V	58	60	72	78	74	86	75	71	79	98

d) As a function of |Miller index|

$\|h\|$	0	1	2	3	4	5	6	7	8	9	10	11	12	13	REST
N	115	241	228	225	206	174	157	132	95	61	26	0	0	0	0
V	93	90	80	78	69	67	67	69	63	52	52	0	0	0	0

$\|k\|$	0	1	2	3	4	5	6	7	8	9	10	11	12	13	REST
N	137	238	235	227	198	190	157	131	89	50	8	0	0	0	0
V	103	81	80	72	73	66	66	66	65	63	74	0	0	0	0

$\|l\|$	0	1	2	3	4	5	6	7	8	9	10	11	12	13	REST
N	167	141	170	135	155	126	141	106	118	95	102	69	58	35	42
V	85	80	87	60	91	63	82	73	70	65	77	61	54	48	71

N = Number of reflections in the group; $V = 100[M\Sigma(w|F_o-F_c|^2)/N\Sigma w]^{\frac{1}{2}}$; M = Total number of reflections.

TABLE 4.8 Fractional Atomic Coordinates ($x10^4$) with estimated standard deviations in parentheses for Compound (11)

Atom	*x/a*	*y/b*	*z/c*
P(1)	6539(-)	593(2)	4654(-)
O(1)	7083(5)	-540(5)	3964(3)
O(2)	5958(5)	2132(5)	4323(4)
O(3)	5304(5)	-334(5)	5217(4)
O(4)	7766(5)	964(5)	5586(3)
C(31)	4394(7)	356(7)	5839(5)
C(32)	4504(8)	-84(9)	6829(5)
C(33)	3576(8)	539(8)	7465(6)
C(34)	2554(8)	1627(8)	7089(5)
C(35)	2410(8)	2108(8)	6096(5)
C(36)	3344(7)	1451(8)	5468(5)
N(34)	1535(9)	2334(10)	7752(6)
O(341)	1676(9)	1906(10)	8611(6)
O(342)	620(9)	3237(10)	7397(7)
C(41)	8750(7)	-138(7)	6020(5)
C(42)	8763(7)	-404(7)	7028(5)
C(43)	9780(7)	-1418(8)	7504(5)
C(44)	10783(8)	-2125(8)	6969(5)
C(45)	10794(8)	-1858(8)	5967(5)
C(46)	9797(7)	-849(7)	5473(5)
N(44)	11904(7)	-3191(8)	7464(5)
O(441)	12733(7)	-3872(8)	6970(5)
O(442)	11932(7)	-3347(8)	8368(5)

TABLE 4.8 Cont/....

TABLE 4.8 Continued

Atom	*x/a*	*y/b*	*z/c*
N(10)	6497(6)	5060(6)	3879(4)
C(100)	6671(10)	4877(11)	2777(6)
C(110)	6823(10)	6355(11)	2236(7)
C(200)	5076(9)	5954(10)	3952(6)
C(210)	4474(10)	5709(11)	4918(6)
C(300)	7775(8)	5748(10)	4515(7)
C(310)	9098(9)	4714(10)	4715(7)
H(32)	5269(8)	-862(9)	7088(5)
H(33)	3633(8)	217(8)	8181(6)
H(35)	1651(8)	2896(8)	5844(5)
H(36)	3279(7)	1769(8)	4751(5)
H(42)	8033(7)	137(7)	7413(5)
H(43)	9789(7)	-1633(8)	8234(5)
H(45)	11540(8)	-2402(8)	5596(5)
H(46)	9812(7)	-633(7)	4745(5)
H(10)	6440(91)	3856(18)	4003(59)
H(100)	7591(10)	4257(11)	2723(6)
H(101)	5793(10)	4301(11)	2448(6)
H(110)	6967(10)	6030(11)	1541(7)
H(111)	5949(10)	7066(11)	2219(7)
H(112)	7731(10)	6908(11)	2541(7)
H(200)	5279(9)	7084(10)	3869(6)
H(201)	4321(9)	5601(10)	3402(6)
H(210)	3572(10)	6365(11)	4954(6)
H(211)	4260(10)	4621(11)	5118(6)
H(212)	5313(10)	6135(11)	5381(6)

TABLE 4.8 Cont/....

TABLE 4.8 Continued

Atom	*x/a*	*y/b*	*z/c*
H(300)	7430(8)	6024(10)	5173(7)
H(301)	8088(8)	6712(10)	4181(7)
H(310)	9911(9)	5261(10)	5138(7)
H(311)	9021(9)	3622(10)	4954(7)
H(312)	9321(9)	4710(10)	4004(7)

Hydrogen atoms were subjected to constrained refinement.

TABLE 4.9 Anisotropic and Isotropic Thermal Motion Parameters ($Å^2 \times 10^3$) of the Non-Hydrogen Atoms with estimated standard deviations in parentheses for Compound (11)

Atom	U_{11}	U_{22}	U_{33}	U_{12}	U_{13}	U_{23}
P(1)	44(1)	28(1)	43(1)	-1(1)	11(1)	3(1)
O(1)	57(3)	45(3)	39(3)	7(2)	7(2)	-4(2)
O(2)	54(3)	38(3)	72(3)	0(2)	11(2)	15(2)
O(3)	52(3)	33(2)	60(3)	-3(2)	23(2)	2(2)
O(4)	53(3)	38(2)	54(3)	-1(2)	5(2)	-12(2)
N(34)	66(5)	97(6)	82(6)	-35(5)	32(4)	-39(5)
O(341)	126(6)	166(8)	71(4)	-50(6)	48(4)	-36(5)
O(342)	84(5)	124(7)	135(7)	11(5)	47(5)	-39(6)
N(44)	61(4)	56(4)	57(4)	-6(3)	-4(3)	3(3)
O(441)	79(4)	97(5)	90(5)	38(4)	19(4)	13(4)
O(442)	90(5)	102(5)	70(4)	24(4)	-15(3)	12(4)

Atom	U_{iso}	*Atom*	U_{iso}
C(31)	39(1)	N(10)	49(1)
C(32)	51(2)	C(100)	81(2)
C(33)	59(2)	C(110)	91(3)
C(34)	52(2)	C(200)	76(2)
C(35)	51(2)	C(210)	86(3)
C(36)	47(2)	C(300)	88(3)
C(41)	39(1)	C(310)	86(3)
C(42)	44(2)		
C(43)	49(2)		
C(44)	44(2)		
C(45)	47(2)		
C(46)	44(2)		

4.2.3 DISCUSSION

The "high-energy" bond of biochemically energetic compounds such as ATP is in fact a group transfer potential and the free energy of phosphorylation is dependent on the nature of the reaction products as well as that of the reactants. It would be misleading therefore to analyse the molecular parameters of reactant molecules in isolation and make predictions as to their thermodynamic properties. Nevertheless certain geometrical observations can be made, and the results obtained for the title compounds may be compared with those of related structures.

Perspective views of compounds (10) and (11) with atomic nomenclature are shown in Figures 4.2 and 4.3 respectively. Bond lengths and angles are listed in Tables 4.10 and 4.11.

In substrates (10) and (11) the phosphorus is tetrahedrally coordinated to two 4-nitrophenoxy groups and two oxygen atoms. The geometry however is not perfectly regular, a slight widening of the O(1)-P-O(2) angles with concomitant narrowing of the PNPO-P-OPNP angles occurs as a result of the repulsive effect of the delocalised electron on the oxygen atoms.
In both compounds (10) and (11) the P-O(3) and P-O(4) bond lengths (on average 1,592Å for (10) and 1,622Å for (11)) are longer than the corresponding bonds (on average, 1,556Å) in dibenzylphosphoric acid[58]. This is in agreement with the 4-nitrophenoxy substituent being a better leaving group than the benzyloxy moiety. The P-O(1) and P-O(2) bonds may be regarded as chemically equivalent in both structures (10) and (11), with the electron pair delocalised between them.

The 4-nitrophenoxy ligands in (10) and (11) are planar to within 0,02Å and lie almost parallel with respect to each other, with a mere discrepancy of 9° in

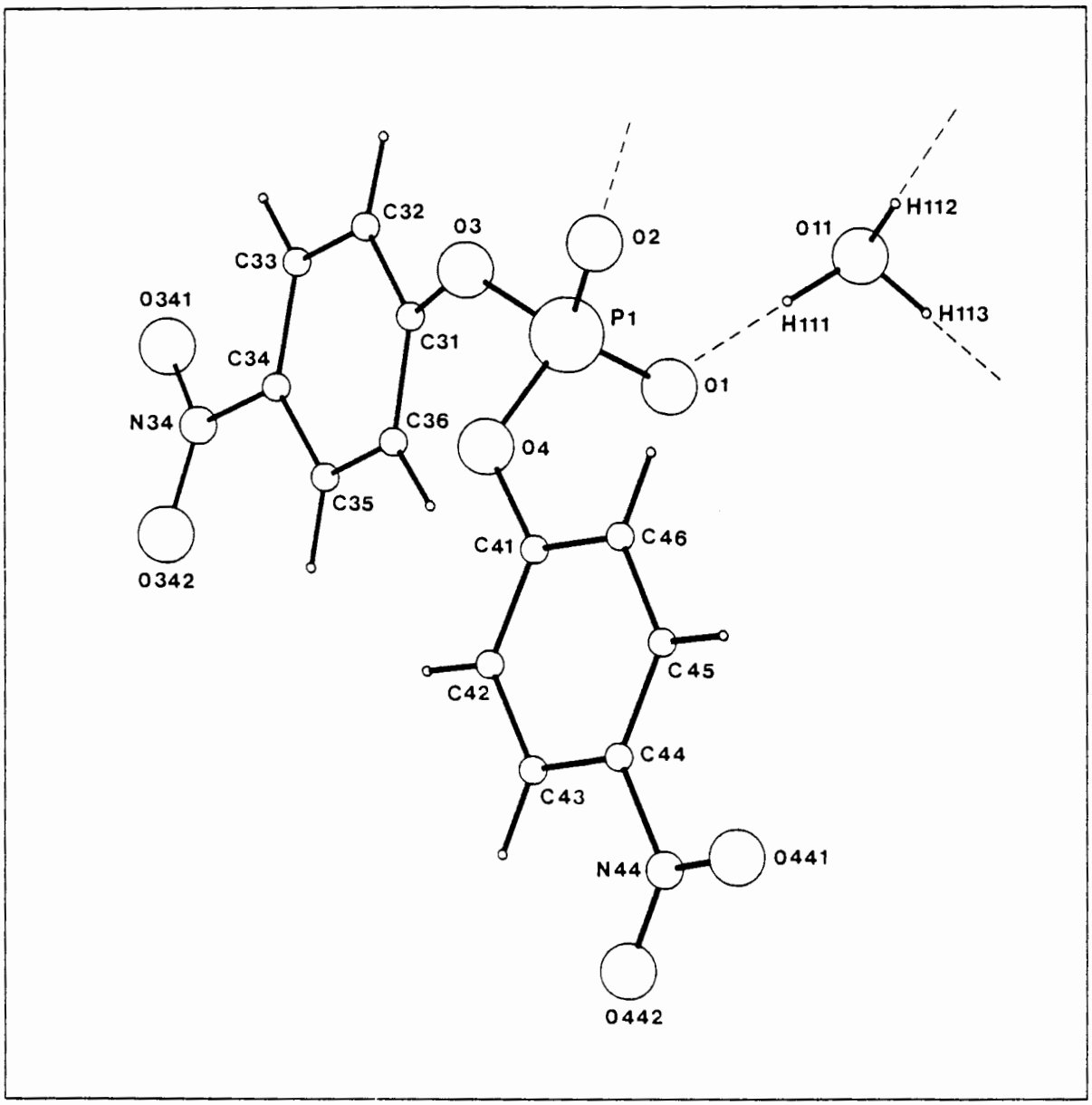

FIGURE 4.2 A perspective view of the oxonium bis(4-nitrophenyl)phosphate salt (10).

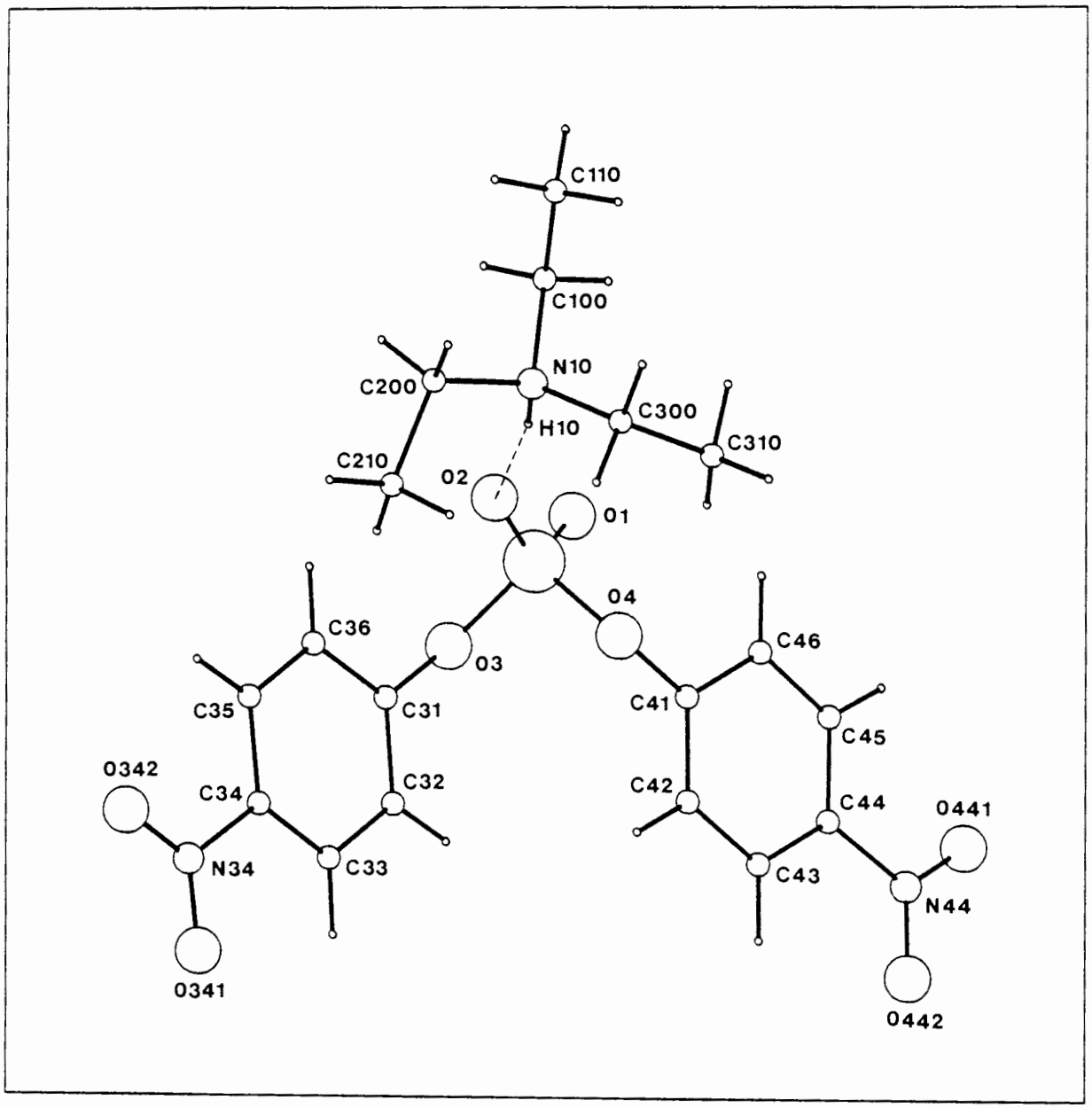

FIGURE 4.3 A perspective view of the triethylammonium bis(4-nitrophenyl)-phosphate salt (11).

TABLE 4.10 Bond Lengths (Å) and Angles (°) with estimated standard deviations in parentheses for Compound (10)

Bond Lengths	
P(1) - O(1)	1,483(2)
P(1) - O(2)	1,471(2)
P(1) - O(3)	1,589(2)
P(1) - O(4)	1,595(2)
O(3) - C(31)	1,387(3)
C(31) - C(32)	1,379(3)
C(32) - C(33)	1,371(3)
C(33) - C(34)	1,370(3)
C(34) - C(35)	1,376(3)
C(35) - C(36)	1,378(3)
C(36) - C(31)	1,379(3)
C(34) - N(34)	1,469(3)
N(34) - O(341)	1,225(2)
N(34) - O(342)	1,222(3)
O(4) - C(41)	1,395(3)
C(41) - C(42)	1,374(3)
C(42) - C(43)	1,377(4)
C(43) - C(44)	1,378(3)
C(44) - C(45)	1,379(4)
C(45) - C(46)	1,380(3)
C(46) - C(41)	1,378(3)
C(44) - N(44)	1,468(3)
N(44) - O(441)	1,216(3)
N(44) - O(442)	1,220(3)

TABLE 4.10 Cont/....

TABLE 4.10 Continued

O(11) - H(111)	1,00(1)
O(11) - H(112)	0,99(1)
O(11) - H(113)	1,00(1)

Bond Angles

O(1) - P(1) - O(2)	119,4(1)
O(1) - P(1) - O(3)	111,0(1)
O(1) - P(1) - O(4)	109,2(1)
O(2) - P(1) - O(3)	105,7(1)
O(2) - P(1) - O(4)	110,2(1)
O(3) - P(1) - O(4)	99,6(1)
P(1) - O(3) - C(31)	128,3(1)
O(3) - C(31) - C(32)	115,0(2)
C(36) - C(31) - C(32)	121,1(2)
C(31) - C(32) - C(33)	119,8(2)
C(32) - C(33) - C(34)	118,8(2)
C(33) - C(34) - C(35)	122,0(2)
C(33) - C(34) - N(34)	119,2(2)
C(34) - C(35) - C(36)	119,2(2)
C(35) - C(36) - C(31)	118,9(2)
C(34) - N(34) - O(341)	118,5(2)
C(34) - N(34) - O(342)	117,8(2)
O(341) - N(34) - O(342)	123,8(2)
P(1) - O(4) - C(41)	124,6(1)
O(4) - C(41) - C(42)	116,2(2)
C(46) - C(41) - C(42)	121,9(2)
C(41) - C(42) - C(43)	119,5(2)
C(42) - C(43) - C(44)	118,6(3)

TABLE 4.10 Cont/....

TABLE 4.10 Continued

C(43) - C(44) - C(45)	122,2(3)
C(43) - C(44) - N(44)	118,7(3)
C(44) - C(45) - C(46)	118,9(2)
C(45) - C(46) - C(41)	118,9(3)
C(44) - N(44) - O(441)	118,2(3)
C(44) - N(44) - O(442)	118,1(3)
O(441) - N(44) - O(442)	123,7(3)
H(111) - O(11) - H(112)	108(3)
H(111) - O(11) - H(113)	114(3)
H(112) - O(11) - H(113)	109(3)

Hydrogen Bonds

Atom - Atom Distances

O(1)...O(11)	2,60
$O(1)^{(i)}$...O(11)	2,64
$O(2)^{(ii)}$...O(11)	2,44

Intermolecular Bond Angles

O(11) - H(111)...O(1)	171
O(11) - H(112)...$O(1)^{(i)}$	176
O(11) - H(113)...$O(2)^{(ii)}$	179

Symmetry Codes

(i) $1-x, \frac{1}{2}+y, -\frac{1}{2}-z$

(ii) $1-x, -\frac{1}{2}+y, -\frac{1}{2}-z$

O(3) - C(31) - C(36)	123,8(2)
N(34) - C(34) - C(35)	118,8(2)
O(4) - C(41) - C(46)	121,8(2)
N(44) - C(44) - C(45)	119,1(3)

TABLE 4.11 Bond Lengths (Å) and Angles (°) with estimated standard deviations in parentheses for Compound (11)

Bond Lengths	
P(1) - O(1)	1,470(5)
P(1) - O(2)	1,477(5)
P(1) - O(3)	1,628(5)
P(1) - O(4)	1,616(4)
O(3) - C(31)	1,374(8)
C(31) - C(32)	1,379(9)
C(32) - C(33)	1,374(11)
C(33) - C(34)	1,376(10)
C(34) - C(35)	1,393(10)
C(35) - C(36)	1,382(10)
C(36) - C(31)	1,394(9)
C(34) - N(34)	1,484(12)
N(34) - O(341)	1,208(11)
N(34) - O(342)	1,198(11)
O(4) - C(41)	1,388(7)
C(41) - C(42)	1,376(9)
C(42) - C(43)	1,378(9)
C(43) - C(44)	1,363(10)
C(44) - C(45)	1,371(10)
C(45) - C(46)	1,372(9)
C(46) - C(41)	1,403(9)
C(44) - N(44)	1,475(9)
N(44) - O(441)	1,208(10)
N(44) - O(442)	1,222(9)

TABLE 4.11 Cont/....

TABLE 4.11 Continued

N(10) - C(100)	1,519(10)
C(100) - C(110)	1,481(13)
N(10) - C(200)	1,513(10)
C(200) - C(210)	1,481(13)
N(10) - C(300)	1,487(9)
C(300) - C(310)	1,495(11)

Bond Angles

O(1) - P(1) - O(2)	122,6(3)
O(1) - P(1) - O(3)	105,3(2)
O(1) - P(1) - O(4)	111,9(2)
O(2) - P(1) - O(3)	109,9(2)
O(2) - P(1) - O(4)	104,5(2)
O(3) - P(1) - O(4)	100,7(2)
P(1) - O(3) - C(31)	124,1(4)
O(3) - C(31) - C(32)	119,0(6)
C(36) - C(31) - C(32)	120,5(6)
C(31) - C(32) - C(33)	120,7(7)
C(32) - C(33) - C(34)	118,1(7)
C(33) - C(34) - C(35)	123,0(7)
C(33) - C(34) - N(34)	119,8(7)
C(34) - C(35) - C(36)	117,8(6)
C(35) - C(36) - C(31)	119,9(6)
C(34) - N(34) - O(341)	116,3(8)
C(34) - N(34) - O(342)	118,4(8)
O(341) - N(34) - O(342)	125,3(9)
P(1) - O(4) - C(41)	123,3(4)
O(4) - C(41) - C(42)	117,7(6)
C(46) - C(41) - C(42)	120,7(6)

TABLE 4.11 Cont/....

TABLE 4.11 Continued

C(41) - C(42) - C(43)	119,9(6)
C(42) - C(43) - C(44)	119,3(6)
C(43) - C(44) - C(45)	121,4(6)
C(43) - C(44) - N(44)	120,4(6)
C(44) - C(45) - C(46)	120,6(7)
C(45) - C(46) - C(41)	118,0(6)
C(44) - N(44) - O(441)	119,5(6)
C(44) - N(44) - O(442)	117,2(6)
O(441) - N(44) - O(442)	123,3(7)
C(100) - N(10) - C(200)	107,2(6)
C(100) - N(10) - C(300)	116,6(6)
C(200) - N(10) - C(300)	112,1(6)
N(10) - C(100) - C(110)	114,6(7)
N(10) - C(200) - C(210)	112,5(7)
N(10) - C(300) - C(310)	115,2(7)

Hydrogen Bonds

Atom - Atom Distances and Angle

O(2)...N(10)	2,65
O(2)...H(10)	1,62
O(2)...H(10) - N(10)	165

O(3) - C(31) - C(36)	120,4(6)
N(34) - C(34) - C(35)	117,1(6)
O(4) - C(41) - C(46)	121,2(6)
N(44) - C(44) - C(45)	118,2(6)

(10) and 3° in (11) between the normals to their planes. The equations of the least-squares mean planes and atomic deviations therefrom are listed in Tables 4.12 and 4.13.

The oxonium ion in compound (10) exhibits its usual pyramidal geometry with H-O-H angles varying between 108° and 114°. In their review of hydrated proton complexes, Lungren and Olovsson[57b] state that the H-O-H angles in oxonium ions do vary considerably, from 98° to 133°, presumably in order to accommodate the energetics of hydrogen bond formation. The oxonium hydrogens each form an almost linear hydrogen bond with the phosphoryl oxygens. These are detailed in Table 4.10. The average O...O distance in compounds containing the oxonium ion is 2,57Å[59], thus the O(11)-H(113)...O(2)$^{(ii)}$ bond with an O...O distance of 2,44Å observed in compound (10) is remarkably strong. In addition the O-H...O angle is 179°, practically linear as is expected for strong hydrogen bonds. A packing diagram of the structure which views the unit cell in the [100] direction is shown in Figure 4.4. The oxonium ions link columns of the phosphate anions by double ribbons of hydrogen bonds running close to the two-fold screw axis, parallel to *b*.

The triethylammonium cation in (11) is in a tetrahedral arrangement but the individual C-N-C angles subtended at the nitrogen deviate significantly from the ideal value of 109,5°. The hydrogen bonding detailed in Table 4.11 is also strong. Typical N...O distances vary from 2,7Å to 3,1Å[57a]. The N(10)-H(10)...O(2) distance of 2,65Å obtained for (11) is therefore very short but the N-H...O angle of 165° deviates significantly from linearity. This bond is similar in strength to the intramolecular bond found in methylphenyl[*syn*, α-(tosylhydrazono)benzyl]phosphinate which has a N...O distance of 2,66Å and a N-H...O angle of 143°[60]. Three other compounds of the general formula (E) reported in the literature[61,62,63] exhibit the similar interaction.

TABLE 4.12 Least-Squares Planes for Compound (10)

1 (a) Equations of least-squares planes are expressed in orthogonalised space as $pX + qY + rZ = S$.

Plane 1 : The 4-nitrophenyl ring atoms (C(31), C(32), C(33), C(34), C(35), C(36))

$4,1355X + 1,9260Y + 19,9087Z = 0,2340$

Plane 2 : The 4-nitrophenyl ring atoms (C(41), C(42), C(43), C(44), C(45), C(46))

$4,9139X + 2,5060Y + 17,2767Z = 1,8893$

(b) Deviations from the planes ($\AA \times 10^3$)

Atom	*Plane* 1	*Atom*	*Plane* 2
P(1)	-261	P(1)	-936
O(1)	-1652	O(1)	-2340
O(2)	101	O(2)	-382
O(3)	172	O(3)	-691
O(4)	747	O(4)	16
C(31)*	22	C(41)*	-4
C(32)*	-15	C(42)*	7
C(33)*	-6	C(43)*	-3
C(34)*	18	C(44)*	-4
C(35)*	-10	C(45)*	7
C(36)*	-10	C(46)*	-3
N(34)	91	N(44)	-12
O(341)	-48	O(441)	33
O(342)	31	O(442)	-68

(c) Angle between normals to planes ($^\circ$)

Plane 1 and Plane 2	9,02

TABLE 4.13 Least-Squares Planes for Compound (11)

1 (a) Equations of least-squares planes are expressed in orthogonalised space as $pX + qY + rZ = S$.

Plane 1 : The 4-nitrophenyl ring atoms (C(31), C(32), C(33), C(34), C(35), C(36))

$5{,}8245X + 6{,}2900Y + 2{,}1895Z = 4{,}0615$

Plane 2 : The 4-nitrophenyl ring atoms (C(41), C(42), C(43), C(44), C(45), C(46))

$5{,}5958X + 6{,}5481Y + 1{,}8323Z = 5{,}9201$

(b) Deviations from the planes ($\text{Å} \times 10^3$)

Atom	*Plane* 1	*Atom*	*Plane* 2
P(1)	1139	P(1)	-1020
O(1)	592	O(1)	-1584
O(2)	1696	O(2)	-398
O(3)	-40	O(3)	-2215
O(4)	2291	O(4)	80
C(31)*	0	C(41)*	-11
C(32)*	4	C(42)*	7
C(33)*	-5	C(43)*	-1
C(34)*	2	C(44)*	-1
C(35)*	3	C(45)*	-3
C(36)*	-4	C(46)*	9
N(34)	-2	N(44)	19
O(341)	-2	O(441)	-53
O(342)	-44	O(442)	99

(c) Angle between normals to planes ($^\circ$)

Plane 1 and Plane 2	2,81

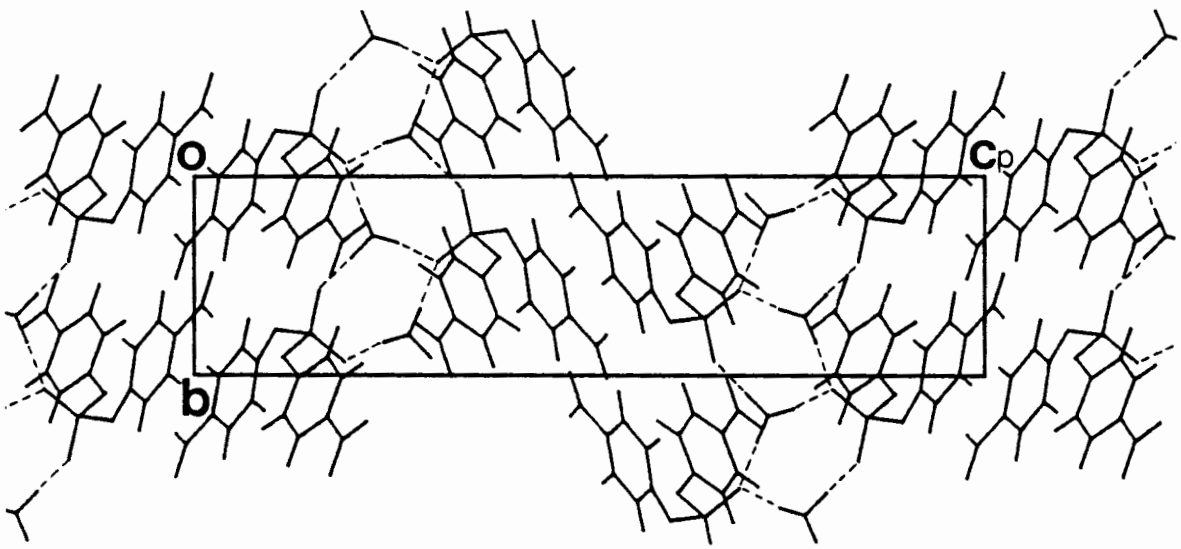

FIGURE 4.4 A packing diagram of the oxonium salt (10) viewed along the [100] direction showing hydrogen bonds as dashed lines.

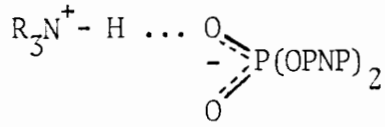

(E)

Their N...O distances vary from 2,69Å to 2,80Å and their N^+-H...O^- angles range between 117° and 169°.

Compound (11) has only the one hydrogen bonding donor, H(10), but two possible acceptors, O(1) and O(2). Structure (11) gives no indication of a bifurcated hydrogen bond formation as the N(10)...O(1) distance is 3,82Å, far greater than the corresponding sum of the van der Waals radii of 2,94Å. The packing of the molecules in the unit cell viewed along [010] is shown in Figure 4.5. The single hydrogen bond between the protonated nitrogen and a phosphoryl oxygen atom groups the ions in distinct pairs.

By comparing molecular parameters of bis(4-nitrophenyl) phosphates (10) and (11) essentially the following proton transfer equilibrium is being studied:

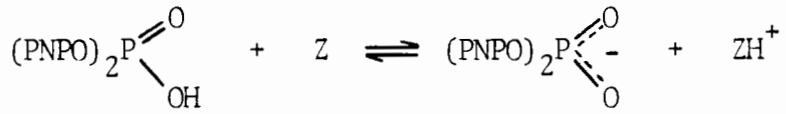

PNPO = 4-$NO_2C_6H_4O$ Z = H_2O or Et_3N

A relationship between the acidity of the ZH^+ and the geometry of the phosphate anion is noticed. This relation is summarised in Table 4.14 and depicted in Figure 4.6, which also includes *p*-carboethoxyanilinium bis(*p*-nitrophenyl) phosphate (12) described in the literature[61]. The stronger the acid ZH^+, the greater is its tendency to protonate the phosphate anion and by decreasing the electron density within the PO_2 fragment, to drive the O-$\bar{P}$-O angle toward a regular tetrahedral value. This is in agreement with other observations

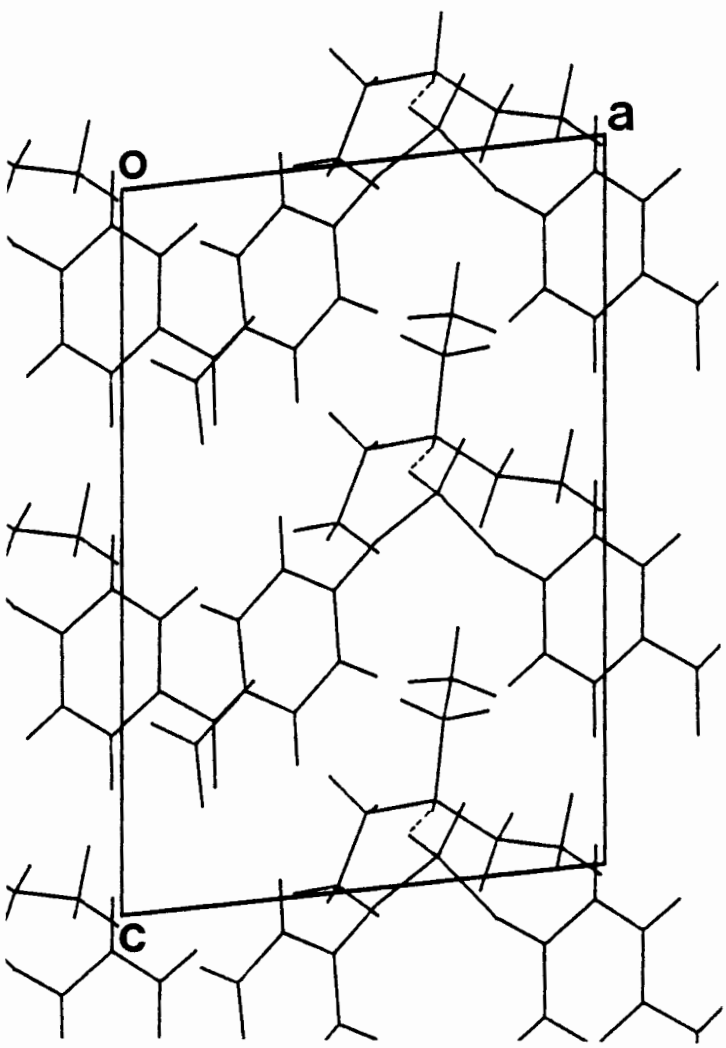

FIGURE 4.5 A packing diagram of the triethylammonium salt (11) viewed along the [010] direction showing hydrogen bonds as dashed lines.

TABLE 4.14 The O-P-O angle of the PO_2^- group in bis(4-nitrophenyl) phosphate salts, $(PNPO)_2PO_2^-$ ZH^+

Compound	ZH^+	pK_{ZH^+}	O-P-O (^{O})
(10)	H_3O^+	-1,74	119,4
(12)	p-$EtO_2CC_6H_4NH_3^+$	2,51[a]	120,1
(11)	Et_3NH^+	10,75	122,6

[a]Calculated from the equation:[64] $pK_a = 4,58 - 2,88\sigma$

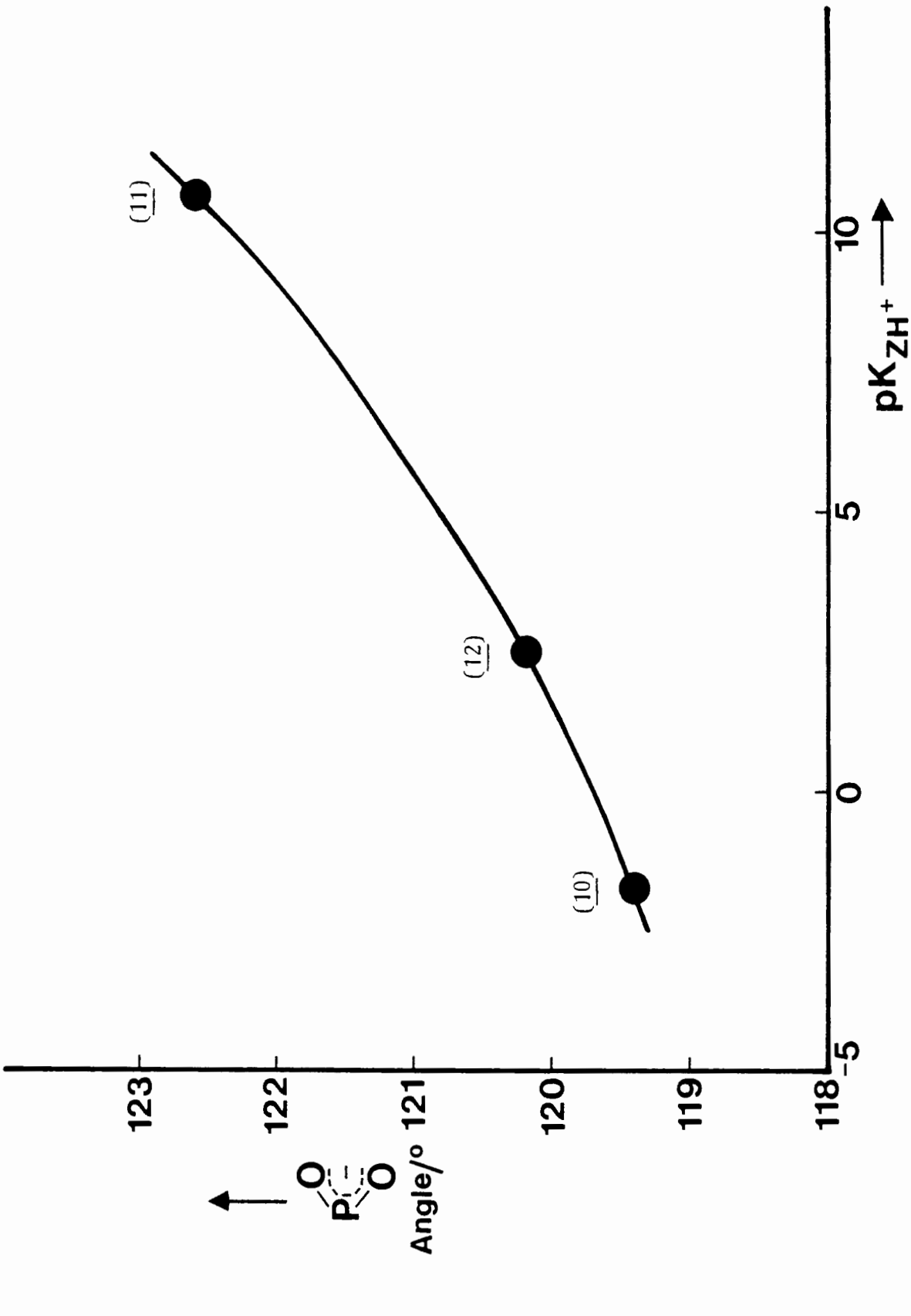

FIGURE 4.6 A plot of the O-P-O angle of the PO_2^- group as a function of acid strength of the cation, ZH^+.

(in Chapters 2 and 5) on the effect of the electron density within the PO_2 group on the value of the O-P-O angle.

Comparison of the three bis(4-nitrophenyl) phosphate salts shows that as the acid ZH^+ becomes dramatically weaker, the O-P-O angle increases from $119,4^o$ to $122,6^o$.

It must be noted however that in order to observe meaningful changes in molecular parameters, as determined by X-ray diffraction, cations ZH^+ of greatly different acidities had to be used. While the acidities of ions ZH^+ used for the comparison vary by more than twelve orders of magnitude, the resulting change in the O-P-O angle is only $3,2^o$. This relatively low sensitivity precludes any more detailed (e.g. Hammett relationship-like) correlations between acidic properties determined in solutions with those demonstrated in a crystalline state.

CHAPTER 5

CHAPTER 5

STRUCTURAL AND BONDING CHARACTERISTICS OF *N*-PHOSPHORYLATED DIMETHYLSULFOXIMIDES

5.1 INTRODUCTION

In recent years a widespread interest has developed in the chemistry of the sulfoximides ($R_2S\lessgtr^{O}_{N-X}$). The sulfur atom, bound in organic molecules can exist in numerous oxidation states and so-doing provides for a wide variety of regional and stereochemical substitution patterns. This unique structural versatility allows sulfur molecules to be tailored for specific functions[65]. Sulfoximides and their derivatives are useful as reagents in the syntheses of oxiranes, aziridines, cyclopropanes, alcohols and alkenes, all of which, except the alkenes, have been prepared in optically active forms when the chiral sulfoximide reagents were used. In addition their biological activity is of interest[66] as some *N*-sulfonylated sulfoximides have shown anti-malarial effects[67].

To date no structural reports on phosphorylated or thiophosphorylated sulfoximides have been found in the literature. Recently developed synthetic methods[68] have made *N*-phosphorylated dimethylsulfoximides (I) easily available substances. These substituted sulfoximides incorporate a phosphorus and a sulphur atom into a single molecular framework via a nitrogen link, thereby providing, in addition to possible biological effects, an interesting topic for structural and bonding studies.

Furthermore the conformation of the OPNSO fragment in these new compounds could possibly allow for metal ion chelation. Such chelating properties could be enhanced by structural modifications, for example by substituting

the thiophosphoryl for the phosphoryl group or by introducing substituents that possess sites for metal ion chelation.

An X-ray crystallographic study of three unique *N*-phosphorylated dimethyl= sulfoximides: $(RO)_2P(O)-N=S(O)Me_2$ (I)

(13) R = *i*Pr

(14) R = Ph

(15) $(RO)_2$ = 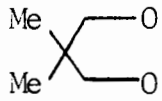

was undertaken in order to investigate the geometry of the OPNSO molecular backbone, the hybridisation and bonding arrangement at the nitrogen atom, conjugation effects and possible secondary interactions.

The structural characteristics of these model compounds may now be compared with a variety of related organophosphorus and organosulfur structures for which ample structural and bonding data are available. In this way information pertinent to various chemical aspects, including the nature of the P-N bond, may be accumulated.

5.2 CRYSTAL AND MOLECULAR STRUCTURES OF THREE *N*-PHOSPHORYLATED DIMETHYL= SULFOXIMIDES (I):

N-(DIISOPROPOXYPHOSPHINYL)-*S*,*S*-DIMETHYLSULFOXIMIDE (13)

N-(DIPHENOXYPHOSPHINYL)-*S*,*S*-DIMETHYLSULFOXIMIDE (14)

N-(2-OXO-5,5-DIMETHYL-1,3,2-DIOXAPHOSPHORINAN-2-YL)-*S*,*S*-DIMETHYL= SULFOXIMIDE (15)

5.2.1 EXPERIMENTAL

The three title compounds were synthesised by Wieczorkowski, Jakobsen and Treppendahl[68] as follows:

Method 1. Preparation of (13)

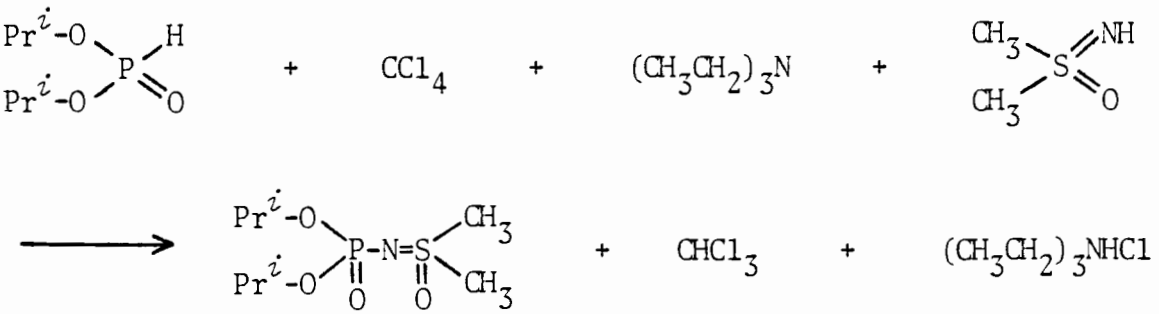

(13)

Dimethylsulfoximide was prepared by the action of hydrazoic acid on dimethyl= sulfoxide[69].

To a mixture of dimethylsulfoximide (0,1mol), triethylamine (0,1mol) and carbon tetrachloride (20ml) dissolved in chloroform (50ml), diisopropylphosphite (0,1mol) was added dropwise with stirring. The temperature rose from 20° to 70°C. The reaction mixture was stirred for 4 hours at room temperature and then evaporated to dryness (40°C bath).

*Benzene (25ml) was added and evaporated again to remove traces of chloroform. Dry benzene (100ml) was then added to the residue and the triethylamine hydro=

chloride precipitate was filtered off and washed with benzene (50ml). The filtrate and washings were then combined and the solvent was evaporated off*.

The crude colourless *N*-(diisopropyloxyphosphinyl)-*S*,*S*-dimethylsulfoximide solid (13) was recrystallised to yield transparent needle crystals suitable for X-ray photography purposes. Yield 79%. b.p. 115°C/0,001mmHg. m.p.66-68°C. Anal. Calculated for $C_8H_{20}NO_4PS$: C = 37,34%, H = 7,83%, N = 5,44%, S = 12,46%. Found: C = 37,12%, H = 7,83%, N = 5,32%, S = 12,38%. ^1H NMR ($CDCL_3$): δ1,30 (6H's,s), δ1,40 (6H's,s), δ3,30 (6H's,s), δ4,32-4,94 (2H's,m). IR (CCL_4, cm^{-1}): 2990(s), 1250(s), 1170(s).

Method 2. Preparation of (14) and (15)

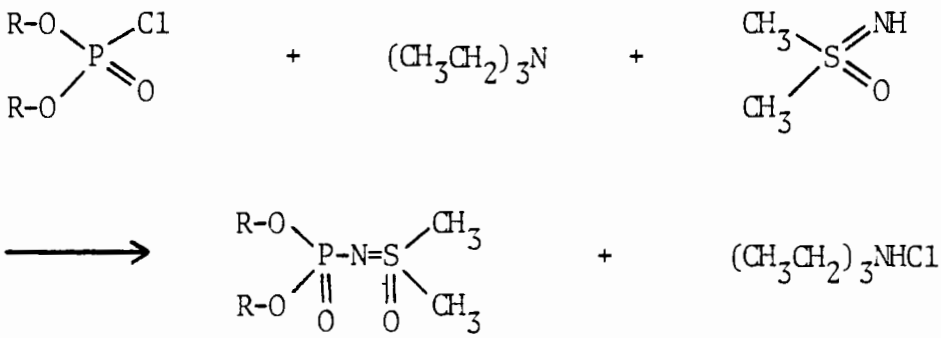

(14) R=Ph (15) $R_2=(Me)_2C(CH_2)_2$

A solution of the appropriate dialkyl phosphorochloridate (0,1mol) in chloroform (15ml) was added dropwise into a stirred solution of sulfoximide (0,1mol, prepared as before[69]) and triethylamine (0,1mol) in chloroform (60ml). This reaction was slightly exothermic. The reaction mixture was then refluxed (64°C) for 15 minutes and stirred for a further 2 hours at room temperature and evaporated to dryness (40°C bath). The reaction mixture was then worked up analogous to Method 1 (see between *'s).

The crude, white *N*-(dipenoxyphosphinyl)-*S*,*S*-dimethyl-sulfoximide solid (14)

was recrystallised from a methylethyl ketone-hexane mixture to yield a white microscopic crystalline material. Yield 60%. m.p. 91-92°C. Anal. Calculated for $C_{14}H_{16}NO_4PS$: C = 51,69%, H = 4,96%, N = 4,30%, S = 9,85%. Found: C = 51,75%, H = 4,96%, N = 4,37%, S = 9,91%. ^{1}H NMR ($CDCl_3$): δ3,16 (6H,s), δ7,31 (10H,s). IR ($CHCl_3$, cm^{-1}): 1595(m), 1500(s), 1250(s), 1160(s).

The crude *N*-(2-oxo-5,5-dimethyl)-1,3,2-dioxaphosphorinan-2-yl)-*S*,*S*-dimethyl= sulfoximide (15) was recrystallised from butanone to produce a white powder. Yield 68%. m.p. 126°C. Anal. Calculated for $C_7H_{16}NO_4PS$: C = 34,85%, H = 6,68%, N = 5,81%, S = 13,29%. Found: C = 34,82%, H = 6,58%, N = 5,47%, S = 13,36%. ^{1}H NMR ($CDCl_3$): δ0,90 (3H,s), δ1,22 (3H,s), δ3,30 (6H,s), δ3,89-4,12 (4H,m). IR ($CHCl_3$, cm^{-1}): 2960(m), 1270(s), 1170(s), 1060(s).

Both the above compounds were recrystallised from a mixture of petroleum spirit (80-100°C) and chloroform to produce transparent needles (14) and colourless rectangular-shaped crystals (15) suitable for X-ray crystallo= graphic work.

Crystal densities were determined by flotation in a mixture of saturated potassium iodide and water (for (14)) and in a calibrated density column[43] containing the same mixture (for (13) and (15)).

For each compound, suitable crystals were selected under the polarising microscope and accurate unit cell dimensions were obtained by a least-squares analysis of a number of high order reflections automatically located and centred on the CAD4 diffractometer using graphite monochromated MoK_α radiation. Reflection data were collected at room temperature and corrected by a Lorentz-polarisation factor but not for absorption as the absorption correction factor, A^*[23], remained equal to 1,0 over the entire range of θ values scanned by the

diffractometer (for (13), μR max.= 0,09, μR min.= 0,05; for (14), μR max.= 0,08, μR min.= 0,03; for (15), μR max.= 0,07, μR min.= 0,04).

5.2.2 SOLUTION AND REFINEMENT

All pertinent crystallographic data for the three structures are given in Table 5.1.

The structures were solved by the preliminary direct methods routine of the SHELXS-84 program system[26]. *E*-maps located the positions of virtually all the non-hydrogen atoms in each of the three structures. After a few cycles of least-squares refinement, difference electron-density maps were calculated and the positions of the remaining heavy atoms as well as most of the hydrogen atoms were revealed.

For compounds (13) and (15), the final refinement was carried out with all the non-hydrogen atoms treated anisotropically, with the methyl hydrogens refined as rigid groups and the remaining hydrogen atoms constrained at 1,00±0,01Å from their respective carbon atoms, their positions dictated by the molecular geometry. As a final check on the accuracy of the structure determinations, final electron-density maps were computed. In compound (13), three high residual peaks of > 0,5eÅ^{-3} were situated at ±1,0Å from the sulfur or phosphorus atoms. This is recognised as arising from imperfect modelling of the anisotropic thermal motion of the sulfur and phosphorus atoms. The other residual peaks were all well less than 0,5eÅ^{-3} which was deemed satisfactory. In the final cycle of refinement, the shift to error ratio was on average 0,04. For compound (15) the average shift to error ratio was 0,02 and in the final refinement no peaks of height > 0,2eÅ^{-3} were revealed. Furthermore the weighting scheme ($1/\sigma^2_F + 0{,}002F^2$) was chosen as this provided by comparison the best

TABLE 5.1 Crystal Data and Experimental and Refinement Parameters for the Structure Analyses

Compound	(13)	(14)	(15)
Crystal Data			
Molecular formula	$C_8H_{20}NO_4PS$	$C_{14}H_{16}NO_4PS$	$C_7H_{16}NO_4PS$
Molecular weight	257,3gmol^{-1}	325,32gmol^{-1}	241,25gmol^{-1}
Space group	$P2_1/c$	$P2_12_12_1$	$P\bar{1}$
a	13,486(6)Å	8,857(2)Å	6,5220(4)Å
b	9,132(4)Å	10,682(3)Å	7,600(3)Å
c	10,815(13)Å	16,120(4)Å	11,762(1)Å
α	90°	90°	89,77(2)°
β	98,36(6)°	90°	100,673(8)°
γ	90°	90°	93,16(2)°
V	1317,76Å^3	1525,12Å^3	572,05Å^3
Z	4	4	2
D_m	1,28gcm^{-3}	1,40gcm^{-3}	1,39gcm^{-3}
D_c	1,30gcm^{-3}	1,42gcm^{-3}	1,40gcm^{-3}
$\mu(MoK_\alpha)$	3,12cm^{-1}	2,79cm^{-1}	3,57cm^{-1}
$F(000)$	552	680	256
Data Collection			
Crystal dimensions	0,30 x 0,18 x 0,16mm	0,30 x 0,25 x 0,11mm	0,19 x 0,16 x 0,11mm
Scan mode	ω-2θ	ω-2θ	ω-2θ
Scan width ($\Delta\omega$)	(1,37 + 0,35tanθ)°	(0,40 + 0,35tanθ)°	(0,74 + 0,35tanθ)°

TABLE 5.1 Cont/....

TABLE 5.1 Continued

Aperture width (Horizontal)	(1,73 + 1,05tanθ)mm	(1,10 + 1,05tanθ)mm	(1,13 + 1,05tanθ)mm
Aperture width (Vertical)	4mm	4mm	4mm
Range scanned	$1^{o} \leq \theta \leq 25^{o}$	$1^{o} \leq \theta \leq 25^{o}$	$1^{o} \leq \theta \leq 25^{o}$
Stability of standard reflections	1,28%	1,74%	1,25%
Number of reflections collected	2610	1575	2117
Number of "observed" reflections with $I_{rel} > 2\sigma I_{rel}$	998	734	1436
Final Refinement			
Number of variables	156	118	141
$R=\Sigma\|\|F_o\|-\|F_c\|\|/\Sigma\|F_o\|$	0,084	0,058	0,037
$R_w=\Sigma w^{\frac{1}{2}}\|\|F_o\|-\|F_c\|\|/\Sigma w^{\frac{1}{2}}\|F_o\|$	0,082	0,053	0,045
Weighting scheme w	$(\sigma^2 F + 0,002F^2)^{-1}$	$(\sigma^2 F)^{-1}$	$(\sigma^2 F + 0,002F^2)^{-1}$
U_{iso} (aromatic H's)	-	$0,085(13)\text{Å}^2$	-
U_{iso} (methyl H's)	$0,077(11)\text{Å}^2$	$0,062(14)\text{Å}^2$	$0,086(4)\text{Å}^2$
U_{iso} (methylene H's)	-	-	$0,053(5)\text{Å}^2$
U_{iso} (methine H)	$0,037(21)\text{Å}^2$	-	-

model for the structure in terms of the smallest standard deviations and lowest R value.

In addition, for compound (13), to improve the goodness of fit between F_o and F_c, fifteen reflections having $||F_o|-|F_c||/|F_o| \geq 0,3$ were individually omitted and this was manifested in the lowering of the reliability index value, R, from 0,09 to 0,08. The need for this improvement is ascribed to poor crystal quality. A wide mosaic spread, which manifests itself in relatively large values for the scan and aperture widths (see Table 5.1) is observed.

However, for compound (14), in the final refinement only the phosphorus atom, its three oxygen ligands and the sulfur atom were treated anisotropically.* The methyl and aromatic hydrogens were refined as indicated above. In the final cycle of refinement the average shift to error ratio was less than 0,02. A final difference electron-density map calculated after the final refinement revealed no peaks of height > $0,4 e\text{Å}^{-3}$. Upon reversal of all the atomic co-ordinates, the final refinement yielded an identical R value and therefore the absolute structure could not be established by the Hamilton's test[45] of the R-ratio. A second more sophisticated procedure (Appendix 3) was employed to establish the absolute structure but this also failed.

Analyses of variance computed after the final cycles of refinement are given in Tables 5.2, 5.3 and 5.4. Final fractional atomic coordinates and thermal motion parameters are listed in Tables 5.5 to 5.10. Observed and calculated structure factors are given on Microfilm in Appendix 2.

*

Anisotropic treatment of the remaining non-hydrogen atoms was not possible because there were insufficient reflection data for the required number of parameters.

TABLE 5.2 Analysis of Variance for Compound (13)

a) By parity groups

Group	*ggg*	*ugg*	*gug*	*uug*	*ggu*	*ugu*	*guu*	*uuu*	All
N	144	129	124	122	110	119	136	114	998
V	260	238	193	215	242	233	224	224	230

b) As a function of sinθ

sinθ	0,00 - 0,17	0,22 - 0,25	0,27 - 0,30	0,32 - 0,34	0,36 - 0,39	0,43
N	107	116	105	78	134	89	94	81	99	95
V	367	254	239	198	186	194	191	196	193	194

c) As a function of $\sqrt{(F/F_{max})}$

$\sqrt{(F/F_{max})}$	0,00 - 0,28	0,30	0,32	0,34	0,36	0,39	0,42	0,47	0,54	1,00
N	130	90	108	91	89	114	85	106	93	92
V	187	206	212	177	198	243	238	199	205	384

d) As a function of |Miller index|

$\|h\|$	0	1	2	3	4	5	6	7	8	9	10	11	12	13	REST
N	56	109	123	100	96	103	85	71	67	51	49	29	32	16	11
V	370	296	242	231	202	203	196	194	207	149	158	175	193	240	241

$\|k\|$	0	1	2	3	4	5	6	7	8	9	10	11	12	13	REST
N	89	158	141	143	102	106	105	66	51	23	14	0	0	0	0
V	212	206	260	212	261	223	253	230	208	208	192	0	0	0	0

$\|l\|$	0	1	2	3	4	5	6	7	8	9	10	11	12	13	REST
N	74	122	127	114	124	102	91	78	59	43	35	20	9	0	0
V	278	307	290	224	210	197	164	162	150	169	200	225	157	0	0

N = Number of reflections in the group; $V = 100[M\Sigma(w|F_o-F_c|^2)/N\Sigma w]^{\frac{1}{2}}$; M = Total number of reflections.

TABLE 5.3 Analysis of Variance for Compound (14)

a) By parity groups

Group	*ggg*	*ugg*	*gug*	*uug*	*ggu*	*ugu*	*guu*	*uuu*	All
N	121	88	91	82	82	86	97	87	734
V	151	136	156	159	124	138	133	136	143

b) As a function of sinθ

sinθ	0,00 - 0,15	0,19 - 0,23	0,25 - 0,28	0,30 - 0,32	0,34 - 0,38	0,43
N	79	71	88	59	93	72	69	61	84	58
V	177	149	156	135	129	127	124	139	110	171

c) As a function of $\sqrt{(F/F_{max})}$

$\sqrt{(F/F_{max})}$	0,00 - 0,21	0,24 - 0,25	0,27 - 0,30	0,32 - 0,34	0,37 - 0,43	1,00
N	73	113	35	75	95	74	63	67	74	65
V	141	114	123	149	149	146	149	155	153	143

d) As a function of |Miller index|

$\|h\|$	0	1	2	3	4	5	6	7	8	9	10	11	12	13	REST
N	98	108	108	99	85	81	60	41	35	14	5	0	0	0	0
V	155	149	147	127	147	136	127	145	109	205	113	0	0	0	0

$\|k\|$	0	1	2	3	4	5	6	7	8	9	10	11	12	13	REST
N	85	105	106	85	72	79	61	49	38	31	13	8	2	0	0
V	146	141	125	158	169	149	127	139	122	138	112	137	158	0	0

$\|l\|$	0	1	2	3	4	5	6	7	8	9	10	11	12	13	REST
N	57	69	71	67	59	57	47	53	43	32	32	31	31	23	27
V	168	143	163	136	139	119	160	112	144	152	123	114	131	161	134

N = Number of reflections in the group; $V = 100[M\Sigma(w|F_o-F_c|^2)/N\Sigma w]^{\frac{1}{2}}$; M = Total number of reflections.

TABLE 5.4 Analysis of Variance for Compound (15)

a) By parity groups

Group	*ggg*	*ugg*	*gug*	*uug*	*ggu*	*ugu*	*guu*	*uuu*	All
N	184	181	186	177	175	182	178	173	1436
V	42	50	45	50	42	44	46	48	46

b) As a function of sinθ

sinθ	0,00 - 0,18	0,18 - 0,23	0,23 - 0,27	0,27 - 0,30	0,30 - 0,32	0,32 - 0,34	0,34 - 0,36	0,36 - 0,39	0,39 - 0,41	0,41 - 0,43
N	147	141	171	171	124	130	127	195	142	88
V	57	52	41	39	39	43	40	45	48	53

c) As a function of $\sqrt{(F/F_{max})}$

$\sqrt{(F/F_{max})}$	0,00 - 0,21	0,21 - 0,24	0,24 - 0,26	0,26 - 0,29	0,29 - 0,31	0,31 - 0,34	0,34 - 0,38	0,38 - 0,43	0,43 - 0,51	0,51 - 1,00
N	201	132	112	168	121	138	158	142	135	129
V	60	51	53	48	49	36	45	39	33	28

d) As a function of |Miller index|

$\lvert h \rvert$	0	1	2	3	4	5	6	7	8	9	10	11	12	13	REST
N	145	294	278	244	216	145	84	30	0	0	0	0	0	0	0
V	42	50	46	45	42	46	45	54	0	0	0	0	0	0	0

$\lvert k \rvert$	0	1	2	3	4	5	6	7	8	9	10	11	12	13	REST
N	105	259	234	219	197	163	132	72	54	1	0	0	0	0	0
V	44	52	44	48	47	39	41	41	46	35	0	0	0	0	0

$\lvert l \rvert$	0	1	2	3	4	5	6	7	8	9	10	11	12	13	REST
N	97	163	163	147	137	133	125	120	104	84	70	47	32	14	0
V	58	43	44	45	45	47	42	40	43	46	50	51	55	62	0

N = Number of reflections in the group; $V = 100[M\Sigma(w|F_o-F_c|^2)/N\Sigma w]^{\frac{1}{2}}$; M = Total number of reflections.

TABLE 5.5 Fractional Atomic Coordinates ($x10^4$) with estimated standard deviations in parentheses for Compound (13)

Atom	*x/a*	*y/b*	*z/c*
S(1)	5913(2)	1463(3)	2430(2)
P(1)	7260(2)	3695(3)	3268(3)
O(1)	6575(6)	4459(9)	3966(6)
O(2)	8356(6)	3597(8)	3940(7)
O(3)	7425(6)	4463(8)	2003(6)
O(11)	5240(6)	1356(9)	3330(7)
N(1)	6967(7)	1984(10)	2838(8)
C(11)	6066(10)	-228(12)	1783(11)
C(12)	5317(9)	2501(14)	1157(10)
C(2)	8555(10)	2940(14)	5212(11)
C(21)	9362(12)	1850(17)	5180(16)
C(22)	8876(11)	4173(17)	6130(13)
C(3)	7354(10)	6051(12)	1833(11)
C(31)	7187(13)	6308(16)	440(12)
C(32)	8309(12)	6732(15)	2474(14)
H(111)	5405(10)	-655(12)	1418(11)
H(112)	6425(10)	-927(12)	2405(11)
H(113)	6479(10)	-47(12)	1102(11)
H(121)	5803(9)	2758(14)	577(10)
H(122)	5018(9)	3418(14)	1450(10)
H(123)	4772(9)	1872(14)	709(10)
H(2)	7955(10)	2446(14)	5467(11)
H(211)	9536(12)	1305(17)	5984(16)
H(212)	9991(12)	2196(17)	4884(16)
H(213)	8989(12)	1186(17)	4538(16)

TABLE 5.5 Cont/....

TABLE 5.5 Continued

Atom	*x/a*	*y/b*	*z/c*
H(221)	9069(11)	3905(17)	7030(13)
H(222)	8248(11)	4770(17)	6032(13)
H(223)	9427(11)	4756(17)	5843(13)
H(3)	6796(10)	6507(12)	2215(11)
H(311)	7237(13)	7360(16)	698(12)
H(312)	6539(13)	6141(16)	-120(12)
H(313)	7758(13)	6057(16)	-17(12)
H(321)	8254(12)	7779(15)	2201(14)
H(322)	8929(12)	6291(15)	2227(14)
H(323)	8342(12)	6680(15)	3403(14)

Hydrogen atoms were subjected to constrained refinement.

TABLE 5.6 Anisotropic Thermal Motion Parameters ($Å^2 \times 10^3$) of the Non-Hydrogen Atoms with estimated standard deviations in parentheses for Compound (13)

Atom	U_{11}	U_{22}	U_{33}	U_{12}	U_{13}	U_{23}
S(1)	43(2)	27(2)	25(2)	-3(1)	7(1)	-2(1)
P(1)	39(2)	23(2)	28(2)	-1(1)	5(1)	0(1)
O(1)	45(5)	50(5)	33(4)	6(4)	13(4)	2(4)
O(2)	48(5)	23(4)	44(5)	-13(4)	0(4)	8(4)
O(3)	70(6)	25(4)	23(4)	3(4)	11(4)	7(3)
O(11)	62(5)	44(5)	36(4)	-13(4)	21(4)	-12(4)
N(1)	40(6)	27(5)	41(6)	2(4)	7(5)	-1(4)
C(11)	78(10)	22(6)	34(7)	-13(5)	16(7)	-10(5)
C(12)	48(8)	48(8)	35(7)	6(6)	0(6)	7(6)
C(2)	51(8)	51(8)	31(6)	-11(6)	0(6)	12(6)
C(21)	85(12)	54(10)	91(12)	21(9)	-12(10)	19(9)
C(22)	62(10)	80(11)	47(9)	-9(8)	1(7)	-9(8)
C(3)	54(8)	28(7)	49(7)	-2(6)	13(6)	2(5)
C(31)	101(12)	57(9)	47(8)	16(9)	2(8)	13(8)
C(32)	89(12)	47(9)	72(10)	-13(8)	-11(9)	-18(8)

TABLE 5.7 Fractional Atomic Coordinates ($x10^4$) with estimated standard deviations in parentheses for Compound (14)

Atom	*x/a*	*y/b*	*z/c*
S(1)	-515(3)	5963(3)	3500(2)
P(1)	1078(3)	5713(3)	4992(2)
O(1)	1832(8)	6933(6)	5042(5)
O(2)	2154(8)	4597(7)	4701(4)
O(3)	524(9)	5193(6)	5859(4)
O(11)	452(10)	5393(7)	2903(5)
N(1)	-391(9)	5537(7)	4415(5)
C(11)	-2383(13)	5677(14)	3250(8)
C(12)	-344(15)	7592(10)	3421(8)
C(21)	3549(11)	4361(10)	5088(7)
C(22)	4752(12)	5150(10)	4980(7)
C(23)	6127(15)	4813(12)	5339(7)
C(24)	6272(14)	3750(11)	5778(7)
C(25)	5060(12)	2958(11)	5877(8)
C(26)	3664(14)	3253(11)	5540(7)
C(31)	331(11)	5946(10)	6551(7)
C(32)	-848(12)	6817(10)	6558(8)
C(33)	-1103(14)	7522(12)	7259(7)
C(34)	-164(14)	7340(11)	7962(8)
C(35)	980(14)	6507(10)	7935(8)
C(36)	1210(12)	5823(10)	7221(6)
H(111)	-2556(13)	6112(14)	2709(8)
H(112)	-3025(13)	6072(14)	3689(8)
H(113)	-2655(13)	4773(14)	3195(8)

TABLE 5.7 Cont/....

TABLE 5.7 Continued

Atom	*x/a*	*y/b*	*z/c*
H(121)	-1183(15)	7971(10)	3751(8)
H(122)	-548(15)	7710(10)	2816(8)
H(123)	630(15)	8009(10)	3569(8)
H(22)	4649(12)	5942(10)	4654(7)
H(23)	7023(15)	5373(12)	5268(7)
H(24)	7266(14)	3535(11)	6036(7)
H(25)	5188(12)	2160(11)	6194(8)
H(26)	2772(14)	2691(11)	5619(7)
H(32)	-1504(12)	6924(10)	6058(8)
H(33)	-1934(14)	8155(12)	7272(7)
H(34)	-352(14)	7831(11)	8480(8)
H(35)	1650(14)	6385(10)	8428(8)
H(36)	2067(12)	5214(10)	7202(6)

Hydrogen atoms were subjected to constrained refinement.

TABLE 5.8 Anisotropic and Isotropic Thermal Motion Parameters ($Å^2 \times 10^3$) of the Non-Hydrogen Atoms with estimated standard deviations in parentheses for Compound (14)

Atom	U_{11}	U_{22}	U_{33}	U_{12}	U_{13}	U_{23}
S(1)	35(2)	57(2)	56(2)	8(2)	3(2)	-6(2)
P(1)	35(2)	46(2)	43(2)	0(2)	3(2)	4(2)
O(1)	44(5)	50(5)	59(5)	-6(4)	3(5)	6(6)
O(2)	38(4)	58(6)	54(6)	-2(4)	7(4)	-11(4)
O(3)	80(5)	30(4)	43(5)	9(5)	6(5)	1(4)

Atom	U_{iso}	*Atom*	U_{iso}
O(11)	73(3)	C(25)	60(4)
N(1)	41(2)	C(26)	53(3)
C(11)	79(4)	C(31)	37(3)
C(12)	64(4)	C(32)	52(3)
C(21)	38(3)	C(33)	66(4)
C(22)	48(3)	C(34)	62(4)
C(23)	63(4)	C(35)	56(4)
C(24)	59(4)	C(36)	44(3)

TABLE 5.9 Fractional Atomic Coordinates ($x10^4$) with estimated standard deviations in parentheses for Compound (15)

Atom	*x/a*	*y/b*	*z/c*
S(1)	1807(1)	11964(1)	6792(1)
P(1)	2588(1)	8348(1)	6942(1)
O(1)	1663(4)	6733(3)	6341(2)
O(2)	2859(3)	8209(3)	8298(2)
O(3)	4890(3)	8833(3)	6741(2)
O(11)	3142(4)	12528(3)	7851(2)
N(1)	1192(4)	10006(3)	6586(2)
C(11)	-580(6)	12954(5)	6634(4)
C(12)	2859(6)	12783(5)	5620(3)
C(2)	4461(5)	7091(4)	8875(3)
C(3)	6466(5)	7678(5)	7304(3)
C(4)	6594(4)	7670(4)	8611(3)
C(41)	7292(5)	9503(5)	9102(3)
C(42)	8153(6)	6315(6)	9141(4)
H(111)	-335(6)	14251(5)	6776(4)
H(112)	-1378(6)	12427(5)	7213(4)
H(113)	-1401(6)	12738(5)	5836(4)
H(121)	1922(6)	12566(5)	4853(3)
H(122)	4136(6)	12096(5)	5665(3)
H(123)	3276(6)	14068(5)	5710(3)
H(21)	4519(5)	7150(4)	9730(3)
H(22)	4099(5)	5850(4)	8598(3)
H(31)	6093(5)	6453(5)	7000(3)
H(32)	7855(5)	8087(5)	7126(3)
H(411)	7422(5)	9441(5)	9962(3)

TABLE 5.9 Cont/....

TABLE 5.9 Continued

Atom	*x/a*	*y/b*	*z/c*
H(412)	6224(5)	10359(5)	8784(3)
H(413)	8672(5)	9900(5)	8906(3)
H(421)	9596(6)	6627(6)	9004(4)
H(422)	7702(6)	5100(6)	8838(4)
H(423)	8143(6)	6357(6)	9990(4)

Hydrogen atoms were subjected to constrained refinement.

TABLE 5.10 Anisotropic Thermal Motion Parameters ($Å^2 \times 10^3$) of the Non-Hydrogen Atoms with estimated standard deviations in parentheses for Compound (15)

Atom	U_{11}	U_{22}	U_{33}	U_{12}	U_{13}	U_{23}
S(1)	50(1)	34(0)	40(0)	4(0)	-1(0)	-1(0)
P(1)	40(1)	32(0)	43(1)	1(0)	-4(0)	-2(0)
O(1)	69(2)	38(1)	73(2)	1(1)	-20(1)	-10(1)
O(2)	36(1)	50(1)	47(1)	7(1)	10(1)	5(1)
O(3)	47(1)	56(1)	36(1)	6(1)	8(1)	8(1)
O(11)	106(2)	47(2)	53(2)	6(1)	-24(1)	-7(1)
N(1)	45(2)	36(2)	63(2)	2(1)	-6(1)	-1(1)
C(11)	67(2)	53(2)	79(3)	19(2)	26(2)	8(2)
C(12)	55(2)	58(2)	60(2)	-2(2)	14(2)	2(2)
C(2)	42(2)	46(2)	43(2)	7(1)	8(1)	10(1)
C(3)	41(2)	66(2)	46(2)	12(2)	11(1)	2(2)
C(4)	37(2)	49(2)	39(2)	7(1)	6(1)	2(1)
C(41)	51(2)	69(2)	51(2)	-8(2)	-3(2)	-1(2)
C(42)	54(2)	86(3)	70(3)	27(2)	10(2)	18(2)

5.2.3 DISCUSSION

Perspective views of the molecules (13), (14) and (15) with atomic nomenclature are shown in Figures 5.1, 5.2 and 5.3 respectively. Bond lengths and angles are given in Tables 5.11, 5.12 and 5.13.

The numerous geometrical arrangements assumed by a phosphorus atom are generally well known. Perhaps less so with regard to the complexity of the stereochemistry of the sulfur atom. Sulfur, like oxygen, has six valence electrons but utilises d in addition to its s and p orbitals and so-doing involves itself in various hybridisation states: sp^2, sp^3, sp^3d_z2, sp^3d^2. The bonding arrangements are therefore numerous: plane triangular, angular, tetrahedral, trigonal pyramidal, trigonal bipyramidal and octahedral.

Various types of ions and molecules exist for the sp^3 sulfur atom in the tetrahedral geometrical arrangement:

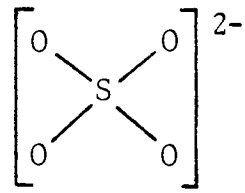

(a)

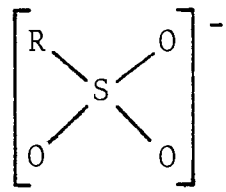

(b)

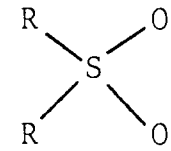

(c)

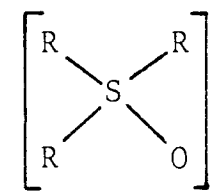

(d)

where R may be a H, N, S, C or halogen atom[46].

Only in type (a) is the geometry a regular tetrahedral one with identical bond lengths and angles of 1,49Å and 109,5° respectively. For compounds of the types (b), (c) and (d), bond orders are rather invariant, typically S=O values range between 1,40-1,47Å; S-C distances, 1,70-1,78Å; S-N values, 1,60-1,67Å, and bond angles vary due to, among other factors, orbital repul= sion effects.

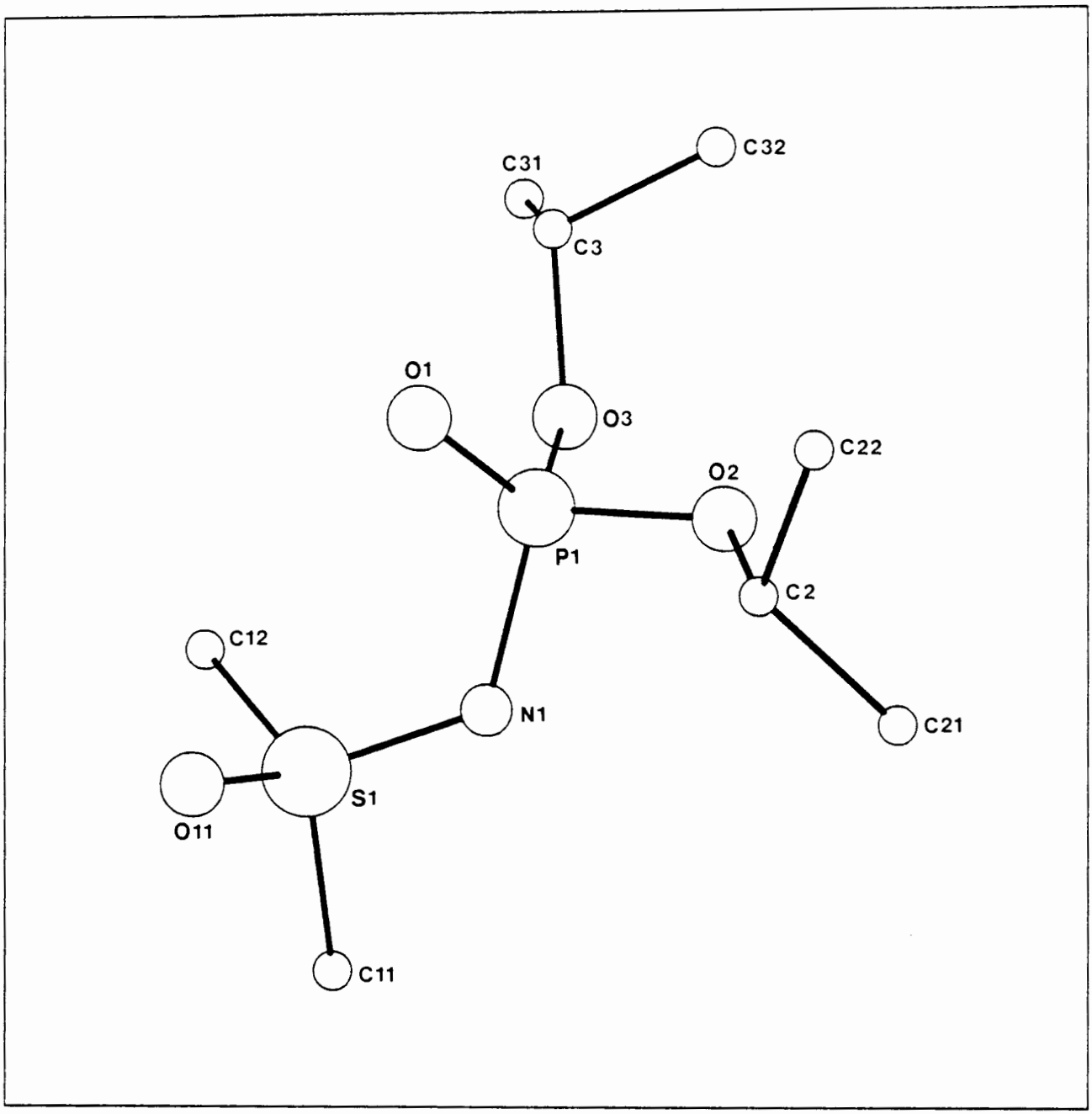

FIGURE 5.1 A perspective view of compound (13).

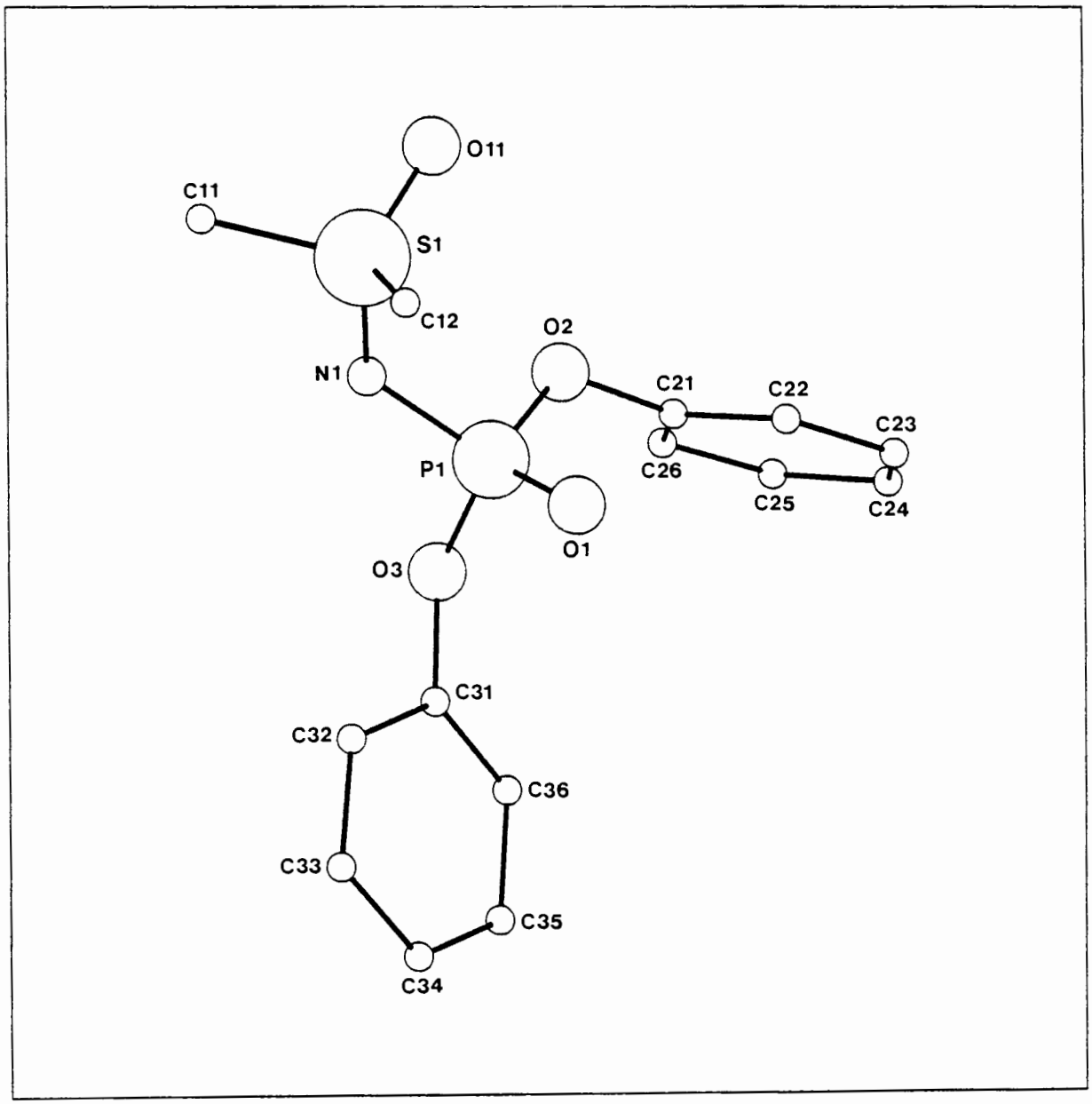

FIGURE 5.2 A perspective view of compound (14).

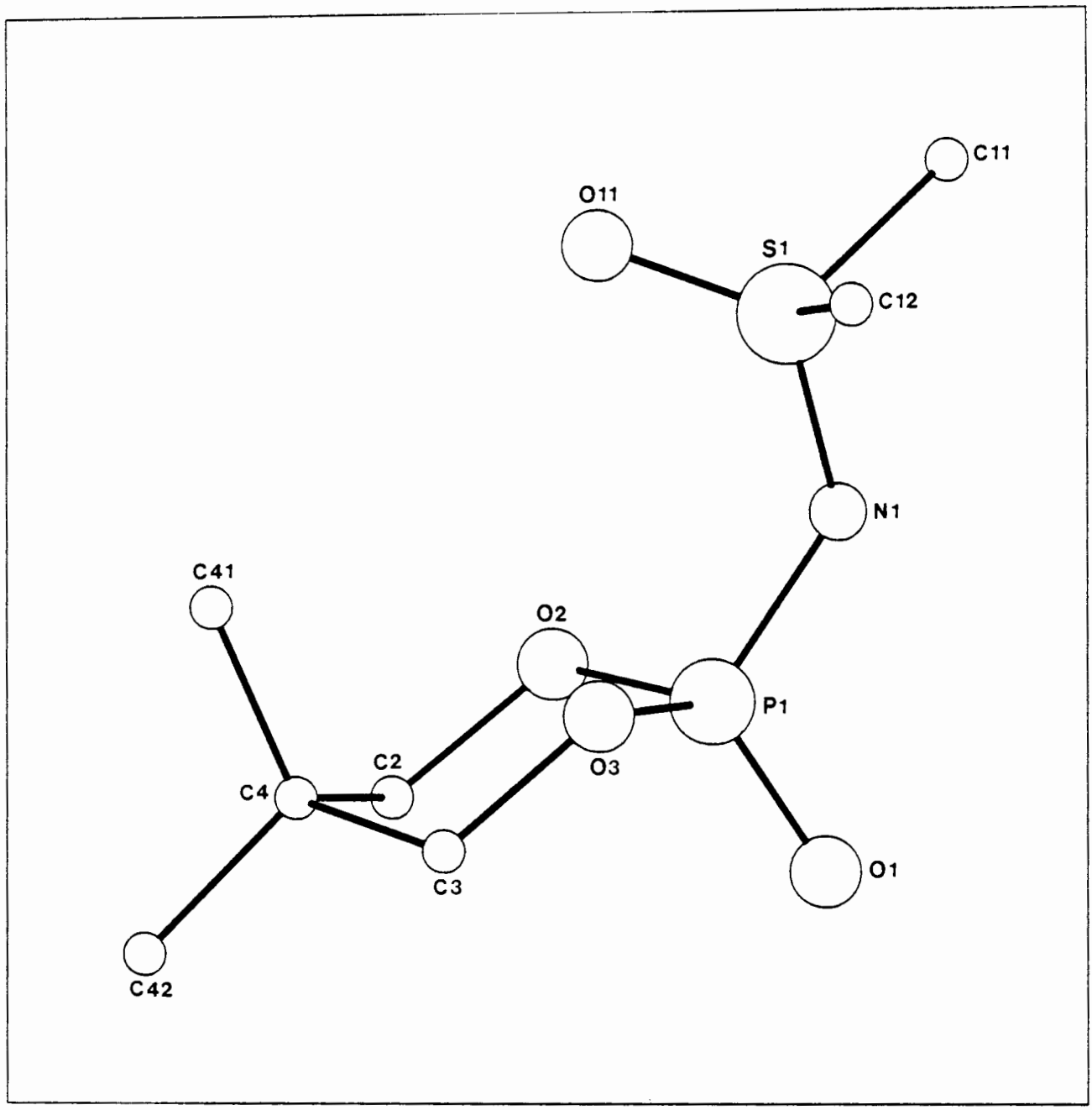

FIGURE 5.3 A perspective view of compound (15).

TABLE 5.11 Bond Lengths (Å) and Angles (°) with estimated standard deviations in parentheses for Compound (13)

Bond Lengths	
P(1) - O(1)	1,454(7)
P(1) - O(2)	1,551(8)
P(1) - O(3)	1,581(7)
P(1) - N(1)	1,661(9)
N(1) - S(1)	1,503(9)
S(1) - O(11)	1,428(8)
S(1) - C(11)	1,720(10)
S(1) - C(12)	1,765(11)
O(2) - C(2)	1,488(13)
C(2) - C(21)	1,479(18)
C(2) - C(22)	1,522(18)
O(3) - C(3)	1,464(13)
C(3) - C(31)	1,509(16)
C(3) - C(32)	1,505(19)
Bond Angles	
O(1) - P(1) - O(2)	114,7(4)
O(1) - P(1) - O(3)	114,6(4)
O(1) - P(1) - N(1)	116,9(5)
O(2) - P(1) - O(3)	100,8(4)
O(2) - P(1) - N(1)	104,4(5)
O(3) - P(1) - N(1)	103,5(4)
P(1) - N(1) - S(1)	123,8(6)
N(1) - S(1) - O(11)	119,3(5)
N(1) - S(1) - C(11)	103,9(6)

TABLE 5.11 Cont/....

TABLE 5.11 Continued

N(1) - S(1) - C(12)	111,3(6)
O(11) - S(1) - C(11)	109,9(6)
O(11) - S(1) - C(12)	107,8(6)
C(11) - S(1) - C(12)	103,5(6)
O(1) - O(2) - C(2)	119,3(7)
O(2) - C(2) - C(21)	106,5(11)
O(2) - C(2) - C(22)	107,5(10)
C(21) - C(2) - C(22)	111,9(11)
P(1) - O(3) - C(3)	122,2(7)
O(3) - C(3) - C(31)	106,1(10)
O(3) - C(3) - C(32)	108,4(10)
C(31) - C(3) - C(32)	112,9(12)

TABLE 5.12 Bond Lengths (Å) and Angles (°) with estimated standard deviations in parentheses for Compound (14)

Bond Lengths	
P(1) - O(1)	1,467(7)
P(1) - O(2)	1,596(8)
P(1) - O(3)	1,583(7)
P(1) - N(1)	1,609(8)
N(1) - S(1)	1,547(8)
S(1) - O(11)	1,426(8)
S(1) - C(11)	1,730(12)
S(1) - C(12)	1,751(11)
O(2) - C(21)	1,408(11)
C(21) - C(22)	1,370(13)
C(22) - C(23)	1,396(15)
C(23) - C(24)	1,344(15)
C(24) - C(25)	1,376(14)
C(25) - C(26)	1,387(15)
C(26) - C(21)	1,394(14)
O(3) - C(31)	1,385(11)
C(31) - C(32)	1,399(13)
C(32) - C(33)	1,376(15)
C(33) - C(34)	1,419(14)
C(34) - C(35)	1,349(14)
C(35) - C(36)	1,380(14)
C(36) - C(31)	1,337(12)
Bond Angles	
O(1) - P(1) - O(2)	114,1(4)
O(1) - P(1) - O(3)	113,8(4)

TABLE 5.12 Cont/....

TABLE 5.12 Continued

O(1) - P(1) - N(1)	120,2(4)
O(2) - P(1) - O(3)	100,5(4)
O(2) - P(1) - N(1)	103,0(4)
O(3) - P(1) - N(1)	102,6(5)
P(1) - N(1) - S(1)	125,0(6)
N(1) - S(1) - O(11)	118,4(5)
N(1) - S(1) - C(11)	103,8(6)
N(1) - S(1) - C(12)	110,8(6)
O(11) - S(1) - C(11)	109,9(6)
O(11) - S(1) - C(12)	108,9(6)
C(11) - S(1) - C(12)	103,9(7)
P(1) - O(2) - C(21)	121,9(7)
O(2) - C(21) - C(22)	121,1(9)
O(2) - C(21) - C(26)	116,6(9)
C(22) - C(21) - C(26)	122,2(10)
C(21) - C(22) - C(23)	117,8(10)
C(22) - C(23) - C(24)	121,3(13)
C(23) - C(24) - C(25)	120,4(13)
C(24) - C(25) - C(26)	120,7(11)
C(25) - C(26) - C(21)	117,5(11)
P(1) - O(3) - C(31)	123,1(6)
O(3) - C(31) - C(32)	119,0(10)
O(3) - C(31) - C(36)	121,4(10)
C(32) - C(31) - C(36)	119,6(11)
C(31) - C(32) - C(33)	119,6(11)
C(32) - C(33) - C(34)	119,0(12)
C(33) - C(34) - C(35)	120,3(12)
C(34) - C(35) - C(36)	119,2(12)
C(35) - C(36) - C(31)	122,4(11)

TABLE 5.13 Bond Lengths (Å) and Angles (°) with estimated standard deviations in parentheses for Compound (15)

Bond Lengths	
P(1) - O(1)	1,463(2)
P(1) - O(2)	1,575(2)
P(1) - O(3)	1,586(2)
P(1) - N(1)	1,604(3)
N(1) - S(1)	1,529(3)
S(1) - O(11)	1,433(2)
S(1) - C(11)	1,745(3)
S(1) - C(12)	1,748(4)
O(2) - C(2)	1,450(3)
O(3) - C(3)	1,452(3)
C(2) - C(4)	1,522(4)
C(3) - C(4)	1,524(4)
C(4) - C(41)	1,523(4)
C(4) - C(42)	1,536(4)
Bond Angles	
O(1) - P(1) - O(2)	113,1(1)
O(1) - P(1) - O(3)	113,0(1)
O(1) - P(1) - N(1)	112,3(1)
O(2) - P(1) - O(3)	103,4(1)
O(2) - P(1) - N(1)	105,8(1)
O(3) - P(1) - N(1)	108,7(1)
P(1) - N(1) - S(1)	128,5(2)
N(1) - S(1) - O(11)	119,7(1)
N(1) - S(1) - C(11)	104,0(2)
N(1) - S(1) - C(12)	108,8(2)

TABLE 5.13 Cont/....

TABLE 5.13 Continued

O(11) - S(1) - C(11)	110,4(2)
O(11) - S(1) - C(12)	109,4(2)
C(11) - S(1) - C(12)	103,2(2)
P(1) - O(2) - C(2)	117,0(2)
P(1) - O(3) - C(3)	115,1(2)
O(2) - C(2) - C(4)	111,1(2)
O(3) - C(3) - C(4)	111,3(2)
C(2) - C(4) - C(3)	109,0(3)
C(2) - C(4) - C(41)	110,9(3)
C(2) - C(4) - C(42)	108,0(3)
C(3) - C(4) - C(41)	109,7(3)
C(3) - C(4) - C(42)	108,7(3)
C(41) - C(4) - C(42)	110,6(3)

The three *N*-phosphorylated dimethylsulfoximides, (13), (14) and (15), have both a phosphorus and a sulfur centre in tetrahedral coordination, with bond angles averaging to 109,2° and 109,8° respectively. This indicates the absence of significant secondary interactions which would have disturbed the tetrahedral geometry at these two acyl centres. However, the individual angles, X-P-Y and W-S-Z show marked deviation from the ideal tetrahedral value of 109,5°. On average, X-P-Y angles range from 101,6° to 116,5° and W-S-Z angles vary between 103,5° and 119,1° (Table 5.14). The bond angles shown in Table 5.14 follow the general trend observed for tetrahedral molecules, which results, among other factors, due to the fact that multiple-bond electrons repel other electrons more strongly than do single-bond electrons[70]. Therefore for P^{IV} derivatives the value of a X-P-Y angle can be taken as an approximate measure of the P-X and/or P-Y bond order and thus can be correlated to bond distances (see Part 2) (and similarly for S^{IV} derivatives). It is observed (Table 5.14) that the bond order to phosphorus decreases in the sequence: P=O > P-N > P-O(ester); and at the sulfonyl centre the order is S=O > S=N > S-C. These sequences are not immediately obvious and deserve some comment. The order P-N > P-O indicates greater back-donation of the nitrogen non-bonding electrons to phosphorus than the donation from the ester oxygen atoms. The same effect has also been observed for the phosphoramidates, $(RO)_2P(O)NR'_2$[86], but it has to be remembered that in compounds (13), (14) and (15) the nitrogen atom is directly bonded to the electron-withdrawing sulfoxide group, S=O. On the other hand, the observed order S=O > S=N can be interpreted in terms of the electron-withdrawing effect of the *N*-phosphinyl group, thus inhibiting the back-donation of electrons from nitrogen to sulfur.

The P=O and P-O(ester) bond lengths of all three compounds lie well within the ranges normally observed[71,72].

In compound (13) the two "identical" isopropyl ester moieties have P-O(*i*Pr)

TABLE 5.14 Deviations from the ideal tetrahedron for the P and S bonds in compounds (I)

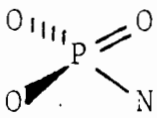	(°)[a]	n[b]	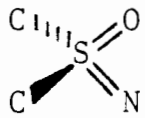	(°)[a]	n[b]
N-P=O	116,5 ± 3,3	3	N=S=O	119,1 ± 0,7	3
O-P=O	113,9 ± 0,7	6	C-S=O	109,4 ± 0,9	6
O-P-N	104,7 ± 2,3	6	C-S=N	107,1 ± 3,6	6
O-P-O	101,6 ± 1,6	3	C-S-C	103,5 ± 0,4	3
	av. 109,2 ± 7,2			av. 109,8 ± 6,7	

[a] average value for (13), (14) and (15)

[b] number of bond angles used for the calculation

distances (1,551 and 1,581Å) which differ by 0,03Å. The shorter P-O(iPr) distance is counterbalanced by a longer O-$C(CH_3)_2$ distance thereby ensuring a constant distance of ∿3,04Å between the phosphorus and dimethyl-substituted carbon atoms. Furthermore, although the C(3)-CH_3 bond lengths are similar (1,505 and 1,509Å) the C(2)-CH_3 distances (1,479 and 1,522Å) indicate a 0,04Å discrepancy.

The phenyl ester groups in compound (14) are planar to within 0,01Å (see Table 5.15). These aromatic rings are orientated almost perpendicularly (95,6°) with respect to each other.

The P-N bond distances in all three compounds are well below the value of 1,78Å, which is considered to be a "pure" P-N single bond distance[73]. The observed values of 1,661Å, 1,609Å and 1,604Å for the P-N bonds correspond closely to the range of 1,61-1,65Å reported for a variety of phosphor= amidates (F)[74], for which a certain degree of p_π-d_π bonding between the phosphorus and the nitrogen atoms has to be taken into account (resonance structure (G)[75].

(F) (G)

In fact, the P-N bond distance in compounds (14) and (15) (∿1,60Å) approxi= mates the value reported for the P-N bond in the sulfimidophosphonium salt (16)[76] which is regarded as a heteroallenic system with the full p_π-d_π P-N bonding.

$$Ph_3\overset{+}{P}=N=SPh_2 \quad SbCl_6^-$$

(16)

TABLE 5.15 Least-Squares Planes for Compound (14)

1 (a) Equations of least-squares planes are expressed in orthogonalised space as $pX + qY + rZ = S$.

Plane 1 : The phenyl ring atoms ((C(21), C(22), C(23), C(24), C(25), C(26))

$-2,2291X + 5,2192Y + 13,4670Z = 8,3371$

Plane 2 : The phenyl ring atoms ((C(31), C(32), C(33), C(34), C(35), C(36))

$5,4649X + 7,5600Y - 5,5468Z = 1,0512$

(b) Deviations from the planes ($\AA \times 10^3$)

Atom	*Plane* 1	*Atom*	*Plane* 2
P(1)	1127	P(1)	1088
S(1)	-396	S(1)	1234
O(1)	1664	O(1)	2394
O(2)	-87	O(2)	993
O(3)	2148	O(3)	-90
N(1)	586	N(1)	472
O(11)	-1714	O(11)	1663
C(11)	-465	C(11)	137
C(12)	309	C(12)	2603
C(21)*	-0	C(31)*	-8
C(22)*	-2	C(32)*	0
C(23)*	-1	C(33)*	8
C(24)*	5	C(34)*	-8
C(25)*	-8	C(35)*	1
C(26)*	5	C(36)*	8

(c) Angle between normals to planes ($^\circ$)

Plane 1 and Plane 2	95,6

The P-N-S linkage in (16) is fully symmetrical (P-N and N-S = 1,60Å) indicative of symmetrical charge delocalisation within this triatomic group.

The P-N bond in (13), (14) and (15) is always longer than the N-S bond; this is in accordance with the conventional structural formula of (I) which implies that the higher bond order exists between the nitrogen and sulfur atoms. Although any value suggested as a bond distance for a "pure" phosphorus-nitrogen double bond must be treated with caution[77,78] there is little doubt that a N→P back-donation effect occurs in (I).

$$(RO)_2P(O)\text{-}N{=}S(O)(Me)_2 \longleftrightarrow (RO)_2P(O^-){=}\overset{+}{N}{=}S(O)(Me)_2$$

(I) (IA)

The bonding represented by (IA) requires both a shortening of the P-N distance as well as a change in the geometry at the nitrogen atom. Structure (I) involves a trigonal nitrogen atom and hence a P-N-S bond angle of 120°, whereas in the allenic structure (IA), a linear P-N-S arrangement is required.

The P-N-S angles in substrates (13), (14) and (15) have values of 123,8, 125,0 and 128,5° respectively, which are greater than 123,6° as reported for the salt (16), and which indicates a significant widening of the bonds at the nitrogen atom beyond the normal value for trigonal geometry[78].

With regard to the OPNSO skeleton, only the sulfoxide bond distance remains virtually constant at 1,43Å in all three compounds, thereby confirming the lack of variation of the S-O bond lengths (1,42-1,44Å) observed for other sulfonyl derivatives[79]. The remaining bonds (P-O, P-N and N-S) show small, but measurable variations in their lengths. It is of interest to note that the sum of the distances for all the four bonds involved remain remarkably constant at 6,05, 6,05 and 6,03Å for (13) (14) and (15) respectively.

A scarcity of structural data regarding the $R_2S(O)=NX$ system makes comparison of the sulfoximide part of compounds (I) with similar derivatives difficult. The only available information relates to three *N*-phtâlimido derivatives (X = 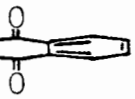)[80] and a single unsubstituted sulfoximide (X = H)[81]. The molecular parameters reported for these compounds generally agree well with those obtained for substrates (I). However, a significant difference is observed with regard to the S=O bond length. In compounds (I) a constant value of 1,43Å is obtained whereas the four compounds reported in the literature exhibit S-O distances ranging from 1,44-1,48Å. These variations probably arise due to differing electronic effects which emanate from the substituents at the nitrogen. Relative to the phosphoryl group in (I), moieties such as hydrogen or phtâlimido increase the contribution of the dipolar structure of the sulfoximide bond:

As mentioned before, the *N*-phosphorylated sulfoximides (I) have both a phosphorus and a sulfur atom in tetrahedral arrangement and each introducing a highly polar functional group, P=O and S=O respectively. The geometry of these substituted sulfoximides (I) should therefore be a result of the bonding requirements at the nitrogen bridge, dipole-dipole interactions between the P=O and S=O groups and steric interactions between the two tetrahedral P^{IV} and S^{IV} centres. The relevant torsion angles for the molecular backbone of (I) are as follows:

	(13)	(14)	(15)
O(1) - P(1) - N(1) - S(1)	36,80°	48,95°	-164,85°
P(1) - N(1) - S(1) - O(11)	-69,84°	63,81°	-37,57°

(Note: The torsion angle $\tau(I\text{-}J\text{-}K\text{-}L)$ is defined as the angle between the vector K-L when viewed down J-K. The sign of τ is positive if J-I is to be rotated clockwise into K-L and negative if counterclockwise[87].)

In compounds (13) and (14) the O-P-N-S torsion angles (36,80° and 48,95° respectively) indicate a nearly gauche relation of the phosphoryl oxygen and sulfur atom. In this arrangement the bulky tetrahedral group, $S(O)Me_2$ is removed from the vicinity of the phosphate ester groups thereby avoiding any interactions between this group and the *i*-propoxy and phenoxy moieties of (13) or (14). In compound (15) the geometry of the phosphate ester groups is restricted by the 1,3,2-dioxaphosphorinan ring, a nearly anti relation of the P=O and N=S groups is thus attained (OPNS torsion angle of 165°). The PNSO torsion angles for all three compounds (I) are similar, ranging from 38 to 70°, i.e. the orientation of the S=O and N-P functions are almost gauche. This implies that the gauche interactions between the tetrahedral phosphoryl moiety, $P(O)(OR)_2$ and the S=O and one S-Me group appear to be more favourable than the similar interactions with two S-Me groups (making PNSO torsion angles of ∿180°).

The molecular structure of compound (15) may be compared with two other 5,5-dimethyl-2-oxo-2-amino-1,3,2-dioxaphosphorinanes, the *N*-phenyl (17)[82] and *N*-formyl (18)[83] derivatives. Projections of these three 1,3,2-dioxa= phosphorinanes are shown below.

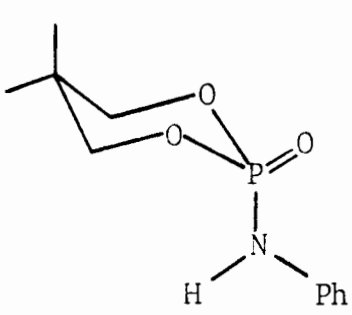

(17)

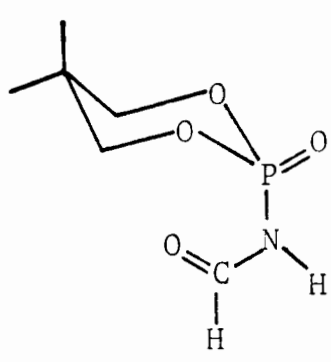

(18)

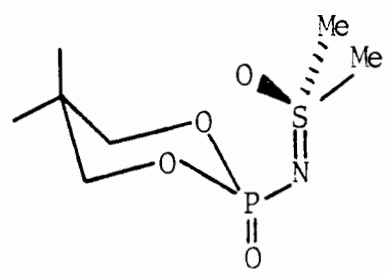

(15)

The phosphoryl oxygen occupies the equatorial position in both the amide (17) and imide (18), in agreement with the generally observed[84] conformational preference of the 2-substituted 1,3,2-dioxaphosphorinan-2-ones. This is as a result of the short P=O bond length which, if positioned axially, would bring the O atom and the two axial hydrogen atoms at C(4) and C(6) unfavourably close together. In this respect compound (15), with its axial location of the phosphoryl oxygen, is an exception. This geometrical change at the exocyclic substituents at phosphorus may arise due to two factors. Firstly, the P-N distance in (15) (1,60Å) is considerably shorter than in (17) (1,65Å) and (18) (1,70Å) thereby making nitrogen more susceptible to the 1,3-steric interactions with the ring hydrogens. Secondly, both the *N*-substituents in (17) (phenyl group) and (18) (formyl group) are planar whereas the nitrogen in (15) is bonded to a tetrahedral group which if located axially will interact with ring hydrogens irrespective of other conformational angles.

The near-gauche orientation of the sulfoxide group with respect to the N-P bond provides for possible secondary interaction between the electron-rich oxygen atom of the S=O group and the electrophilic phosphorus atom (structure (H).

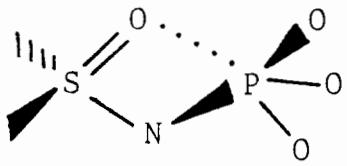

(H)

The non-bonding (S)O...P distances are 4,31, 3,43 and 3,34Å for compounds (13), (14) and (15) respectively (the corresponding sum of the van der Waals radii is 3,30Å[36]).

The analogous long-range interactions between the phosphoryl oxygen atom and the electrophilic sulfur atom (structure (J)) are only possible for (13) and

(14) (in (15) the phosphoryl group has an anti orientation with respect to the N=S bond)

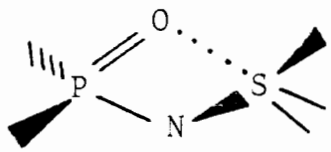

(J)

The (P)O...S distance for (13) is 3,26Å and 3,40Å for (14) (the corresponding sum of the van der Waals radii is 3,25Å).

There is no evidence for any significant donor-acceptor interactions between the P=O and S=O functional groups in compounds (I) (with perhaps the exception of the P=O...S=O contact in (13) where the interatomic distance approximates the sum of the van der Waals radii). In contrast to the above a close contact P=O...C=O, with O...C = 2,97Å (the corresponding sum of the van der Waals radii, 3,25Å) has been observed for *N*-benzoyldimethylphosphoramidate[85], $(MeO)_2P(O)$-NH-C(O)Ph. This difference with regard to the intermolecular interactions suggests a lower flexibility of the P-N=S bridge in compounds (I) relative to that of the P-NH-C linkage in the mixed phosphoric-carboxylic imides.

Molecular Packing

Compound (13) crystallises with four molecules per unit cell and a packing diagram viewed along the [010] direction is shown in Figure 5.4. The molecules appear to pack in pairs running parallel to the *z*-axis with the methyl moieties on the sulfur atoms facing one another.

The molecular packing of the four molecules of compound (14) in the orthor= hombic unit cell viewed along [100] is shown in Figure 5.5. The molecules pair with their phosphoryl oxygen atoms directed towards each other. The

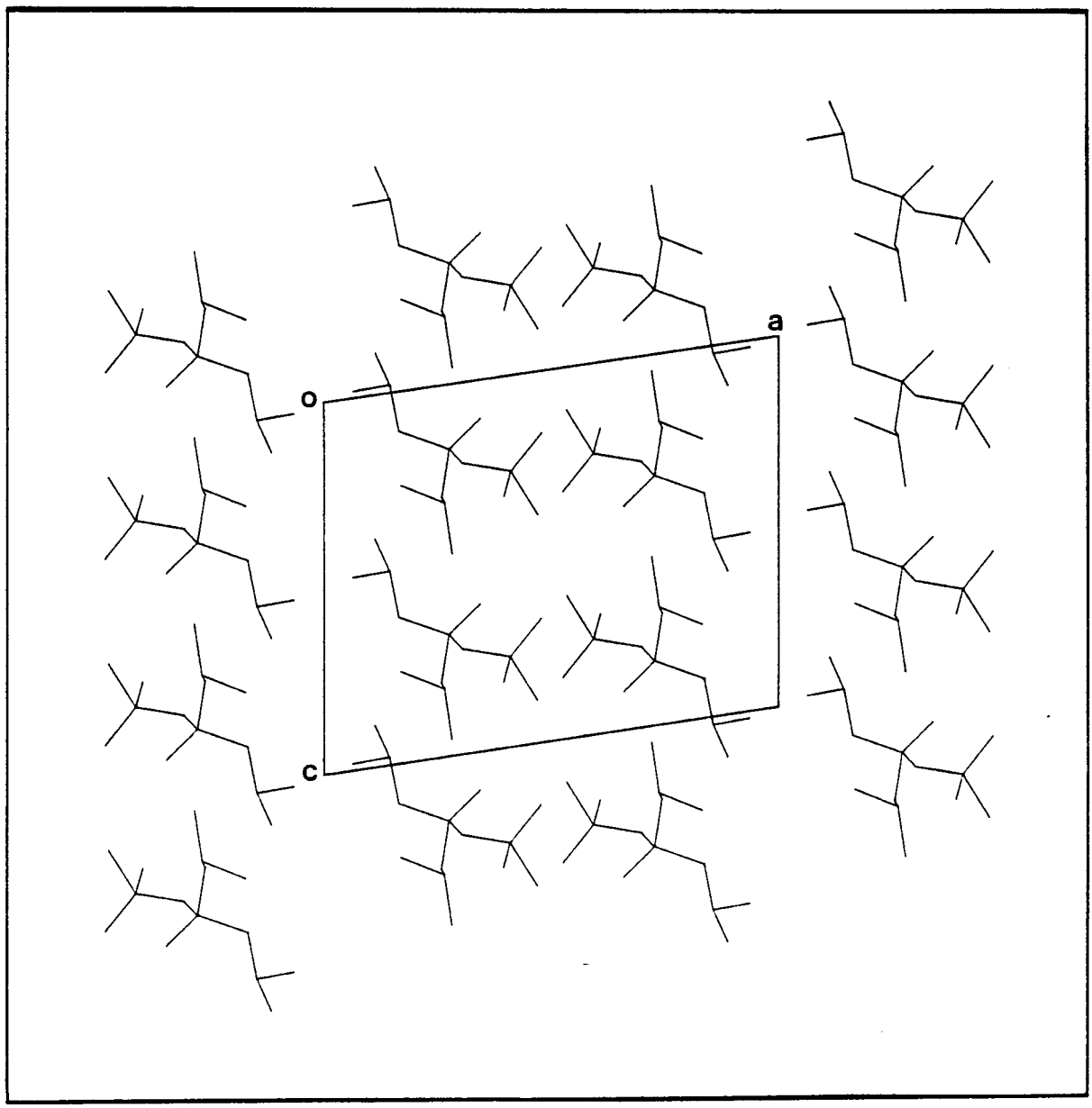

FIGURE 5.4 A packing diagram for compound (13) viewed along [010].

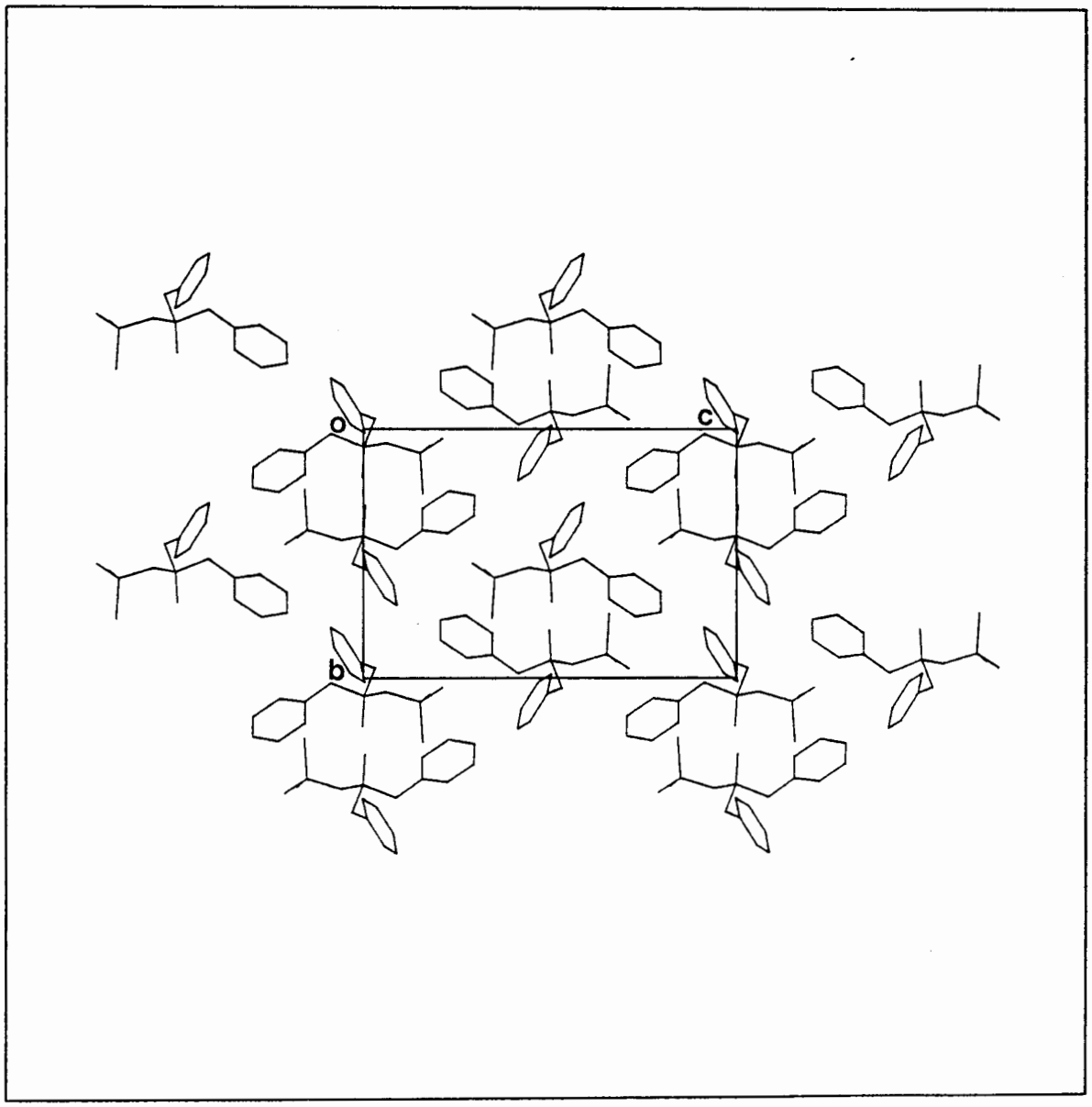

FIGURE 5.5 A packing diagram for compound (14) viewed along [100].

pairs of molecules are aligned in a zig-zag formation parallel to the three axes.

A packing diagram of compound (15) viewed along the [100] direction is shown in Figure 5.6. The molecules simply stack in up-down patterns running parallel to the *z*-axis.

In all three compounds no obvious intramolecular close contacts are observed with exception being perhaps the slight donor-acceptor interaction between the S=O and P=O groups in compound (13) as mentioned above. Furthermore no evidence for any significant intermolecular interactions is found.

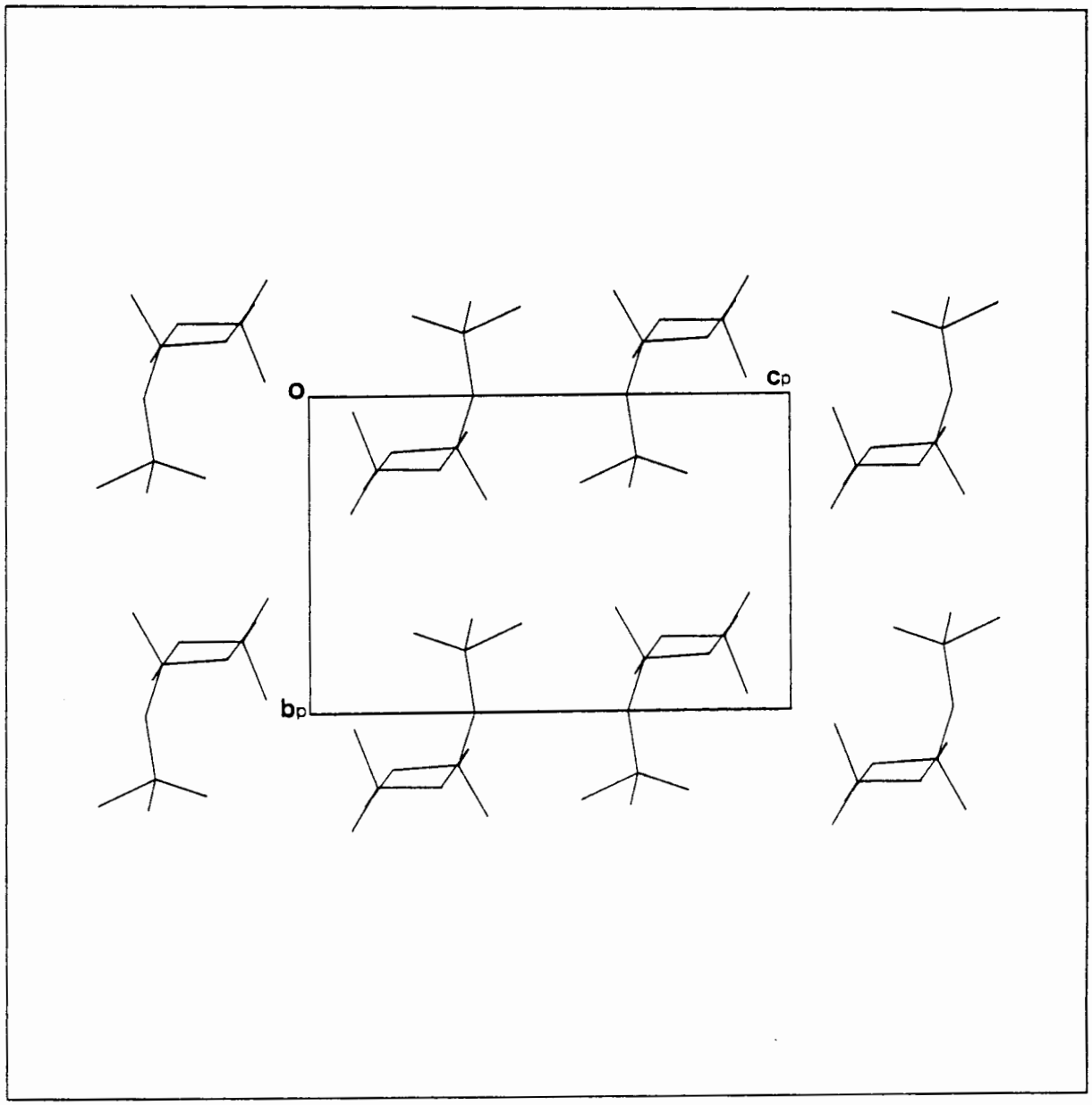

FIGURE 5.6 A packing diagram for compound (15) viewed along [100].

PART 2

CHAPTER 6

CHAPTER 6

STRUCTURAL CORRELATIONS IN ORGANIC PHOSPHATES. A PRELIMINARY STUDY.

During the X-ray analysis of the afore-mentioned phosphate esters, an obvious interrelation was observed between two independent parameters describing each structure, namely: the O-P-O angles and the P-O distances.

Crystal structures of a selected number of organic phosphoric mono-, di- and tri-esters, were retrieved from the literature in order to determine whether such bond length-bond angle correlations were inherent in each of these phosphate compounds. Individual plots of the O-P-O angles versus the sum of the two distances on either side of the angle, for all three classes of compounds produced nearly superimposable linear relationships but each with its own distinctive distribution pattern (see Figure 6.1).

An analogous more comprehensive investigation was undertaken by Baur[89] who examined the shapes of 211 phosphate tetrahedra. The arrangement of the four oxygen atoms around a central phosphorus atom he called a tetrahedral phosphate group because the four oxygen ligands are distributed over the four corners of an irregular tetrahedron. Baur predicted five possible cases of distortion from a regular tetrahedral shape. In addition he observed that the variation of bond lengths and angles from regular tetra= hedral values were not random but that the values of the averaged angles, $\alpha = \langle$(O-P-O) vary inversely with the mean bond length, $d(P\text{-}O)_s$, of the two sides of the angle. The geometrical relationship is

$$\log(\sin \frac{\alpha}{2}) = a + b \log[d(A\text{-}X)_s].$$

This empirical relationship allows prediction of $\langle$(O-P-O) for a known $d(P\text{-}O)_s$

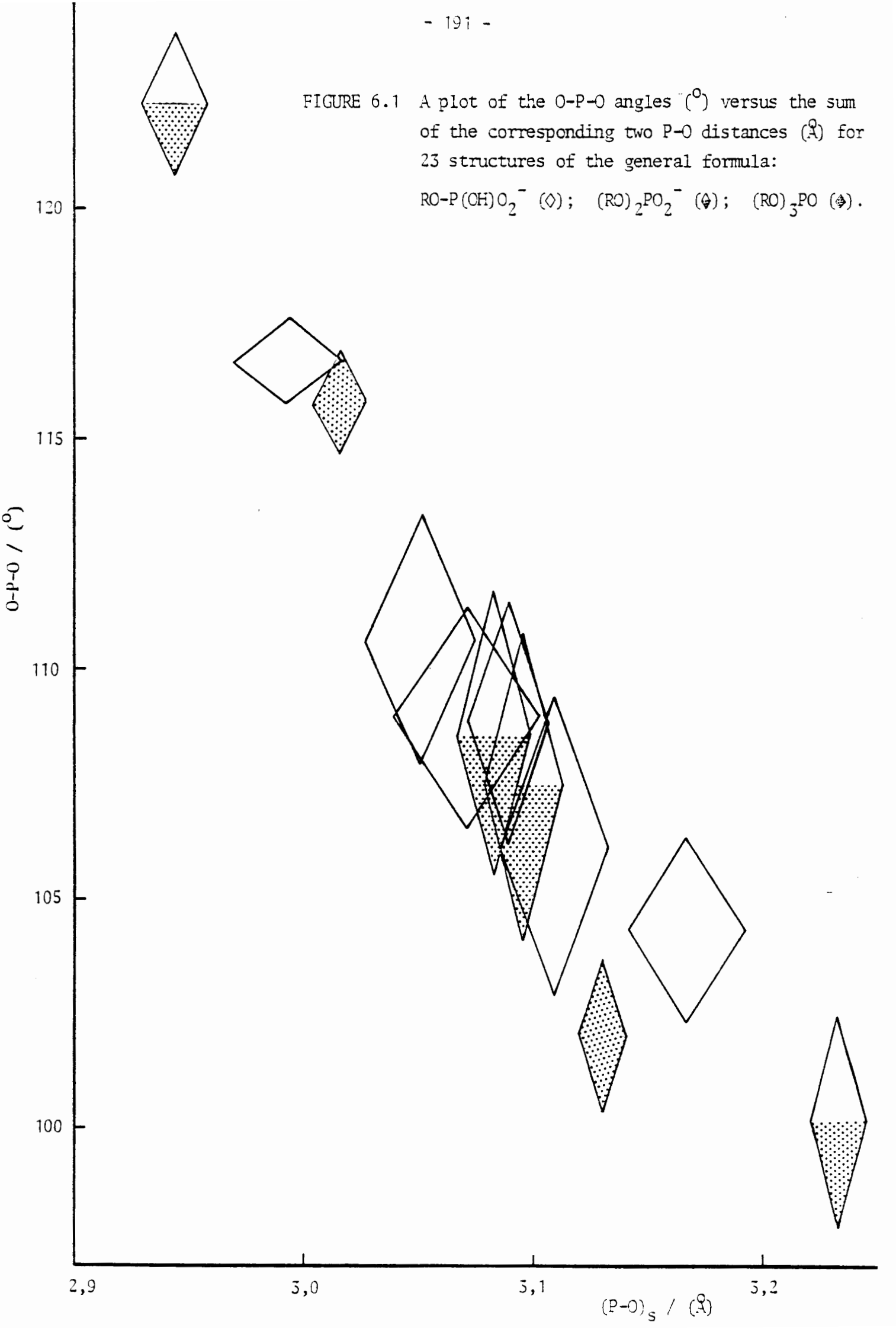

FIGURE 6.1 A plot of the O-P-O angles (°) versus the sum of the corresponding two P-O distances (Å) for 23 structures of the general formula:

$RO\text{-}P(OH)O_2^-$ (◇); $(RO)_2PO_2^-$ (◈); $(RO)_3PO$ (◆).

which in turn can be calculated from the bond strength distribution within the tetrahedron.

In this preliminary investigation this approach was extended to organic phosphates, which include thirteen monoesters[90] (twelve of which were nucleoside derivatives), six diesters[91] and four triesters[92]. The angle-distance correlation observed is graphically presented in Figure 6.2 as a plot of $-\log(\sin\frac{\alpha}{2})$ versus $\log[d(P\text{-}O)_s]$. A slope of -1,46 (r = 0,970) was obtained which is not significantly different from that of the theoretical value of -1,0.[89] This implies that these structures conform to the distortion case in which the two variable parameters are a bond distance, P-O, and an angle, O-P-O (see Figure 6.3). It was noticed that each of the three families of esters (mono-, di- and tri-esters) generates its own distinct set of points thereby indicating that a specific relationship between the structural parameters within each group of compounds exists. This is in accordance with the acknowledged differences in the chemical behaviour of each class. With regard to their phosphorylating properties (i.e. their ability to transfer a $P(O)X_2$ group from one nucleophilic atom to another) the reactivity decreases in the order: monoesters > triesters >> diesters (an example of the latter class being the notoriously stable nucleic acids).

The fundamental difference between the modes of the nucleophilic cleavage of the phosphoric triesters and monoesters is that, while the former react entirely via the associative mechanism, the latter systems are capable of reacting via the dissociative mechanism[93]. It is obvious that structural changes at phosphorus that accompany the associative $S_N2(P)$ and dissociative $S_N1(P)$ pathways must be very different. It was therefore of interest to establish whether the different patterns of nucleophilic substitution avail=able for these two classes of esters, as well as whether the enhanced reactivity of the monoesters would be manifested in the corresponding

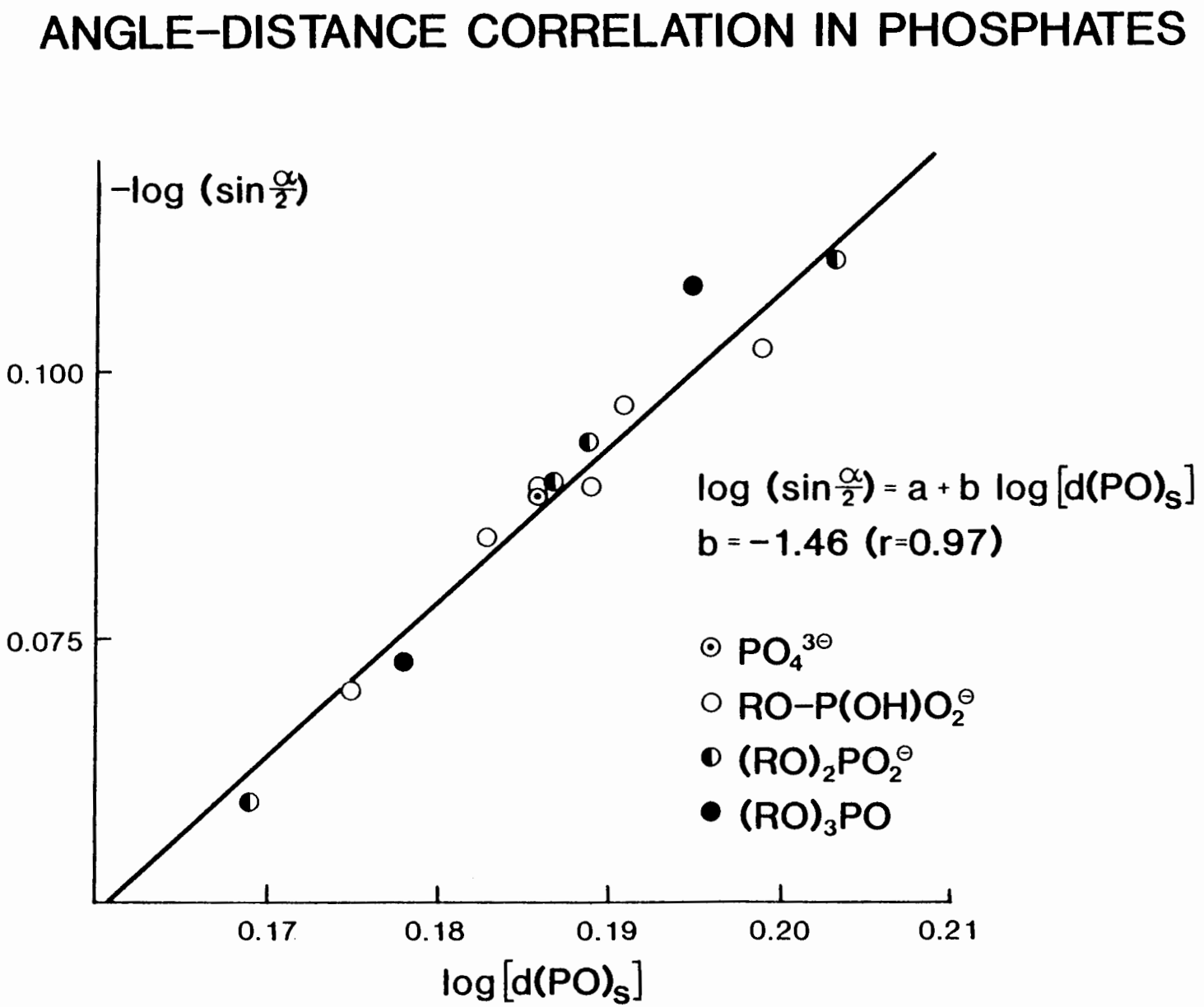

FIGURE 6.2 A plot of $-\log(\sin\frac{\alpha}{2})$ versus $\log[d(PO)_s]$ for the mono-, di- and tri-esters.

APPROXIMATE TREND IN THE DISTORTION OF PO_4 TETRAHEDRA

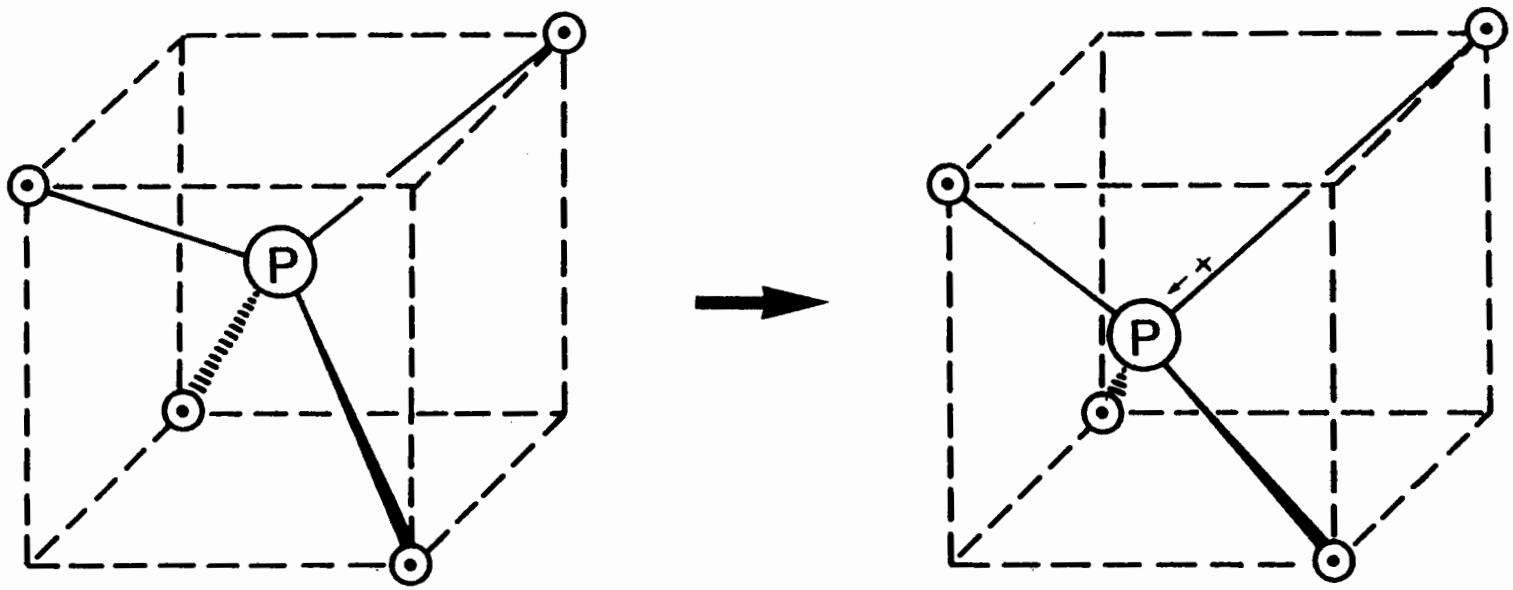

FIGURE 6.3 A bond length - bond angle distortion from the ideal tetrahedron.

structural parameters.

Hydrolysis or any other nucleophilic cleavage of the monoester monoanions (showing a rate maximum at pH 4) is proposed to occur by a $S_N1(P)$ (elimination-addition) mechanism via the metaphosphate intermediate[94]:

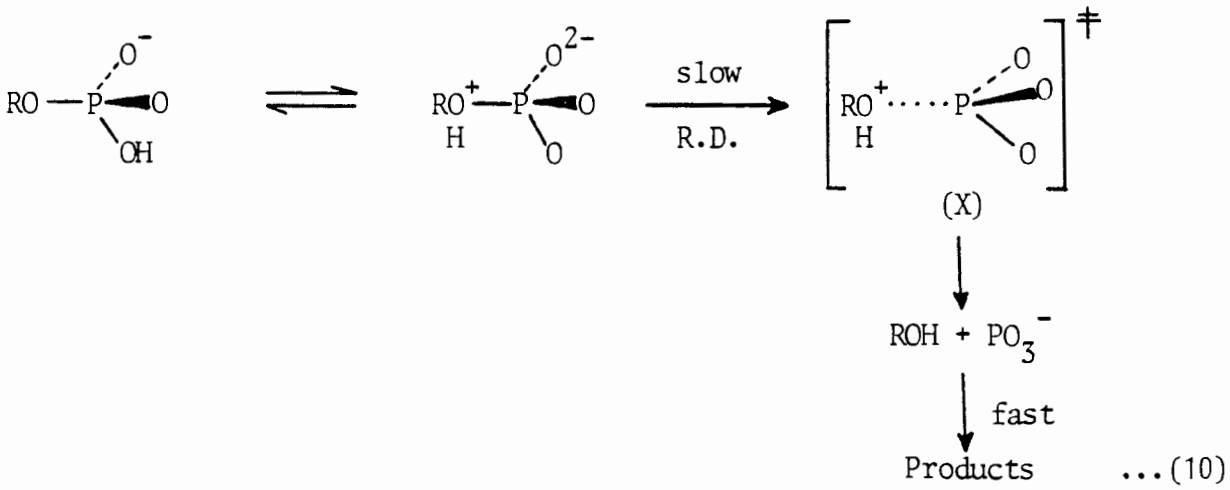

...(10)

For twenty-five monoester monoanions[90,95], for which structural data were retrieved, the RO-P-O angles averaged to 106,3° and the remaining O-P-O angles to 112,1°. These results are consistent with the proposed mechanism of hydrolysis whereby the tetrahedral values of the O-P-O angles tend toward the 90° (x 3) and 120° (x 3) values required by the geometry of the transition state (X). In accordance with the mechanism presented by equation (10) the changes in the O-P-O angles should be accompanied by an increase in the ester(O)-P distance. Whereas the average P-O(ester) bond distance for the triesters[92,96] is 1,563 ± 0,013Å, the corresponding distance for the mono-esters is increased to the average value of 1,607 ± 0,020Å (see Table 6.1).

It is interesting to note that in aromatic phosphate triesters derived from the 1,3,2-dioxaphosphorinane 2-oxide system, the P-OAr bond distances reach a limit at ∿1,600Å for good or very good leaving groups (such as 4-chloro-2-nitrophenoxide or 2,4-dinitrophenoxide) (Kirby and coworkers[88]).

TABLE 6.1 Average Bond Distances calculated for 40 organic structures of the general formula: $(RO)_3PO$, $(RO)_2PO_2^-$, $RO\text{-}P(OH)O_2^-$.

	Triesters (9)	Diesters (6)	Monoesters (25)
RO-P	1,563 ± 0,013Å		1,607 ± 0,020Å
$(\text{-H}\cdots)^-\text{O-P}$		1,486 ± 0,015Å	1,511 ± 0,013Å
O=P	1,445 ± 0,012Å		1,491 ± 0,014Å

The monoester monoanions however, have an ester group (nucleoside) which is derived from an alcohol (carbohydrate) i.e. an intrinsically poor leaving group. In spite of this, the average P-O distance is comparable with that observed only for triesters with very good leaving groups. This small, but meaningful increase in the (ester)O-P bond distance in the monoester mono= anions, as compared with the triesters, suggests some intrinsic weakness of the ester function and is compatible with the "metaphosphate" mechanism proposed for the cleavage reaction. In addition the phosphoryl bond, P=O (average value of 1,491 ± 0,014Å) for the monoesters is considerably longer than the typical value observed for the triesters (average value of 1,445 ± 0,012Å), According to reaction (10) the phosphorus moiety departs as a metaphosphate anion, PO_3^-. Although the metaphosphate species is not avail= able for structural determination, theoretical calculations[97] predict the three identical P-O bond distances in the PO_3^- ion to be ∿1,543Å.

Another approach to correlating structural parameters with chemical behaviour is to derive information about bond orders from structural data.

Dunitz[98] reports a correlation between bond angle and bond number and derives the expression, $n_2 = -3\cos\theta$ where n_2 equals one for the regular tetrahedron and zero for a planar MX_3 system.

In the unimolecular fragmentation of phosphoric monoester monoanions (equation 10) the bond number at phosphorus should reduce from four to three, i.e. the initial bond order for the P-O(ester) bond should change from one to zero. By arbitrarily assuming the bond order for the P-O(ester) function in the triesters to be one, and by applying the Dunitz equation, $n_i = -3\cos\theta$, the "bond number" for the P-O(ester) function in the monoesters is calculated to be 0,84 (θ = <RO-P-O = 106,3°). This value may be interpreted as the measure of progress (∿16%) along the reaction coordinate (equation 10) as observed in the

solid state.

Another way of estimating the "bond number" relates to the bond distance and can be expressed by the Dunitz equation:

$$\Delta r_i = -c \log n_i \qquad \ldots(11)$$

where n_i = "bond number"

Δr_i = change in the bond distance

c = empirical constant; c = 0,47 for P-O bonds.

Once again using the P-O(ester) bond distance for the triesters as a reference (average value of 1,563 ± 0,013Å) and by subtracting the average value of 1,607 ± 0,020Å obtained for the monoesters (Δr_i = 0,044Å), n_i is calculated to be 0,81. This result is in excellent agreement with that obtained from the angle data calculation above.

In conclusion, it is believed that the well known instability of the P-O(ester) bond in the phosphoric acid monoester monoanions is manifested in the molecular parameters of their stable salts, which are therefore considered to be the precursors to the alcohols and metaphosphate ion (equation 10).

APPENDIX 1 AND 3

APPENDIX 1

DETAILS PERTAINING TO THE EQUIPMENT USED IN THE X-RAY ANALYSES

Single Crystal X-ray Photography

Radiation	CuK_α (λ=1,5418Å)
Camera type	Stoe
Camera radius	28,65mm
X-ray generators	Philips (PW1120, PW1140)
Operating conditions	40kV, 20mA
X-ray film	3M medical film

Single Crystal Diffractometry

Radiation	CuK_α (λ=1,5418Å)	MoK_α (λ=0,7107Å)
Diffractometer (4-circle)	Philips PW1100	Enraf-Nonius CAD4
X-ray generator	Philips PW1140	Philips PW1730
Operating conditions	50kV, 20mA	50kV, 20mA
Operating temperature	20°C	20°C
Location	N.P.R.L., C.S.I.R.	U.C.T., C.T.

Computation

All computations were performed on a Univac 1106 computer system located at the computer centre of the University of Cape Town.

(The program SHELX-76[24] and SHELXS-84[26] were employed for structure solution and refinement.

The program XANADU[99] was used to calculate geometrical parameters.

Molecular illustrations and projections were produced by the programs PLUTO[100] and PLUTOX[100].

The program EENY[34] enabled potential energy calculations to be made.)

APPENDIX 3

ABSOLUTE STRUCTURE DETERMINATION

The procedure employed for the determination of the absolute structure, S_o (versus I_o, the inverse structure of S_o) is as follows[101]:

A coordinate set $+x_j$ is found by refining the structure until convergence is reached, employing real scattering factors, that is with all $\Delta f''$ set to zero. Without further refinement, this set of coordinates is then used to calculate two sets of structure factors, one with $\Delta f''$ positive and one with $\Delta f''$ negative, thereby giving two residual factors R_G^+ and R_G^-. A Hamilton's test is then carried out on the ratio of these two residual values.

This method allows all coordinates and the space group to be kept intact, and only the sign of $\Delta f''$ for all atom types need be changed.

However attempts to determine the absolute structures of compounds (7), (11) and (14) were not successful. A Hamilton's test could not be applied as the residuals R^+ and R^- were identical in all three cases.

REFERENCES

REFERENCES

1. Ramirez, F. and Marecek, J.F., *Organophosphorus Chemistry*, (Specialist Periodical Reports, The Royal Society of Chemistry, 1981), Vol. 12, p142 and references cited therein.
2. Cox, J.R. Jr and Ramsay, O.B., *Chemical Reviews*, *64*, p317 (1964).
3. Benkovic, S.J. and Schray, K.J., "*The Enzymes*", Vol. 8, 3rd Edition P.D. Boyer, Ed., Academic Press, New York (1973).
4. Ramirez, F. and Marecek, J.F., *J. of Pure and Appl. Chem.*, *52*, p2213 (1980).
5. Jaffe, E.K. and Cohn, M., *Biochemistry*, *17*, p652 (1978).
6. Jaffe, E.K. and Cohn, M., *J. Biol. Chem.*, *254*, p10839 (1979).
7. Schray, K.J. and Benkovic, S.J., *J. Am. Chem. Soc.*, *93*, p2522 (1971).
8. Khan, S.A., Kirby, A.J., Wakselman, M., Horning, D.P. and Lawlor, J.M., *J. Chem. Soc. B*, p1182 (1970).
9. Bromilow, R.H., Khan, S.A. and Kirby, A.J., *J. Chem. Soc. Perkin Trans. 2*, p911 (1972).
10. Usher, D.A., Richardson, D.I. Jr and Oakenfull, D.G., *J. Am. Chem. Soc.*, *92*, p4699 (1970).
11. Chanley, J.D. and Gindler, E.M., *J. Am. Chem. Soc.*, *75*, p4035 (1953).
12. Chanley, J.D. and Feageson, E., *J. Am. Chem. Soc.*, *77*, p4002 (1955).
13. Bender, M.L. and Lawlor, J.M., *J. Am. Chem. Soc.*, *85*, p3010 (1963).
14. Lazarus, R.A. and Benkovic, S.J., *J. Am. Chem. Soc.*, *101*, p4300 (1979).
15. Loran, J.S. and Williams, A., *J. Chem. Soc., Perkin Trans. 2*, p64 (1977).
16. Allen, G.W. and Haake, P., *J. Am. Chem. Soc.*, *95*, p8080 (1973).
17. Rowley, G.L., Greenleaf, A.L. and Kenyon, G.L. *J. Am. Chem. Soc.*, *93*, p5542 (1971).
18. Lazarus, R.A., Benkovic, P.A. and Benkovic, S.J., *J. Chem. Soc., Perkin Trans. 2*, p373 (1980) and references cited therein.

19. Khan, S.A., Kirby, A.J., Wakselman, M., Horning, D.P. and Lawlor, J.M., *J. Chem. Soc. B*, p1182 (1970).

20. Bürgi, H.B. and Dunitz, J.D., *Acc. Chem. Res., 16*, p153 (1983).

21. a) John, K.P., Schmutzler, R. and Sheldrick, W.S., *J. Chem. Soc. Dalton*, p1841 (1974); b) Ibid., p2466.

22. Cruickshank, D.W.J., *Acta Cryst., 17*, p671 (1964).

23. International Tables for X-ray Crystallography, Vols I, II, III, IV, Kynoch Press, Birmingham.

24. Sheldrick, G.M., The SHELX program in "Computing in Crystallography" Schenk, H., Olthof-Hazenkamp, R., van Koningsveld, H. and Bassi, G.C., Eds) Delft University Press (1978).

25. Murayama, A., Jastorff, B., Cramer, E. and Hettler, H., *J. Org. Chem., 36*, p3029 (1971).

26. Sheldrick, G.M., SHELXS-84 Direct Methods Program. Preliminary version. Private Communication (1983).

27. "*The Hydrogen Bond*", Schuster, P., Zundel, G. and Sandorfy, C., Eds, North-Holland Publ. Co., Vol II, p412 (1976).

28. Singleton, R., *J. Chem. Educ., 50*, p538 (1973).

29. Gillespie, R.J., *J. Chem. Educ., 40*, p295 (1963).

30. Emsley, J. and Hall, D., "*The Chemistry of Phosphorus*", Harper and Row, London, Ch. 8 (1976).

31. Aragona, G., Ghio, C. and Kollman, P., *J. Am. Chem. Soc., 105*, p5226 (1983).

32. Kitaigorodsky, A.I., *Chem. Soc. Rev., 7*, p133 (1978).

33. Mirsky, K., "*Computing in Crystallography*", Schenk, K., Olthof-Hazenkamp, R., van Koningsveld, H. and Bassi, G.C., Eds, Delft University Press (1978).

34. Giglio, E., *Nature, 222*, p339 (1969).

35. Motherwell, W.D.S., EENY Potential Energy Program, Cambridge University (1974).

36. "*Lange's Handbook of Chemistry*", Dean, J.A., Ed., 11th Edition, McGraw-Hill (1973) (van der Waals radii quoted are those of Pauling).

37. Gillis, R.G. and Occolowitz, J.L., "*Analytical Chemistry of Phosphorus Compounds*", Halman, M. Ed., Wiley-Interscience, N.Y., Ch 6.111.F. (1972).

38. Haake, P. and Ossip, P.S., *J. Am. Chem. Soc., 93,* p6919 (1971).

39. Bürgi, H.B., Dunitz, J.D. and Shefter, E., *J. Am. Chem. Soc., 95,* p5065 (1973). An initial survey based on six molecules for which structural data were available.

40. Dunitz, J.D., "*X-ray Analysis and the structure of organic molecules*", Cornell University Press, Ithaca and London, Ch. 7 (1979).

41. a) Schweizer, W.B., Doctoral Dissertation No. 5948, E.T.H., Zürich, (1977);
b) Schweizer, W.B., Procter, G., Kaftory, M. and Dunitz, J.D., *Helv. Chim. Acta, 61,* p2783 (1978).

42. Cocks, S. and Modro, T.A. in preparation.

43. Rodgers, A.L., Nassimbeni, L.R., Mulder, K.J. and Mullins, J.M., *Investigative Urology, 19,* p154 (1981).

44. North, A.C.T., Phillips, D.C. and Mathews, F.S., *Acta Cryst., A24,* p351 (1968).

45. Hamilton, W.C., *Acta Cryst., 18,* p502 (1965).

46. Wells, A.F., "*Structural Inorganic Chemistry*", 5th Edition, Clarendon Press, Oxford (1984).

47. Caughlan, C.N., Wang, C.K. and Fitzgerald, A., *Acta Cryst., A28,* S40, (1972).

48. Davies, W.O. and Stanley, E., *Acta Cryst., 15,* p1092 (1962).

49. Wolfenden, R. and Williams, R., *J. Am. Chem. Soc., 105,* p1028 (1983).

50. Cocks, S. and Modro, T.A., in preparation.

51. Murray-Rust, P. and Glusker, J.P., *J. Am. Chem. Soc., 106,* p1018 (1984).

52. Alagona, G., Ghio, C. and Kollman, P., *J. Am. Chem. Soc., 105,* p5226 (1983).

53. Etter, M.C., *J. Am. Chem. Soc., 104,* p1095 (1982).

54. Pullman, A., Berthod, H. and Gresh, N., *Chem. Phys. Lett., 33,* p11 (1975).

55. Pullman, B., Pullman, A., Berthod, H. and Gresh, N., *Theor. Chim. Acta, 40,* p93 (1975).

56. Main, P., Fiske, S.J., Hull, S.E., Lessinger, L., Germain, G., Declercq, J-P. and Woolfson, M.M., MULTAN-82. A system of computer programs for the automatic solution of crystal structures from X-ray diffraction data. Universities of York, England and Louvain, Belgium (1982).

57. a) "*The Hydrogen Bond*", Schuster, P., Zundel, G. and Sandorfy, C., Eds. North-Holland Publishing Company, Vol. II, Ch. 8, p412 (1976).
b) Ibid. Ch. 10.

58. Dunitz, J.D. and Rollett, J.S., *Acta Cryst., 9*, p327 (1956).

59. Emsley, J., Jones, D.J. and Lucas, J., *Reviews in Inorganic Chemistry, 3*, p109 (1981).

60. Maas, G. and Hoge, R., *Acta Cryst., B36*, p499 (1980).

61. Pletcher, J., Sax, M. and Yoo, C.S., *Acta Cryst., B28*, p378 (1972).

62. Yoo, C.S., Abola, E., Wood, M.K., Sax, M. and Pletcher, J., *Acta Cryst., B31*, p1354 (1975).

63. Sax, M., Pletcher, J. and Gustaffson, B., *Acta Cryst., B26*, p114 (1970).

64. Perrin, D.D., Dempsey, B. and Serjeant, E.P., "*pKa Prediction for Organic Acids and Bases*", Chapman and Hall, London, Ch. 5 (1981).

65. Johnson, C.R., *Acc. Chem. Res., 6*, p341 (1973).

66. Bentley, H.R., McDermott, E.E., Pace, J., Whitehead, J.K. and Moran, T., *Nature, 165*, p150 (1950).

67. Andersen, K.K., Bhattacharyya, J. and Mukhopadhyay, S.K., *J. Med. Chem., 13*, p759 (1970).

68. Wieczorkowski, J., Jakobsen, P. and Treppendahl, S., *Acta Chim. Scand., B37*, p27 (1983).

69. Schmidbaur, H. and Kammel, G., *Chem. Ber., 102*, p4128 (1969).

70. Gillespie, R.J., *J. Chem. Ed., 40*, p295 (1963).

71. Galdecki, Z. and Karolak-Wojciechowska, J., *Lodz. Towarz. Nauk. Wydzial*, III, *Acta Chim., 115*, p7 (1973).

72. du Plessis, M.P., PhD Thesis, U.C.T. (1982).

73. Cruickshank, D.W.J., *J. Chem. Soc.*, p5858 (1961).

74. du Plessis, M.P., Modro, T.A. and Nassimbeni, L.R., *J. Org. Chem., 47,* p2313 (1982).

75. Rünchle, R., Pohl, W., Blaich, B. and Goubeau, J., *Ber. Bunsen Ges. Phys. Chem., 75,* p66 (1971).

76. Reck, R., Zsolnai, L., Huttner, G., Herzberger, S. and Jochims, J.C., *Chem. Ber., 115,* p2981 (1982).

77. Hewlins, M.J.E., *J. Chem. Soc., (B),* p942 (1971).
Report a short P-N distance of 1,57Å for triphenyl-N-(*p*-bromophenyl)-iminophosphorane, $Ph_3P{=}N{-}C_6H_4Br(p)$.

78. Nöth, H., *Z. Naturforsch., 37b,* p1491 (1982).
Report a short P-N distance of 1,54Å and a P-N-P bond angle of ideal linearity for imidotetraphenyldiphosphinic acid, $Ph_2P(O){-}N{=}P(OH)Ph_2$.

79. Kwart, H. and King, K., "*d-Orbitals in the Chemistry of Silicon, Phosphorus and Sulfur*", Springer-Verlag, Berlin, Ch. III (1977).

80. a) Andreetti, G.D., Bocelli, G. and Sgarabotto, P., *Gazz. Chim. Ital., 105,* p165 (1975).

b) Andreetti, G.D., Bocelli, G. and Sgarabotto, P., *Cryst. Struct. Comm, 2,* p171 (1973).

c) Andreetti, G.D., Bocelli, G., Cogni, L. and Sgarabotto, P., *Cryst. Struct. Comm., 3,* p765 (1974).

81. Neidle, S. and Rogers, D., *J. Chem. Soc. (B),* p694 (1970).

82. Cameron, T.S., Galdecki, Z. and Karolak-Wojciechowska, J., *Acta Cryst., Ser. B, B32,* p492 (1976).

83. Cameron, T.S. and Karolak-Wojciechowska, J., *Acta Cryst., Ser. B, B37,* p2342 (1977).

84. White, D.W., McEwen, G.K., Bertrand, R.D. and Verkade, J.G., *J. Chem. Soc. (B),* p1454 (1971).

85. Mizrahi, V. and Modro, T.A., *Cryst. Struct. Comm., 11,* p627 (1982).

86. Emsley, J. and Hall, D., "*The Chemistry of Phosphorus*", Harper and Row, London, Ch. 10 (1976).

87. Klyne, W. and Prelog, V., *Experientia, 16*, p521 (1960).

88. a) Jones, P.G., Sheldrick, G.M., Kirby, A.J. and Briggs, A.J., *Acta Cryst., C41*, p1374 (1985) (and references cited therein).

b) Ibid. p1377 (and references cited therein).

c) Ibid. p1380 (and references cited therein).

89. Baur, W.H., *Acta Cryst., B30*, p1195 (1974).

90. a) Bugg, E. and Marsh, R.E., *J. Mol. Biol., 25*, p67 (1967).

b) Sundaralingam, M., *Acta Cryst., 21*, p495 (1966).

c) Sundaralingam, M. and Jensen, L.H., *J. Mol. Biol., 13*, p914 (1965).

d) Kraut, J. and Jensen, L.H., *Acta Cryst., 16*, p79 (1963).

e) Murayama, W., Nagashima, N. and Shimizu, Y., *Acta Cryst., B25*, p2236 (1969)

f) Adamiak, D.A. and Saenger, W., *Acta Cryst., B35*, p924 (1979).

g) Yamagata, Y., Suzuki, Y., Fujii, S., Fujiwara, T. and Tomita, K-I., *Acta Cryst., B35*, p1136 (1979).

h) Tanaka, K., Fujii, S., Fujiwara, T. and Tomita, K-I., *Acta Cryst., B35*, p929 (1979).

i) Emerson, J. and Sundaralingam, M., *Acta Cryst., B36*, p537 (1980).

j) Viswamitra, M.A., Reddy, B.S., Hung-Yin Lin, G. and Sundaralingam, M., *J. Am. Chem. Soc., 93*, p4565 (1971).

k) Sherfinski, J.S., Marsh, R.E., Chwang, A.K. and Sundaralingam, M., *Acta Cryst., B35*, p2141 (1979).

l) Viswamitra, M.A., Reddy, B.S., James, M.N.G.,and Williams, G.J.B., *Acta Cryst., B28*, p1108 (1972).

m) Li, C-T. and Caughlan, C.N., *Acta Cryst., 19*, p637 (1965).

91. a) Bond, D.R., Modro, T.A., Niven, M.L. and Nassimbeni, L.R., *S. Afr. J. Chem., 38*, p78 (1985).

b) Ref. 61

c) Ref. 62

d) Ref. 63.

e) Sax, M., Pletcher, J., Yoo, C.S. and Stewart, J.M., *Acta Cryst., B27*, p1635 (1971).

f) Bond, D.R., Modro, T.A. and Nassimbeni, L.R., *J. Org. Chem., 50*, p2281 (1985).

92. a) Svetich, G.W., Caughlan, C.N., *Acta Cryst., 19*, p645 (1965).

b) Ul-Haque, M. and Caughlan, C.N., *Acta Cryst., B26*, p1528 (1970).

c) Ref. 91(f).

d) Brennan, R.G., Kondo, N.S. and Sundaralingam, M., *J. Am. Chem. Soc., 106*, p5671 (1984).

93. Bunton, C.A., *Acc. Chem. Res., 3*, p257 (1970).

94. Ref. 86, Ch. 8, p312.

95. a) Shefter, E., Trueblood, K.N., *Acta Cryst., 18*, p1067 (1965).

b) Karle, I.L. and Britts, K., *Acta Cryst., 20*, p118 (1966).

c) Beevers, C.A. and Maconochie, G.H., *Acta Cryst., 18*, p232 (1965).

d) Kraut, J., *Acta Cryst., 14*, p1146 (1961).

e) Sundaralingam, M. and Putkey, E.F., *Acta Cryst., B26*, p790 (1970).

f) Ref. 95(e), p782.

g) Mostad, A. and Rosenquist, E., *Acta Chem. Scand., 25*, p147 (1971).

h) Rao, S.T. and Sundaralingam, M., *J. Am. Chem. Soc., 91*, p1210 (1969).

i) Ul-Haque, M. and Caughlan, C.N., *J. Am. Chem. Soc., 88*, p4124 (1966).

j) Fujiwara, T. and Tomita, K., *Tet. Lett.*, p2819 (1969).

k) Furberg, S. and Mostad, A., *Acta Chem. Scand., 16*, p1627 (1962).

l) Caughlan, C.N. and Ul-Haque, M., *Inorg. Chem., 6*, p1998 (1967).

96. a) Cocks, S., Modro, T.A. and Niven, M.L., submitted to *Acta Cryst., C.*

b) Newton, M.G., Cox, J.R. and Bertrand, J.A., *J. Am. Chem. Soc., 88*, p1503 (1966).

c) Steltz, T.A. and Lipscomb, W.N., *J. Am. Chem. Soc., 87*, p2488 (1965).

d) Van Nuffel, P., Lenstra, A.T.H. and Geise, H.J., *Cryst. Struct. Comm., 9*, p733 (1980).

e) Jones, P.G., Sheldrick, G.M., Kirby, A.J. and Briggs, A.J., *Acta Cryst., C40*, p1061 (1984) (where Ar = Ph only).

97. Loew, L.M. and MacArthur, W.R., *J. Am. Chem. Soc., 99*, p1019 (1977).

98. Ref 40, p358.

99. Roberts, P. and Sheldrick, G.M., Cambridge, unpublished.

100. Motherwell, W.D.S., Cambridge, unpublished.

101. Marsh, R.E., *Acta Cryst., B37*, p1985 (1981).